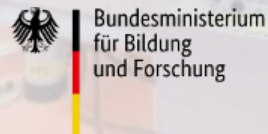
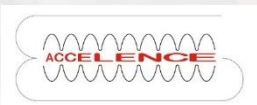




ENERGY-RECYCLING IN A MULTI-TURN ENERGY-RECOVERY LINAC AND PROSPECTS FOR PHOTONUCLEAR REACTIONS

Norbert Pietralla

Michaela Arnold, Jonny Birkhan, Adrian Brauch, Jochim Enders, Ruben Grewe, Johann Isaak, Lars Jürgensen, Jörn Kleemann, Maximilian Meier, Felix Schliessmann, Dominic Schneider, Volker Werner + Norbert Pietralla



Work supported by DFG (GRK 2128, GRK 2891), BMBF (05H21RDRB1), and the State of Hesse (Cluster Project ELEMENTS)



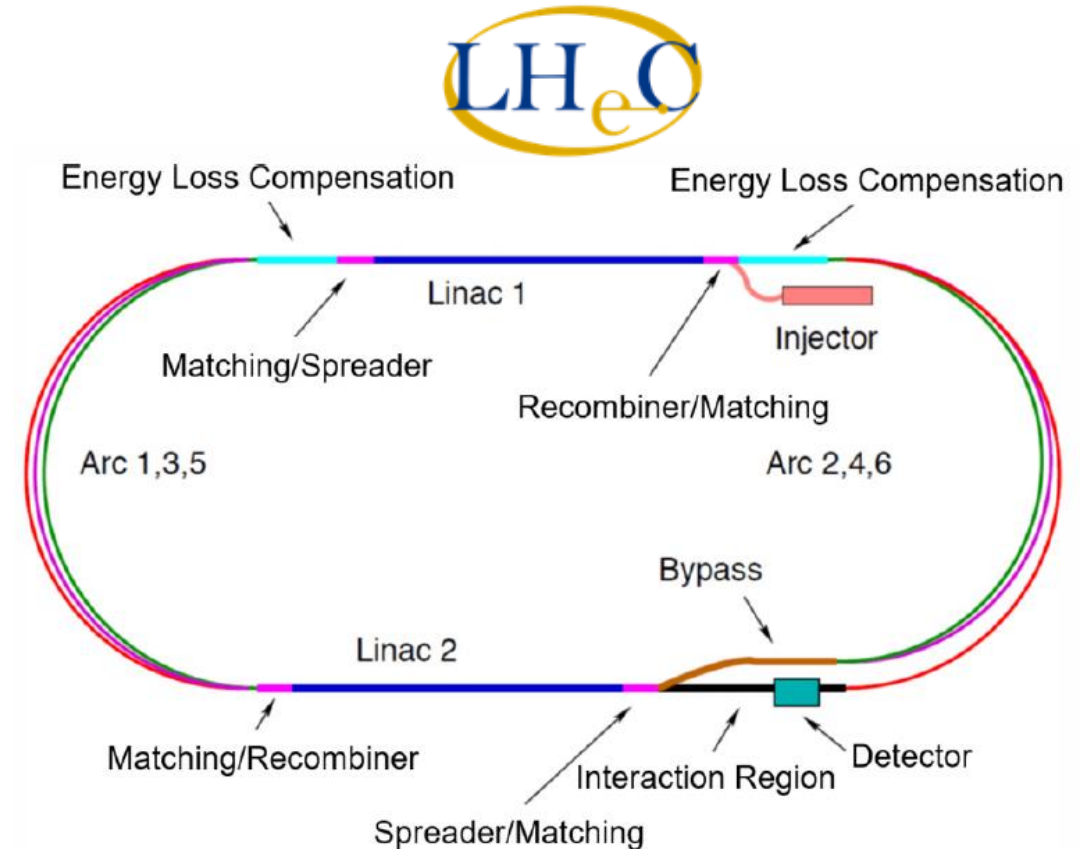
MULTI-TURN ERL MODE OF THE S-DALINAC

MOTIVATION FOR MULTI-TURN ENERGY RECOVERY

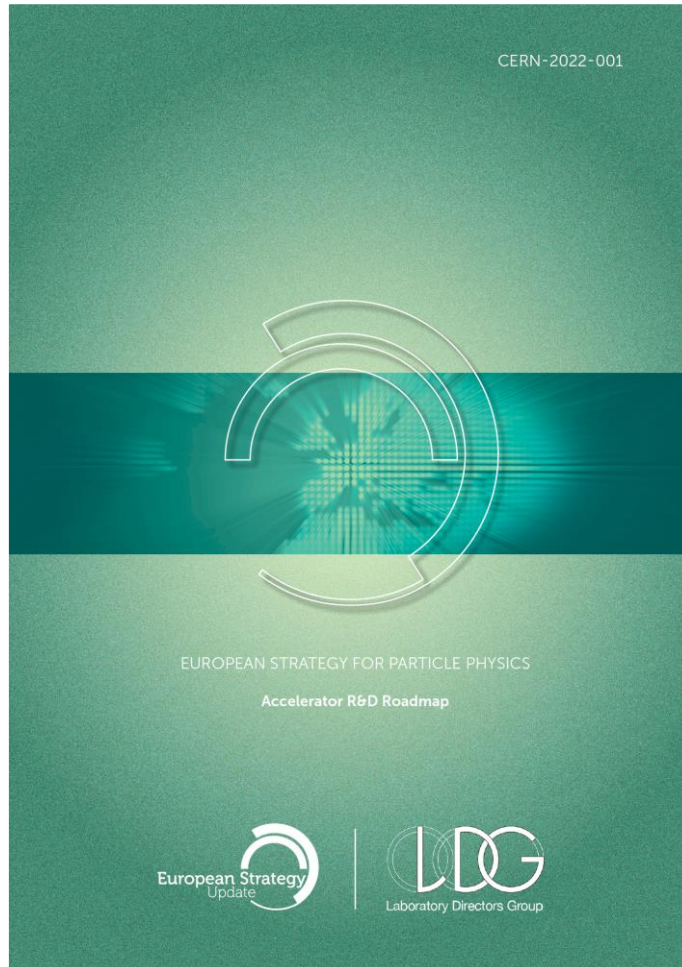
Potential future for CERN beyond 2045

- Collide LHC beam with high power electron beam
- Optimum emittance via use of LINAC
- 50 GeV and 200 mA → 10 GW of (virtual) beam power
- Largest nuclear reactor facility in Europe ca. 8 GW

→ Need for sustainable technology
→ Energy-recovery LINACs



P. Agostini et al., J. Phys. G: Nucl. Part. Phys. **48**, 110501 (2021)



CERN Yellow Reports: Monographs, CERN-2022-001

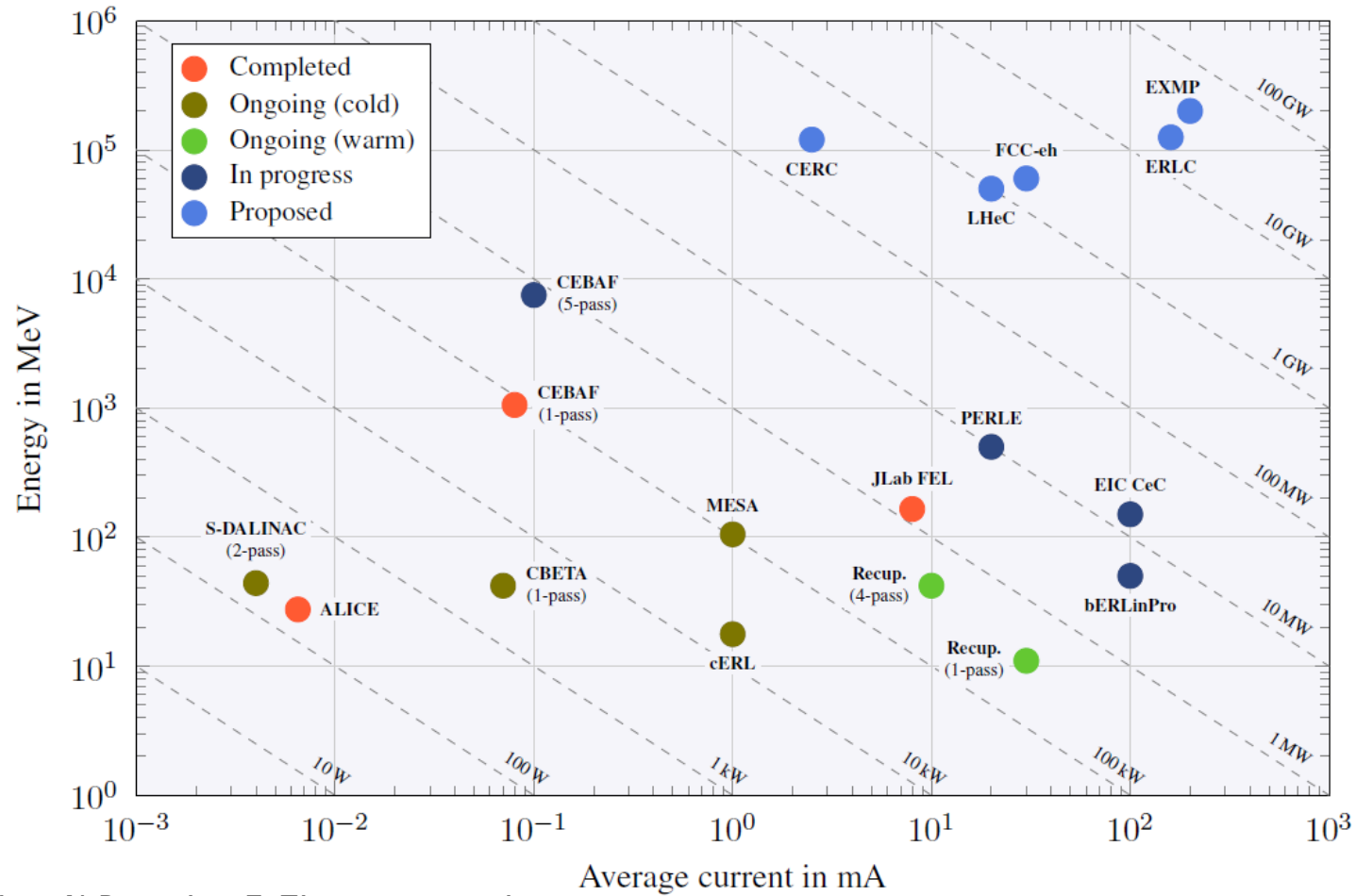
6 Energy-recovery linacs

6.1 Executive summary

Energy Recovery is at the threshold of becoming a key means for the advancement of accelerators. Recycling the kinetic energy of a used beam for accelerating a newly injected beam, i.e. reducing the power consumption, utilising the high injector brightness and dumping at injection energy: these are the key elements of a novel accelerator concept, invented half a century ago [1]. The potential of this

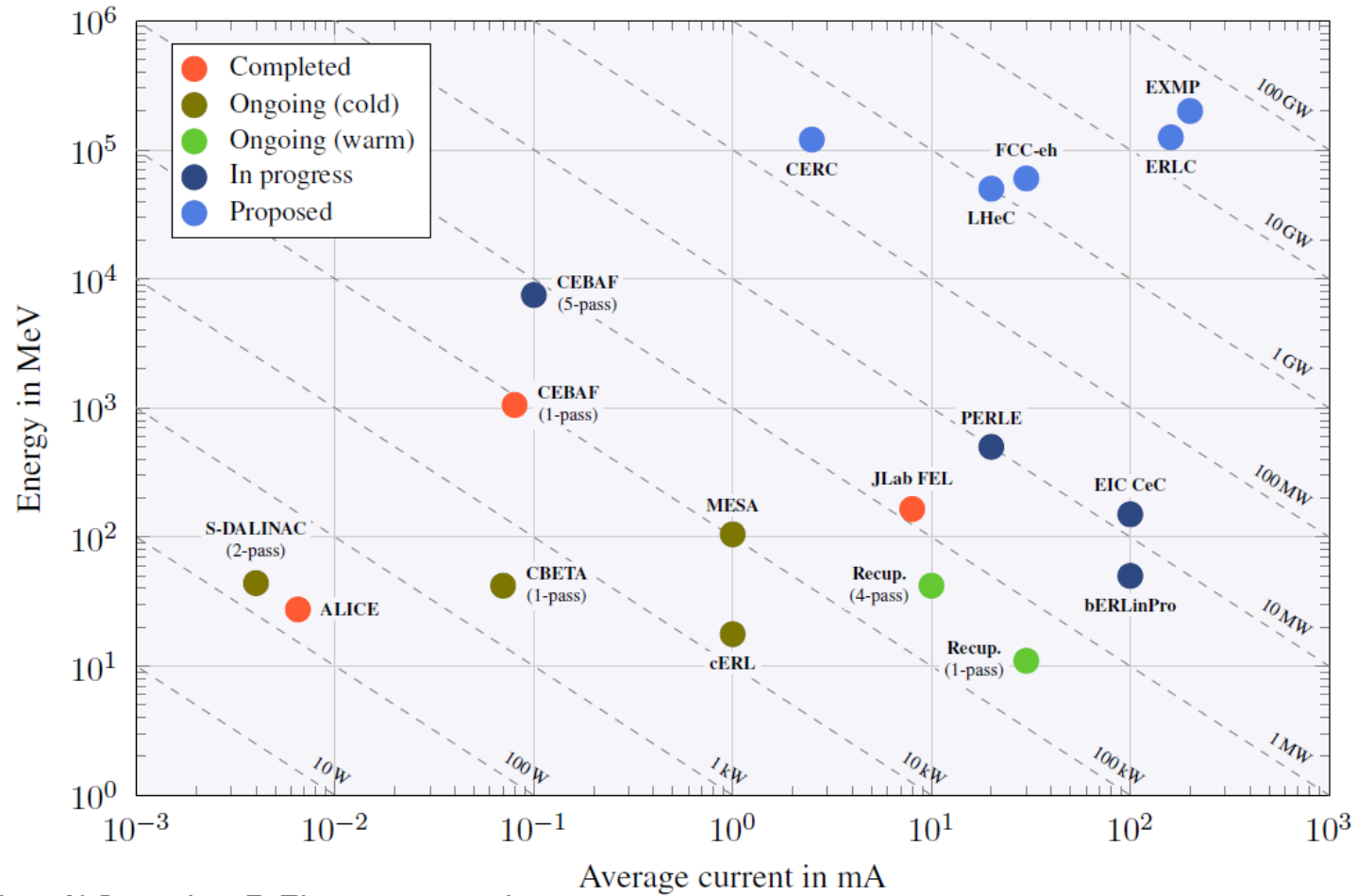
M. Klein, A. Hutton *et int.*, N.P., *et int.* F. Zimmermann, in European Strategy for Particle Physics - Accelerator R&D Roadmap, N. Mounet (ed.), CERN-2022-001 (CERN, Geneva, 2022), pp. 185–228.

ENERGY RECOVERY LINACS (ERLS) WORLDWIDE



M. Klein, A. Hutton *et int.*, N.P., *et int.* F. Zimmermann, in European Strategy for Particle Physics - Accelerator R&D Roadmap, N. Mounet (ed.), CERN-2022-001 (CERN, Geneva, 2022), pp. 185–228.

ENERGY RECOVERY LINACS (ERLS) WORLDWIDE

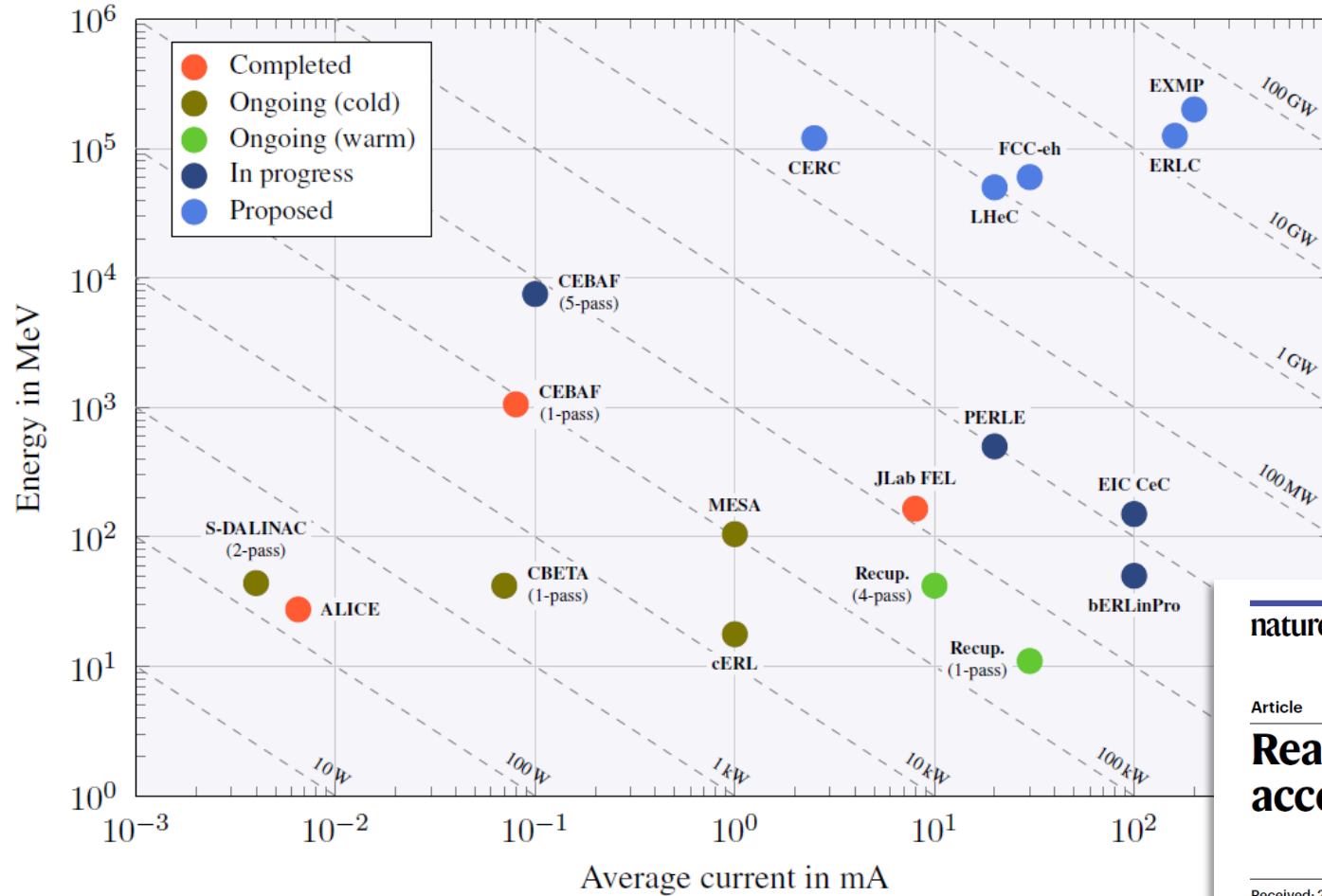


CBETA – first multi-turn SRF-ERL

A. Bartnik et al.,
Phys. Rev. Lett. **125**, 044803
(2020).

M. Klein, A. Hutton *et al.*, N.P., *et al.* F. Zimmermann, in
European Strategy for Particle Physics - Accelerator R&D
Roadmap, N. Mounet (ed.), CERN-2022-001 (CERN, Geneva,
2022), pp. 185–228.

ENERGY RECOVERY LINACS (ERLS) WORLDWIDE



@S-DALINAC

For the first time, measured energy-recycling directly in multi-turn SRF-ERL.

measured energy-recycling of 87%

nature physics

Article

<https://doi.org/10.1038/s41567-022-01856-w>

Realization of a multi-turn energy recovery accelerator

Received: 28 March 2022

Felix Schlessmann, Michaela Arnold, Lars Juergensen,

Accepted: 26 October 2022

Norbert Pietralla, Manuel Dutine, Marco Fischer, Ruben Grewe, Manuel Steinhorst, Lennart Stobbe & Simon Weih

Published online: 26 January 2023

OUTLINE

- 1** Motivation for Multi-Turn Energy Recovery
- 2** Multi-Turn Energy Recovery at the S-DALINAC
- 3** Perspectives for ERL Applications
- 4** Prospects for Photonuclear Reactions

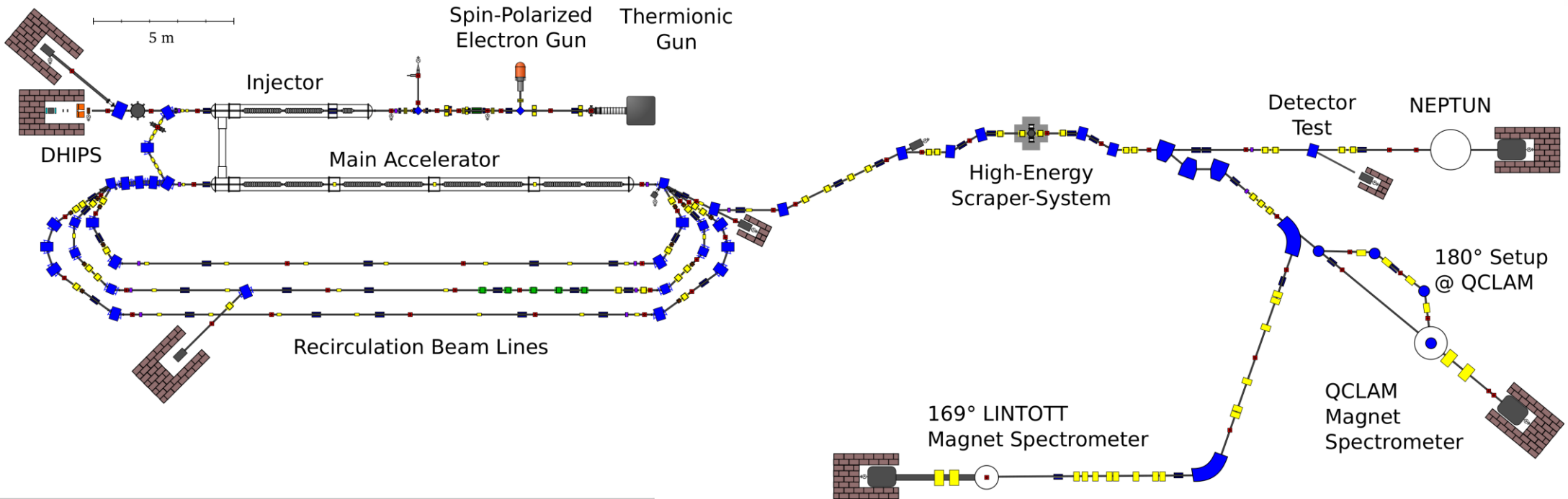


MULTI-TURN ERL MODE OF THE S-DALINAC

MULTI-TURN ENERGY RECOVERY AT THE S-DALINAC

SUPERCONDUCTING DARMSTADT LINEAR ACCELERATOR

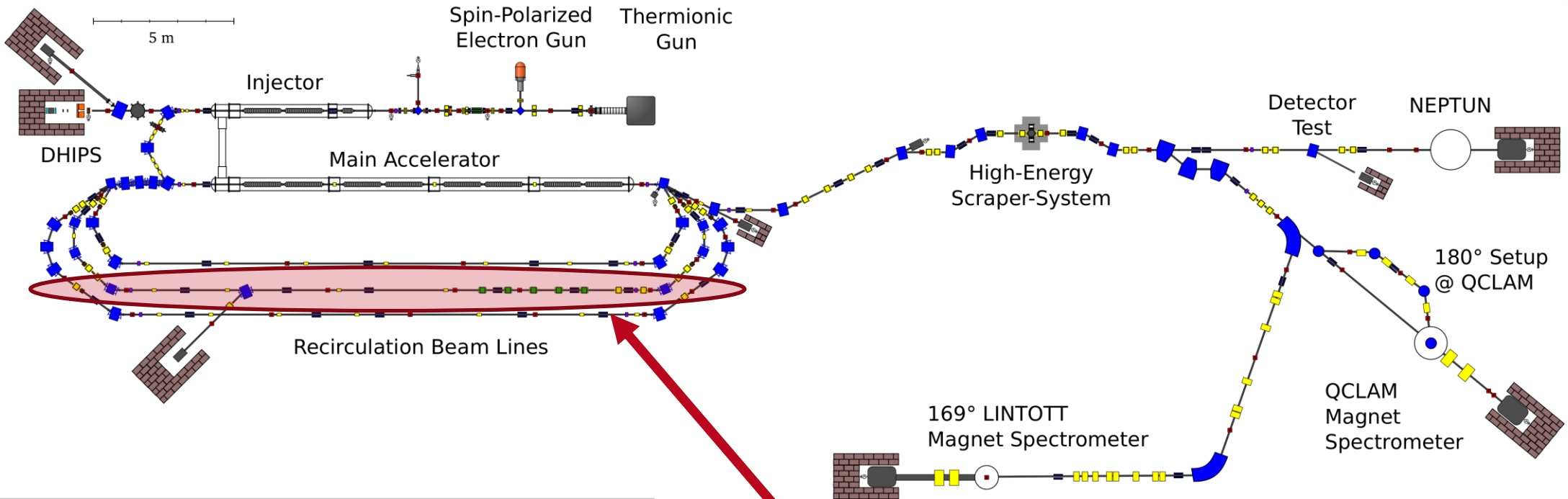
MULTI-TURN ERL MODE OF THE S-DALINAC | INTRODUCTION



Thrice Recirculating Operation

Energy Gain Injector	7.6 MeV
Energy Gain Linac	30.4 MeV
Beam Current	20 μ A

MULTI-TURN ERL MODE OF THE S-DALINAC | INTRODUCTION



Thrice Recirculating Operation

Energy Gain Injector	7.6 MeV
Energy Gain Linac	30.4 MeV
Beam Current	20 μA

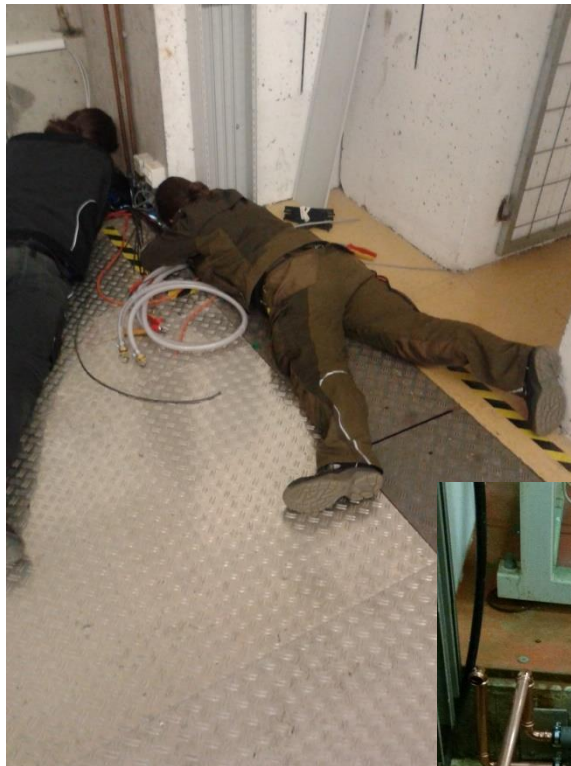
new beamline in 2015/16

2015/16 NEW BEAM LINE

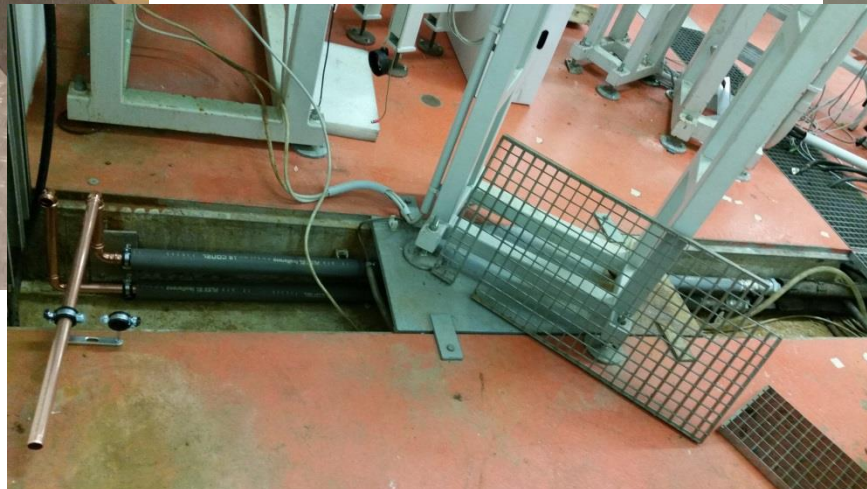


TECHNISCHE
UNIVERSITÄT
DARMSTADT

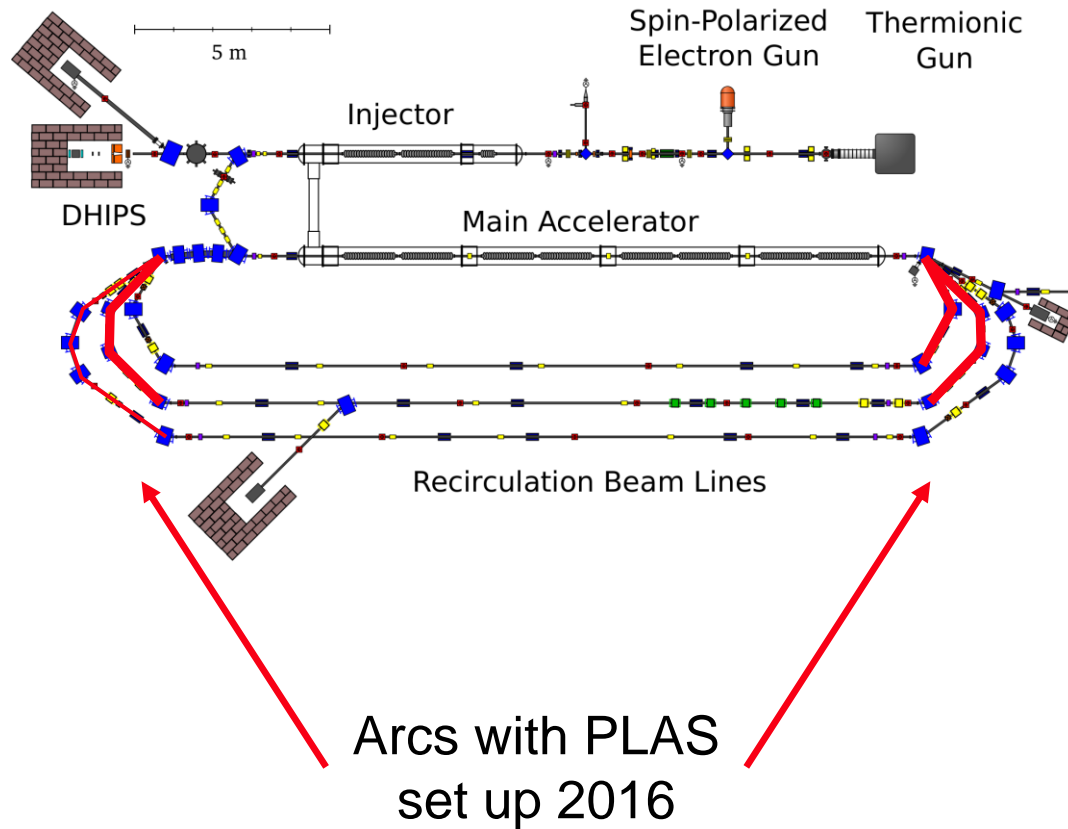




- 500 cables
- 15 km cables
- 500 m copper-pipes for water
- 250 m flexible tubes



MULTI-TURN ERL MODE OF THE S-DALINAC | INTRODUCTION



- Path length adjustment system (PLAS) in arcs of the recirculation beam lines
- PLAS in 1st and 2nd recirculation tunable for
 - Beam acceleration
 - Phase change up to 360°
 - Beam deceleration (Energy Recovery)
- Enables single-fold and two-fold ERL mode

A THIRD RECIRCULATION WITH ERL-OPTION FOR THE S-DALINAC - DESIGN AND IMPLEMENTATION

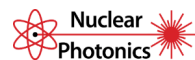
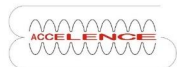


TECHNISCHE
UNIVERSITÄT
DARMSTADT

Fall 2015

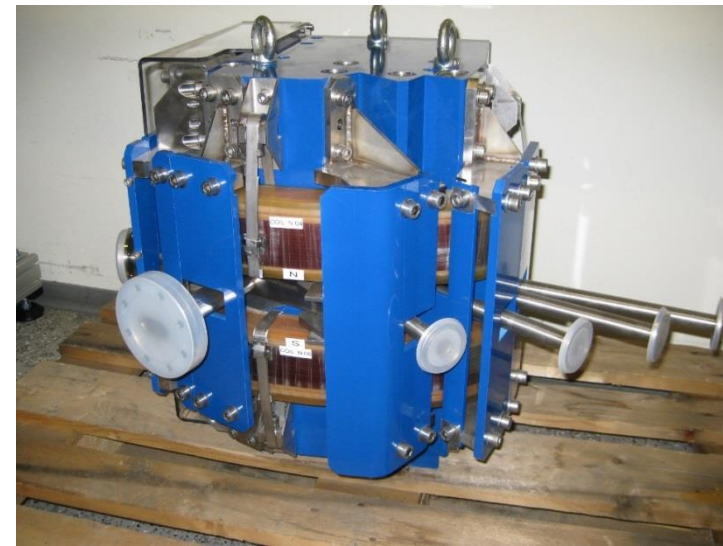
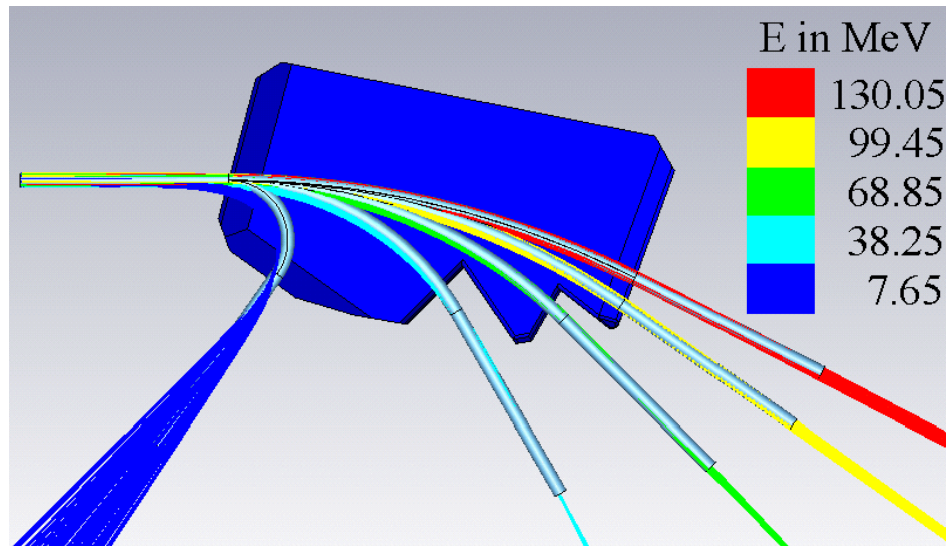


Summer 2016



Separation Dipole

- Particle tracking of all beam energies (CST Particle Studio)
- Acceptance
 - Beam diameter: up to 10 mm
 - Energy spread: up to $1 \cdot 10^{-3}$
 - Angular spread: up to 0.1°



M. Arnold (PhD thesis, TU Darmstadt, 2016).

OVERVIEW OPERATION MODES/COMMISSIONING

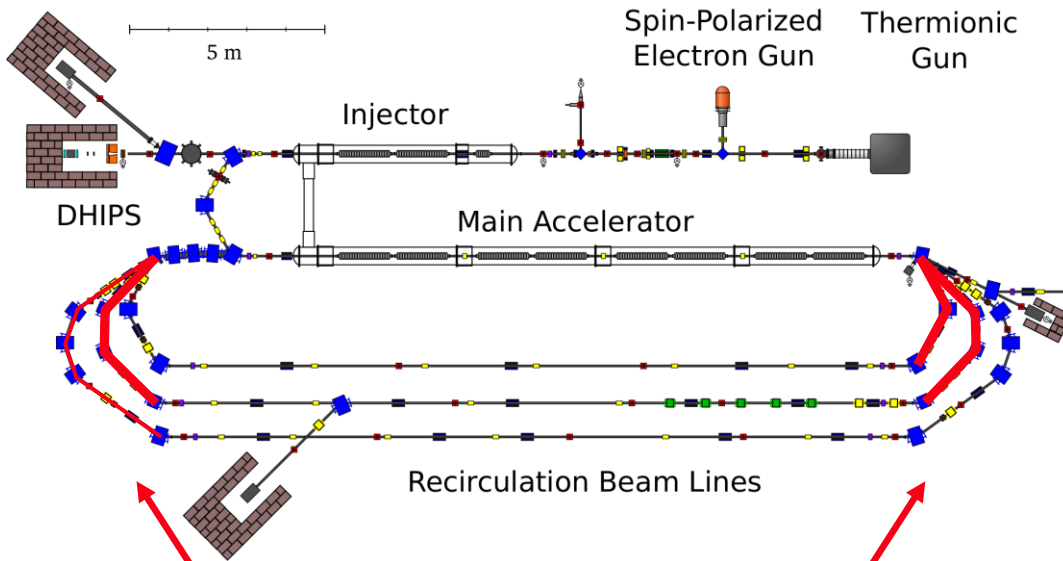


TECHNISCHE
UNIVERSITÄT
DARMSTADT

- Modification lattice 2015/2016
- Commissioning of modes followed beam time schedule



MULTI-TURN ERL MODE OF THE S-DALINAC | INTRODUCTION

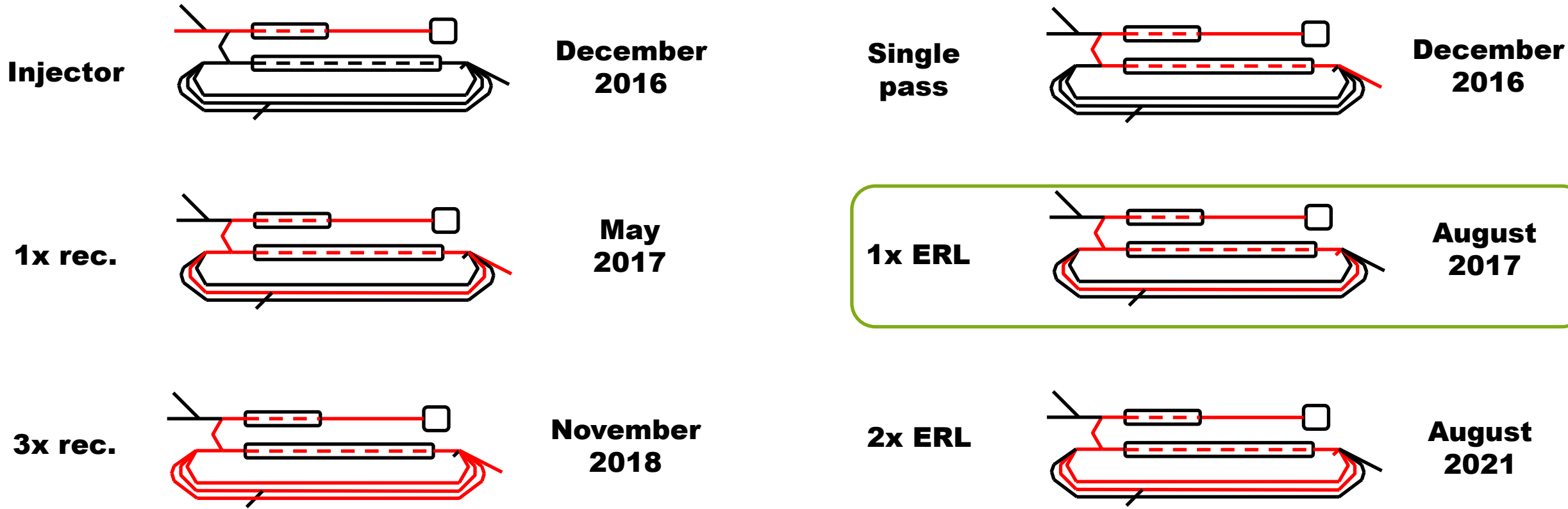


Arcs with PLAS
set up 2016

- Path length adjustment system (PLAS) in arcs of the recirculation beam lines
- PLAS in 1st and 2nd recirculation tunable for
 - Beam acceleration
 - Phase change up to 360°
 - Beam deceleration (Energy Recovery)
- Enables single-fold and two-fold ERL mode
- Research on ERL modes since 2016, e.g.:
 1. M. Arnold *et al.* First operation of the superconducting Darmstadt linear electron accelerator as an energy recovery linac. *Phys. Rev. Accel. Beams* **23**, 020101 (2020).
<https://doi.org/10.1103/PhysRevAccelBeams.23.020101>
 2. F. Schliessmann *et al.* Realization of a multi-turn energy recovery accelerator. *Nat. Phys.* **19**, 597 (2023).
<https://doi.org/10.1038/s41567-022-01856-w>

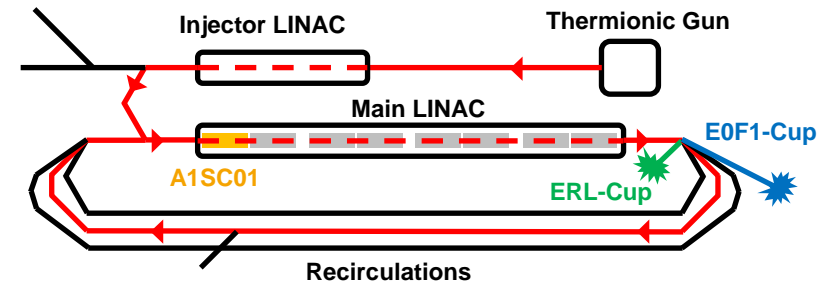
OVERVIEW OPERATION MODES/COMMISSIONING

- Modification lattice 2015/2016
- Commissioning of modes followed beam time schedule



ONCE-RECIRCULATING ERL OPERATION

- Energy gain injector: 2.5 MeV
- Energy gain LINAC: 20.0 MeV
- Current (I_{in}): 1.2 μ A

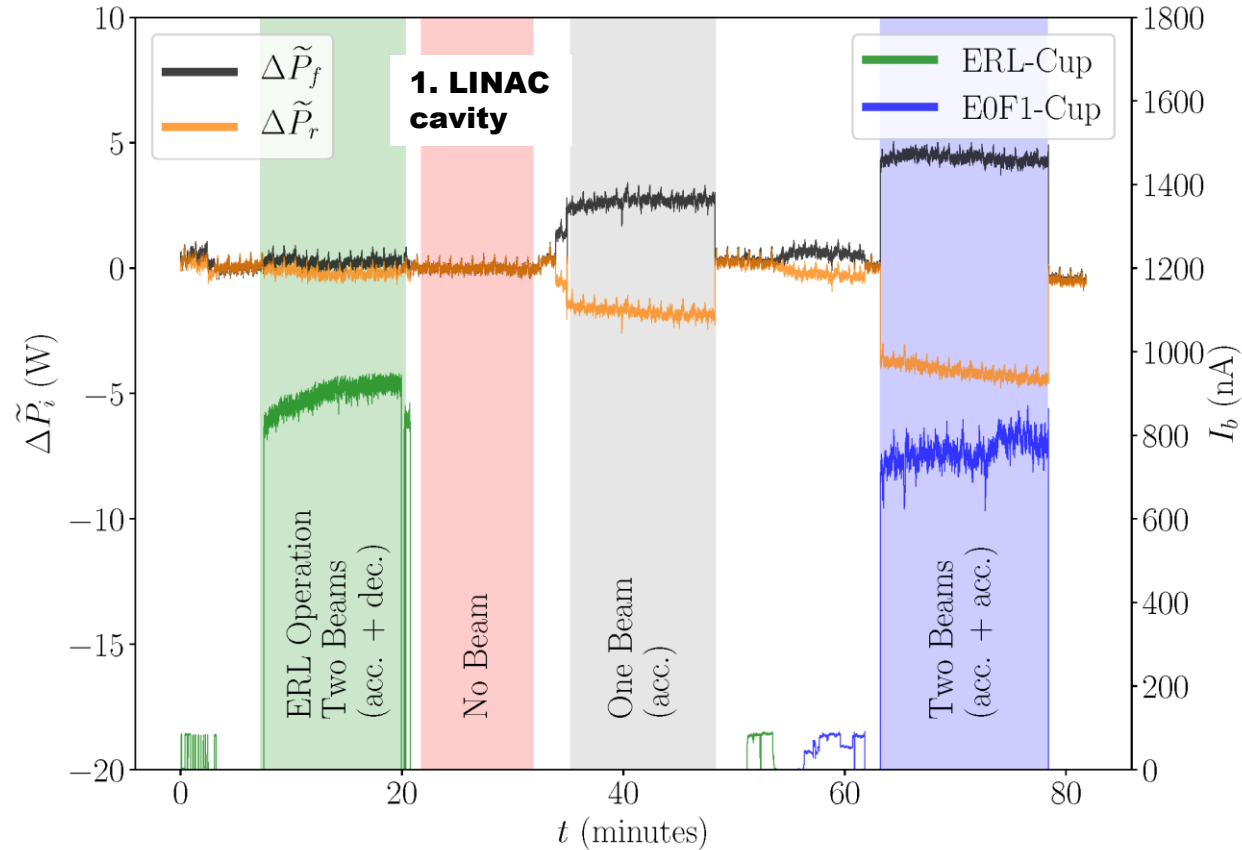


Data taken in four phases:

- Phase 1 (ERL Operation): one accelerated and one decelerated beam
- Phase 2 (no beam): RF operation of cavity without beam
- Phase 3 (1x acc.): one accelerated beam
- Phase 4 (2x acc.): two accelerated beams

„Cavity beam-load“

difference between
forward RF power
and reflected power



1st ERL in Germany,
August 2017



M. Arnold et al.,
First operation of the superconducting Darmstadt linear electron accelerator as an energy recovery linac, *Phys. Rev. Accel. Beams* **23**, 020101 (2020).

Operation	Mean Beam Power in W
No Beam	0.00 ± 0.01
One Beam (acc.)	4.51 ± 0.16
Two Beams (acc. + acc.)	8.59 ± 0.01
ERL (acc. + dec.)	0.45 ± 0.03

RF-recovery effect:

$$\epsilon_{RF} = (90.1 \pm 0.3)\%$$

Value and uncertainty take correlations between fit parameters into account.

8.59 W: about 10% less than 2×4.51 W

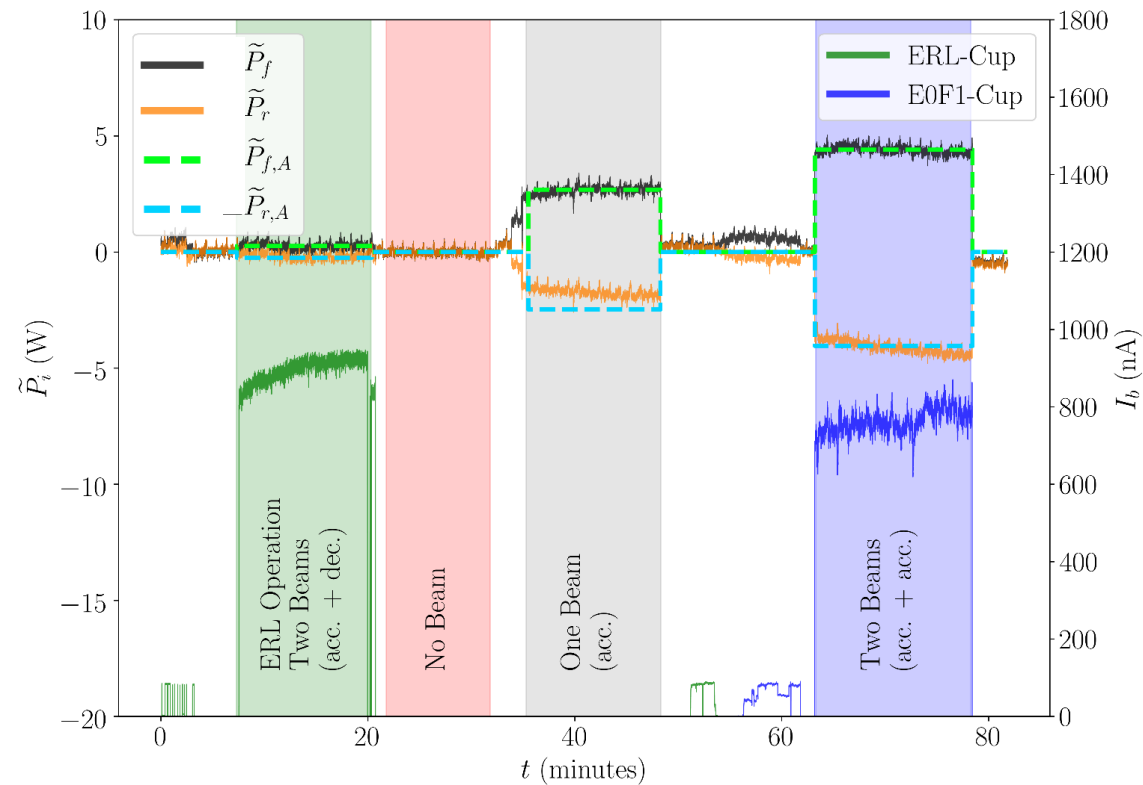
Incomplete transmission due to abstaining from beamline optimization

M. Arnold et al., First operation of the superconducting Darmstadt linear electron accelerator as an energy recovery linac, Phys. Rev. Accel. Beams 23, 020101 (2020).

ANALYTICAL MODEL

$$P_f = P_0 \frac{[\beta_{input} + (1 + \beta_{output} + \beta_{beam})]^2}{4\beta_{input}}$$

$$P_r = P_0 \frac{[\beta_{in} - (1 + \beta_{output} + \beta_{beam})]^2}{4\beta_{input}}$$

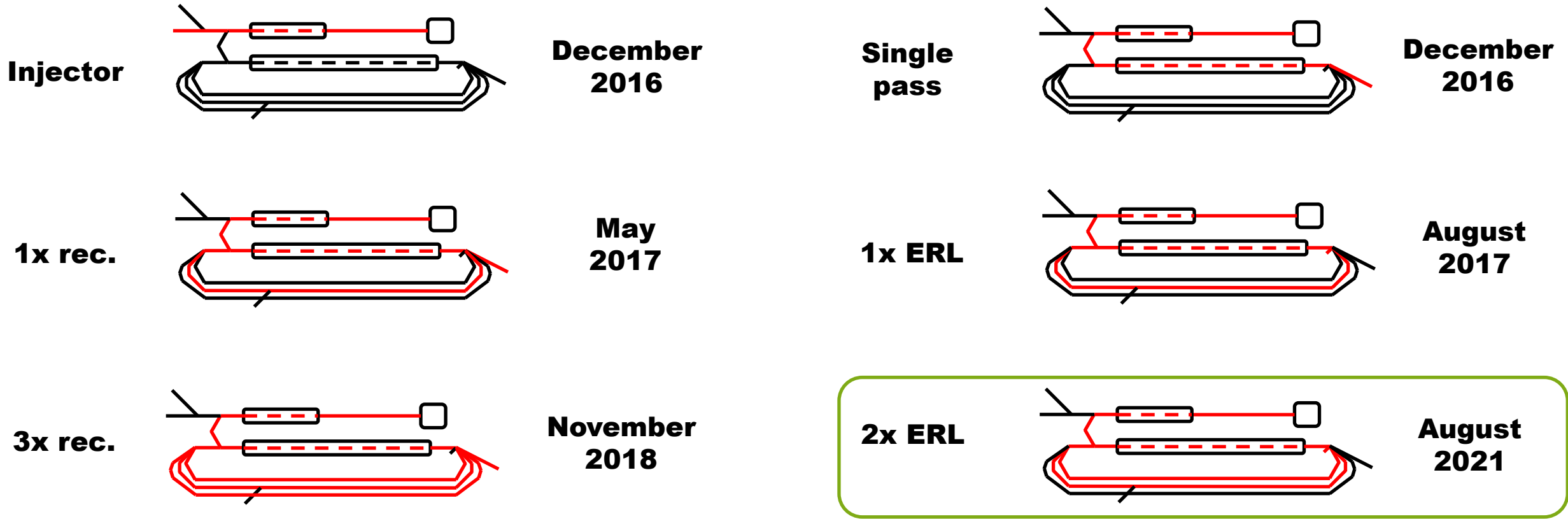


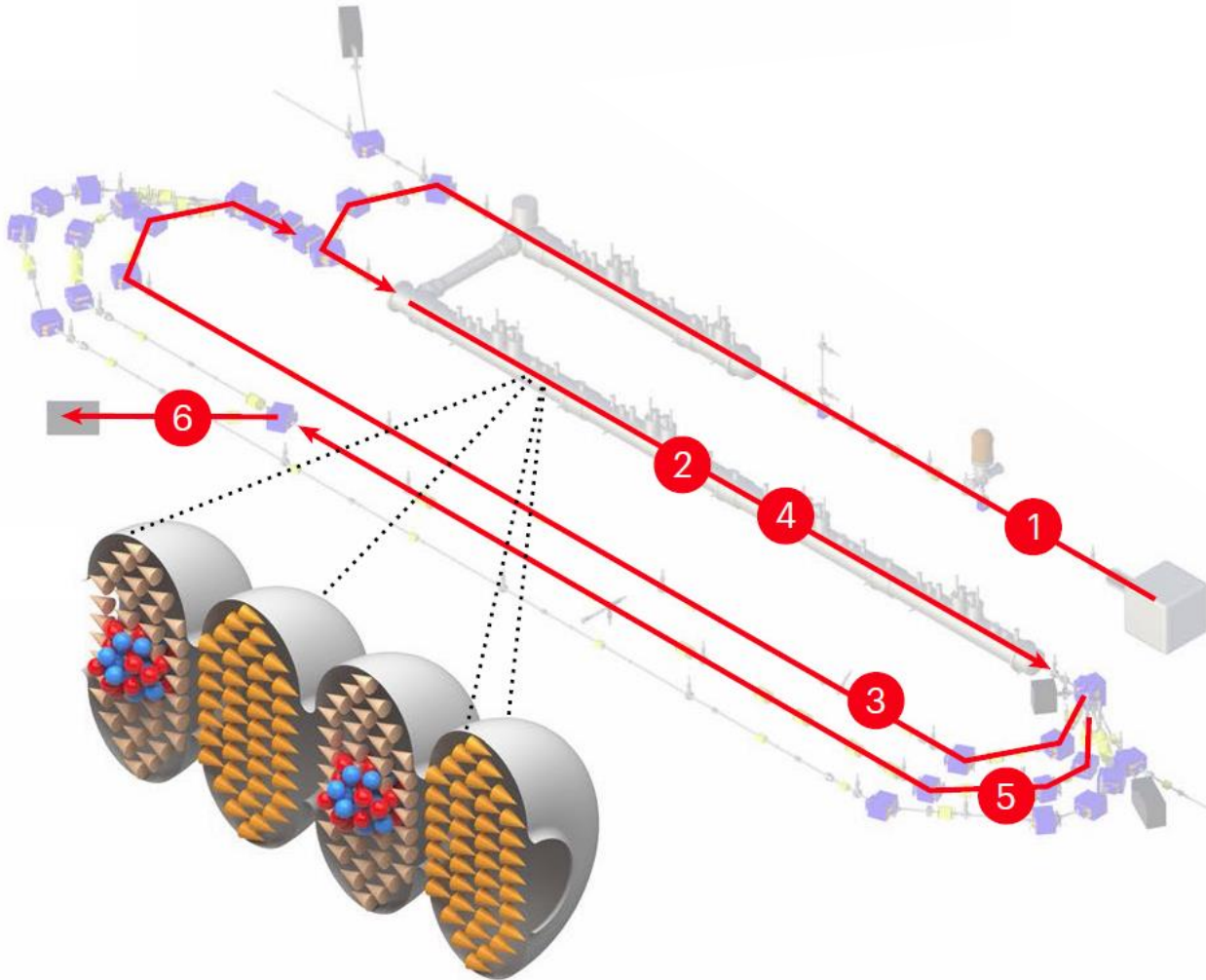
- Curve-fitting to data in P_f
 - $\beta_{beam}=0$: to obtain β_{input} , β_{output} and P_0
 - $\beta_{beam} \neq 0$: to obtain $\beta_{beam,i}$ for each phase i
- Analytical prediction of P_r

M. Arnold et al., *First operation of the superconducting Darmstadt linear electron accelerator as an energy recovery linac*, *Phys. Rev. Accel. Beams* **23**, 020101 (2020).

OVERVIEW OPERATION MODES/COMMISSIONING

- Modification lattice 2015/2016
- Commissioning of modes followed beam time schedule



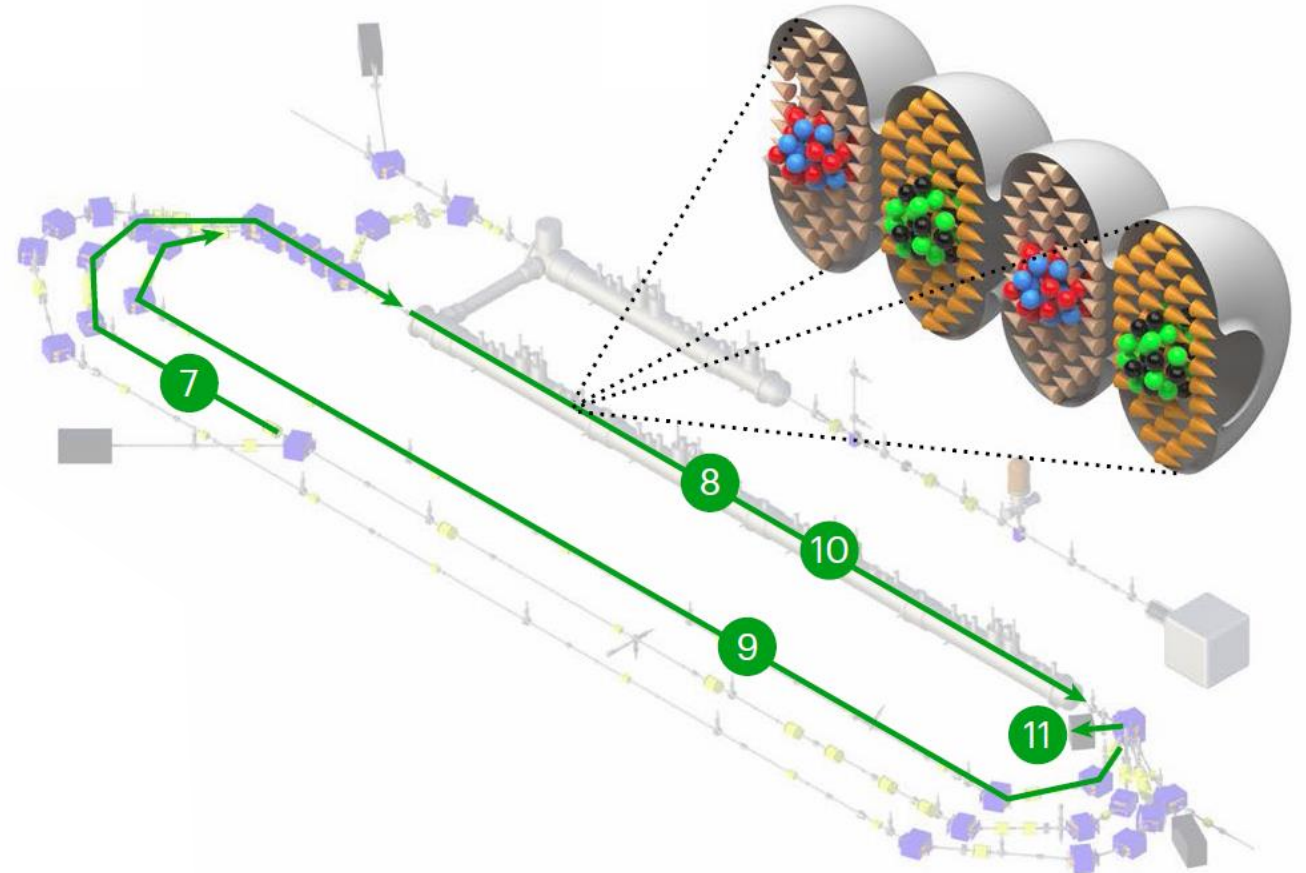


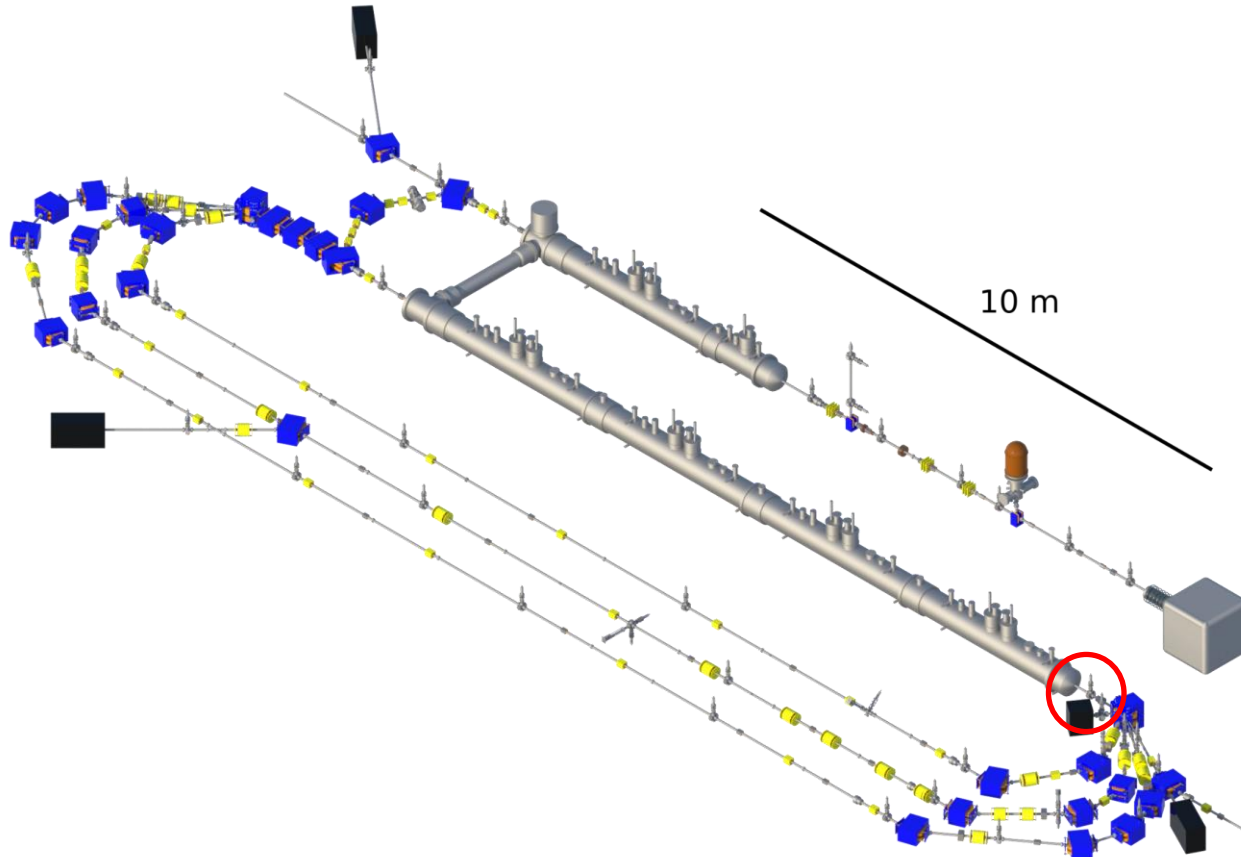
Conventional two-fold Acceleration (CTA)

(1)	Injection	5.00 MeV/c
(2)	1 st acceleration	23.66 MeV/c
(3)	1 st recirculation	0° phase shift
(4)	2 nd acceleration	41.61 MeV/c
(5)	2 nd recirculation	0° phase shift
(6)	Beam dump	

Two-fold Energy Recovery (TER)

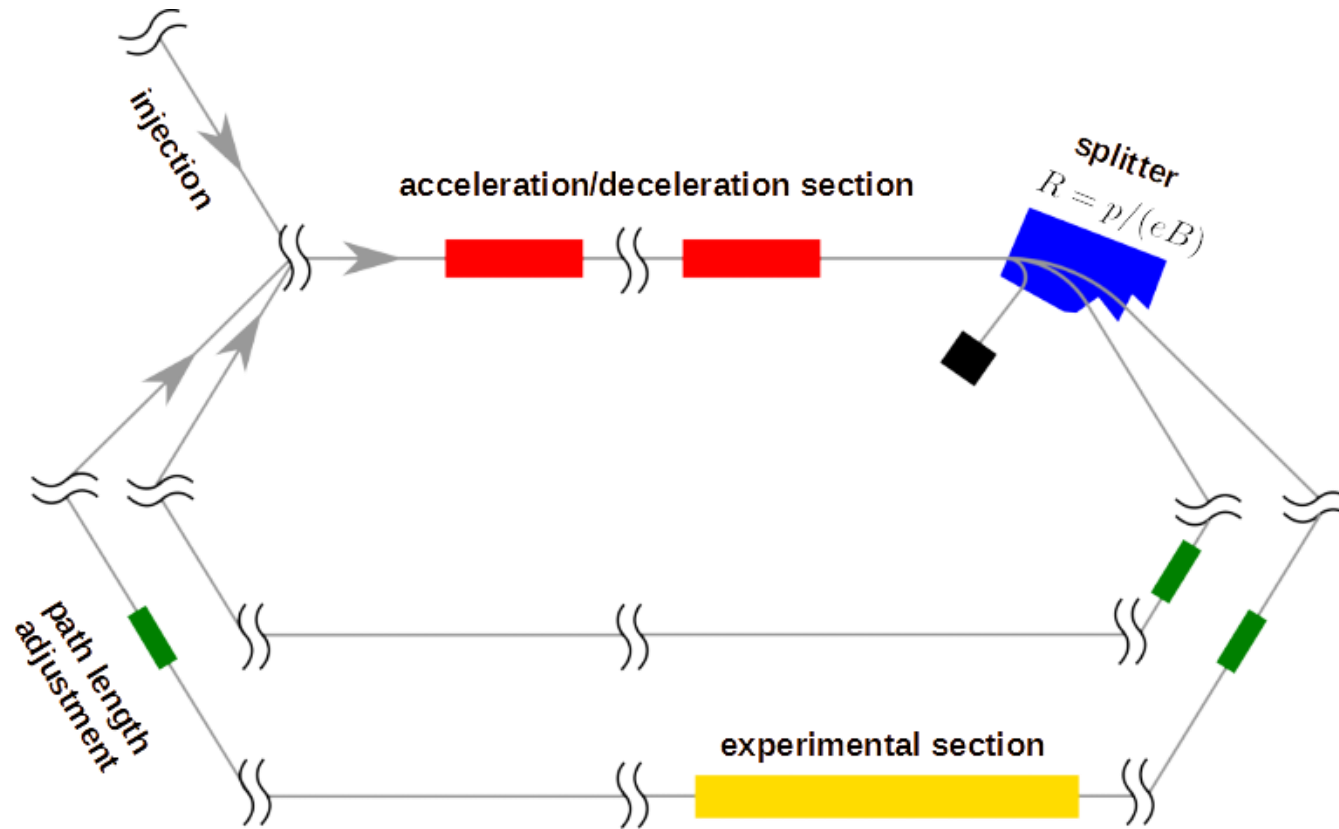
(1) – (6)	As before	41.61 MeV/c
(7)	2 nd recirculation	180° phase shift
(8)	1 st deceleration	23.66 MeV/c
(9)	3 rd recirculation	0° phase shift
(10)	2 nd deceleration	5 MeV/c
(11)	Low energy beam dump	





- Eight accelerating cavities
- Two recirculation arcs
- Degrees of freedom:
 - Amplitudes \vec{A}
 - Phases $\vec{\phi}$
 - Path lengths \vec{L}
 - Longitudinal dispersions \vec{R}_{56}

MULTI-TURN ERL MODE OF THE S-DALINAC | CHALLENGES

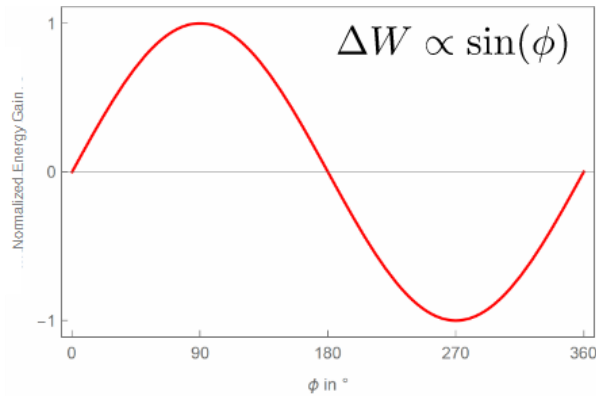


Objective functions result from
splitter magnet ratio:
 $p_I : p_F : p_S = 1 : 4.7 : 8.3$

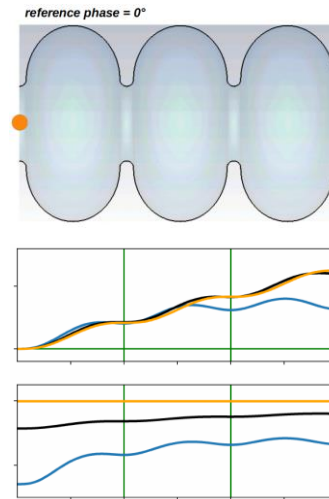
Degrees of freedom:
 $\vec{A}, \vec{\phi}, \vec{L}, \vec{R}_{56}$

Concept based on: R. Koscica et al., *Phys. Rev. Accel. Beams* **22**, 091602 (2019)

Simplified model of energy gain



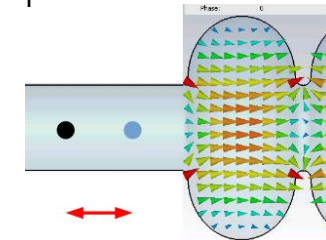
More complex model of energy gain



Speed changes along the cavity

→ Impacts interaction with alternating electric field

→ Numerical simulations required



- Phase slippage not negligible
- Simplified model of energy gain not applicable
- Numerical simulations of interaction between electrons and EM fields required

LONGITUDINAL TARGETS AND DEGREES OF FREEDOM

$$\begin{pmatrix} \bar{p}_{1x \text{ acc.}} \\ \bar{p}_{2x \text{ acc.}} \\ \bar{p}_{1x \text{ dec.}} \\ \bar{p}_{2x \text{ dec.}} \end{pmatrix} = \begin{pmatrix} 4.73 \cdot \bar{p}_{\text{inj.}} \\ 8.32 \cdot \bar{p}_{\text{inj.}} \\ 4.73 \cdot \bar{p}_{\text{inj.}} \\ 1.00 \cdot \bar{p}_{\text{inj.}} \end{pmatrix} \quad \bar{p}_{\text{inj.}} = 5 \text{ MeV}/c$$

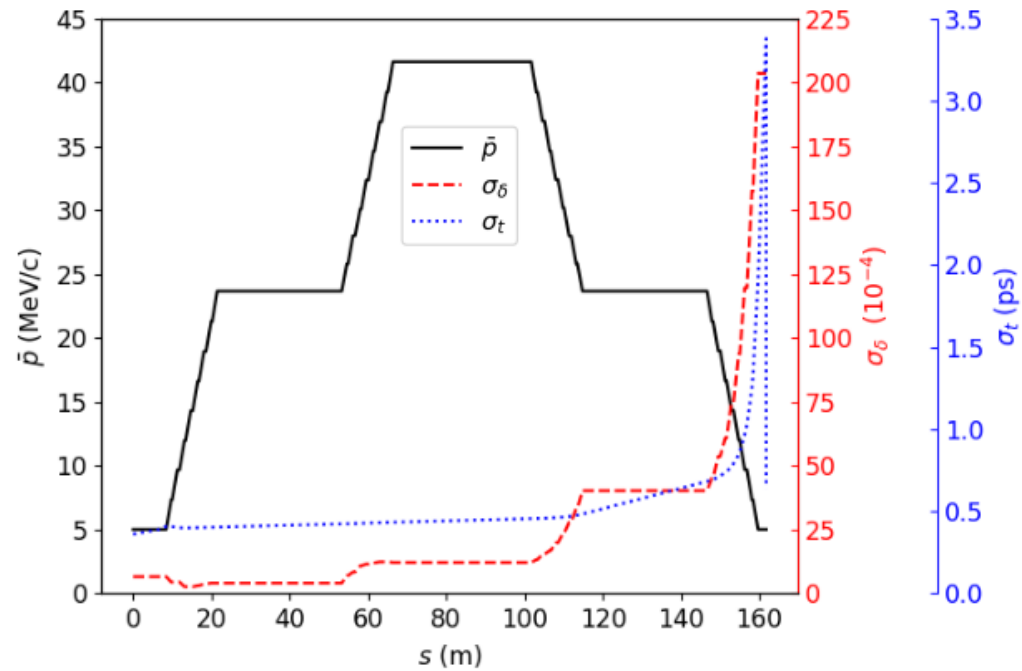
$$\begin{pmatrix} \bar{p}_{1x \text{ acc.}} \\ \bar{p}_{2x \text{ acc.}} \\ \bar{p}_{1x \text{ dec.}} \\ \bar{p}_{2x \text{ dec.}} \end{pmatrix} = \begin{pmatrix} 4.73 \cdot \bar{p}_{\text{inj.}} \\ 8.32 \cdot \bar{p}_{\text{inj.}} \\ 4.73 \cdot \bar{p}_{\text{inj.}} \\ 1.00 \cdot \bar{p}_{\text{inj.}} \end{pmatrix} \quad \bar{p}_{\text{inj.}} = 5 \text{ MeV}/c$$

$$\min \left\| \begin{pmatrix} \text{sene}(\bar{p}_{0,1x \text{ acc.}}, 4.73 \cdot p_{\text{inj.}}, T) \\ \text{sene}(\bar{p}_{0,2x \text{ acc.}}, 8.32 \cdot p_{\text{inj.}}, T) \\ \text{sene}(\bar{p}_{0,1x \text{ dec.}}, 4.73 \cdot p_{\text{inj.}}, T) \\ \text{sene}(\bar{p}_{0,2x \text{ dec.}}, 1.00 \cdot p_{\text{inj.}}, T) \end{pmatrix} \right\|_{1^*} \quad \text{s.t.} \quad \begin{cases} A_i \in [0, 5] \text{ MV/m } \forall i \in \{1, \dots, 8\} \\ \phi_i \in [0, 360)^\circ \forall i \in \{1, \dots, 8\} \\ L_1 \in [0, 74.0] \text{ mm} \\ L_2 \in [0, 101.2] \text{ mm} \end{cases} \quad \|\vec{x}\|_{1^*} := \sum_i x_i$$

$$\text{sene}(V_1, V_2, T) = \begin{cases} 0, & |V_1 - V_2| \leq T \\ ((|V_1 - V_2| - T)/T)^2, & |V_1 - V_2| > T \end{cases} \quad T = 1 \text{ eV}/c$$

SOLUTION FOR LONGITUDINAL QUANTITIES

$$\min \|\dots\|_{1^*}$$



$$\begin{pmatrix} \bar{p}_{1x \text{ acc.}} \\ \bar{p}_{2x \text{ acc.}} \\ \bar{p}_{1x \text{ dec.}} \\ \bar{p}_{2x \text{ dec.}} \end{pmatrix} = \begin{pmatrix} 4.73 \cdot \bar{p}_{\text{inj.}} \\ 8.32 \cdot \bar{p}_{\text{inj.}} \\ 4.73 \cdot \bar{p}_{\text{inj.}} \\ 1.00 \cdot \bar{p}_{\text{inj.}} \end{pmatrix} \quad \bar{p}_{\text{inj.}} = 5 \text{ MeV}/c$$

$$\min \left\| \begin{pmatrix} \text{sene}(\bar{p}_{0,1x \text{ acc.}}, 4.73 \cdot p_{\text{inj.}}, T) \\ \text{sene}(\bar{p}_{0,2x \text{ acc.}}, 8.32 \cdot p_{\text{inj.}}, T) \\ \text{sene}(\bar{p}_{0,1x \text{ dec.}}, 4.73 \cdot p_{\text{inj.}}, T) \\ \text{sene}(\bar{p}_{0,2x \text{ dec.}}, 1.00 \cdot p_{\text{inj.}}, T) \end{pmatrix} \right\|_{1^*} \quad \text{s.t.} \quad \begin{cases} A_i \in [0, 5] \text{ MV/m } \forall i \in \{1, \dots, 8\} \\ \phi_i \in [0, 360)^\circ \forall i \in \{1, \dots, 8\} \\ L_1 \in [0, 74.0] \text{ mm} \\ L_2 \in [0, 101.2] \text{ mm} \end{cases} \quad \|\vec{x}\|_{1^*} := \sum_i x_i$$

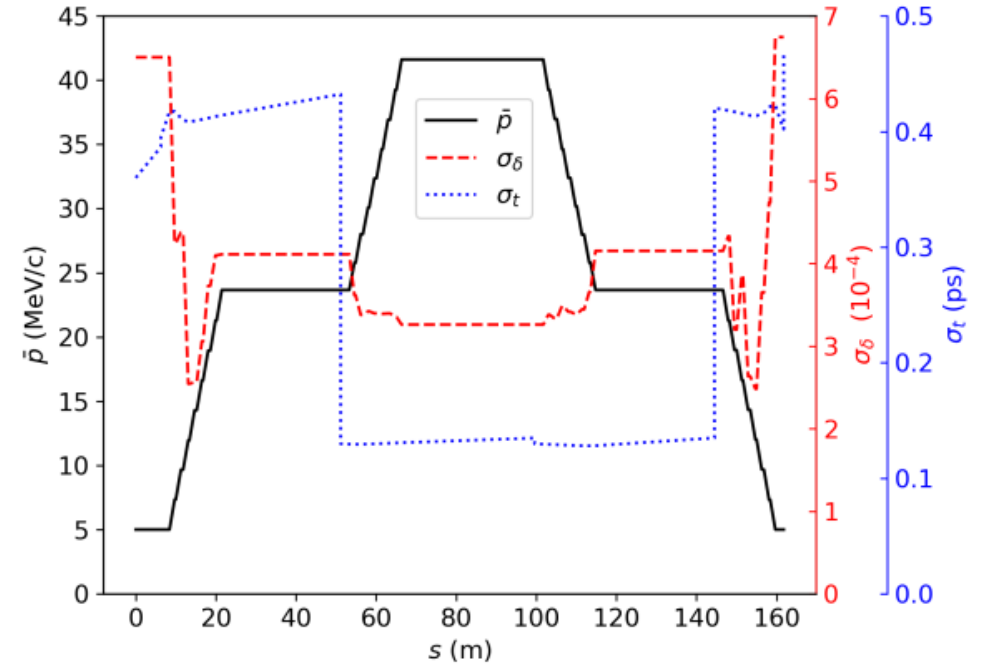
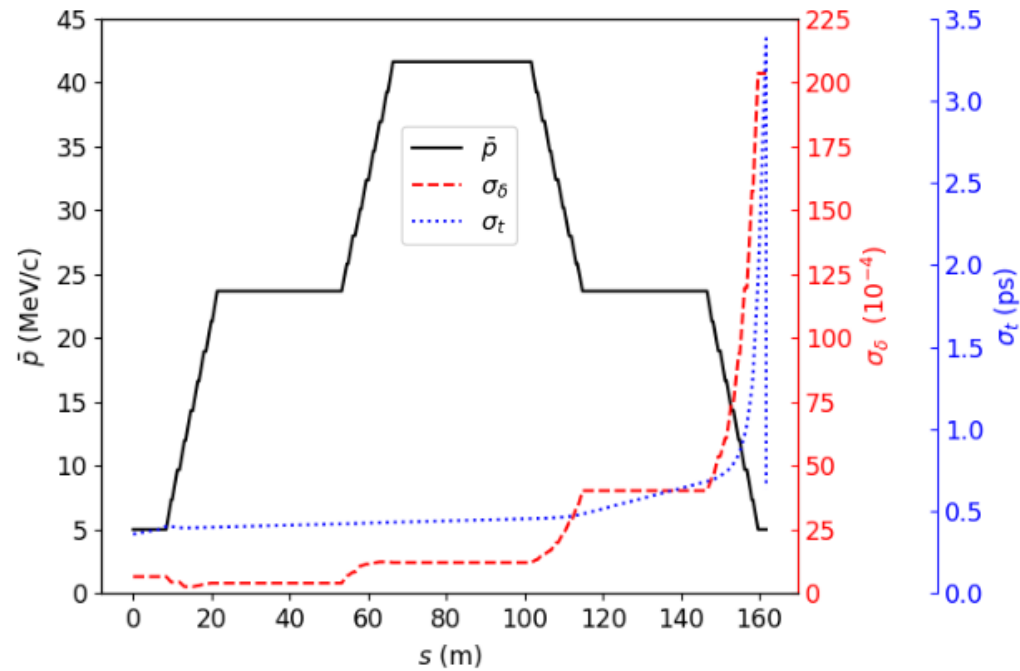
$$\text{sene}(V_1, V_2, T) = \begin{cases} 0, & |V_1 - V_2| \leq T \\ ((|V_1 - V_2| - T)/T)^2, & |V_1 - V_2| > T \end{cases} \quad T = 1 \text{ eV}/c$$

$$\min \sigma_\delta(s) \quad \text{s.t.} \quad \begin{cases} R_{56,I} \in [-0.7, 0.4] \text{ m} \\ R_{56,F} \in [-0.1, 0.8] \text{ m} \\ R_{56,S} \in [-0.7, 0.7] \text{ m} \end{cases}$$

SOLUTION FOR LONGITUDINAL QUANTITIES

$$\min \|\dots\|_{1^*}$$

$$\min \|\dots\|_{1^*} \quad \text{and} \quad \min \sigma_\delta(s)$$



LONGITUDINAL SETUP

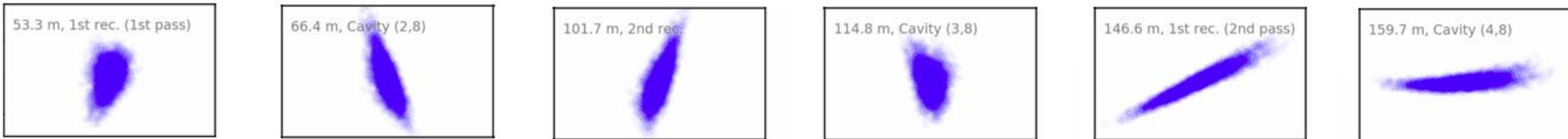
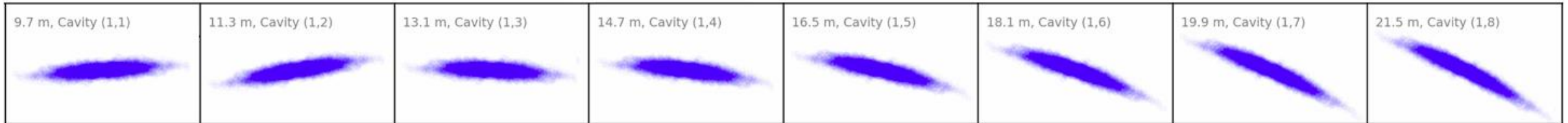
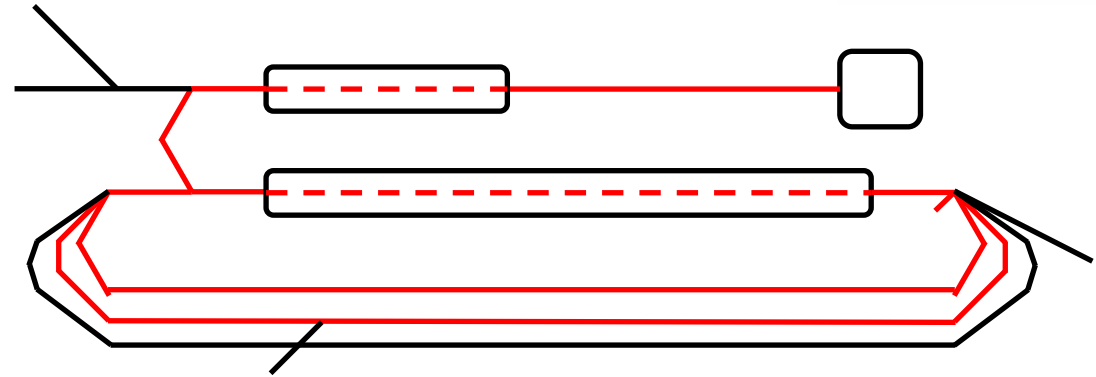
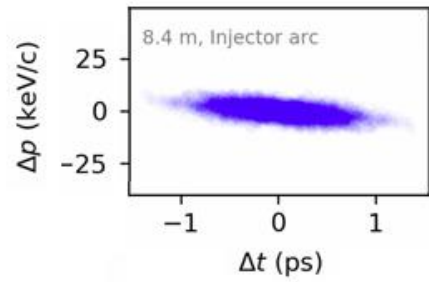
LINAC Cavity	#1	#2	#3	#4	#5	#6	#7	#8
Off-crest phase (°) (during 1st LINAC pass)	-9.7	-5.7	13.2	4.0	6.1	7.2	5.6	3.2
Off-crest momentum gain (MeV/c) (during 1st LINAC pass)	2.34	2.32	2.29	2.34	2.33	2.33	2.35	2.36
On-crest momentum gain (MeV/c) (during 1st LINAC pass)	2.37	2.33	2.35	2.35	2.34	2.34	2.36	2.37

$$R_{56,I} = -0.01 \text{ m}$$

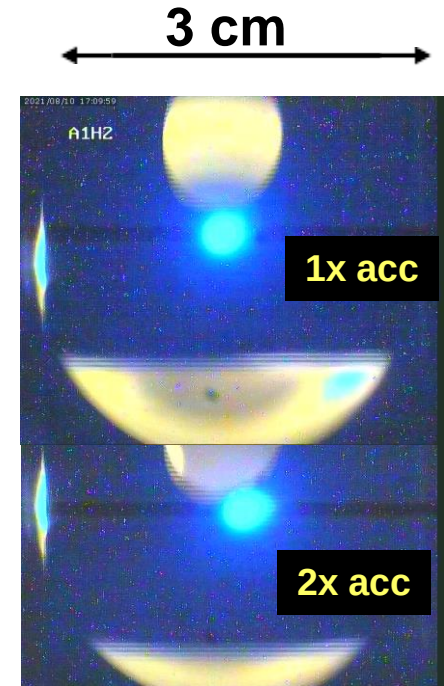
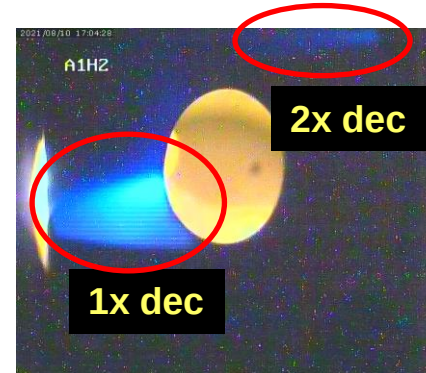
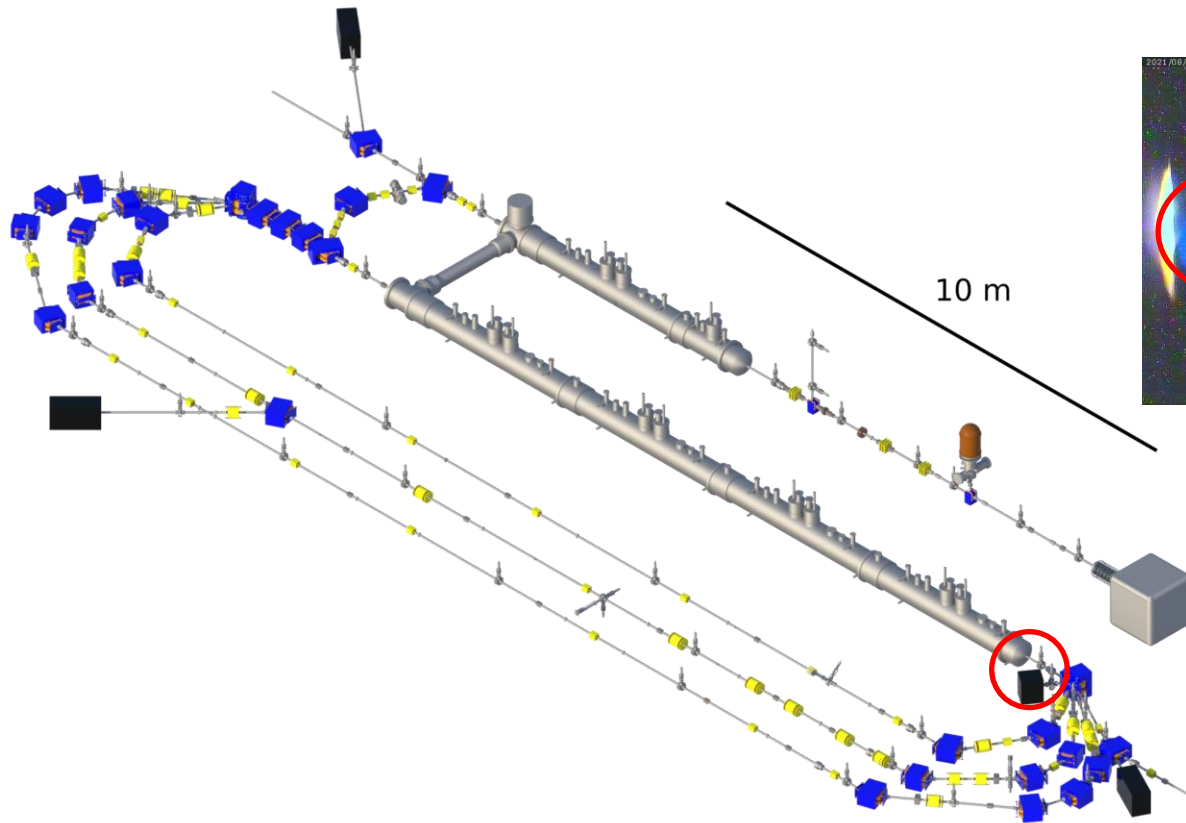
$$R_{56,F} = +0.33 \text{ m}$$

$$R_{56,S} = +0.18 \text{ m}$$

LONGITUDINAL PHASE SPACE



MULTI-TURN ERL MODE OF THE S-DALINAC | CHALLENGES



- Limits of transverse beam tuning

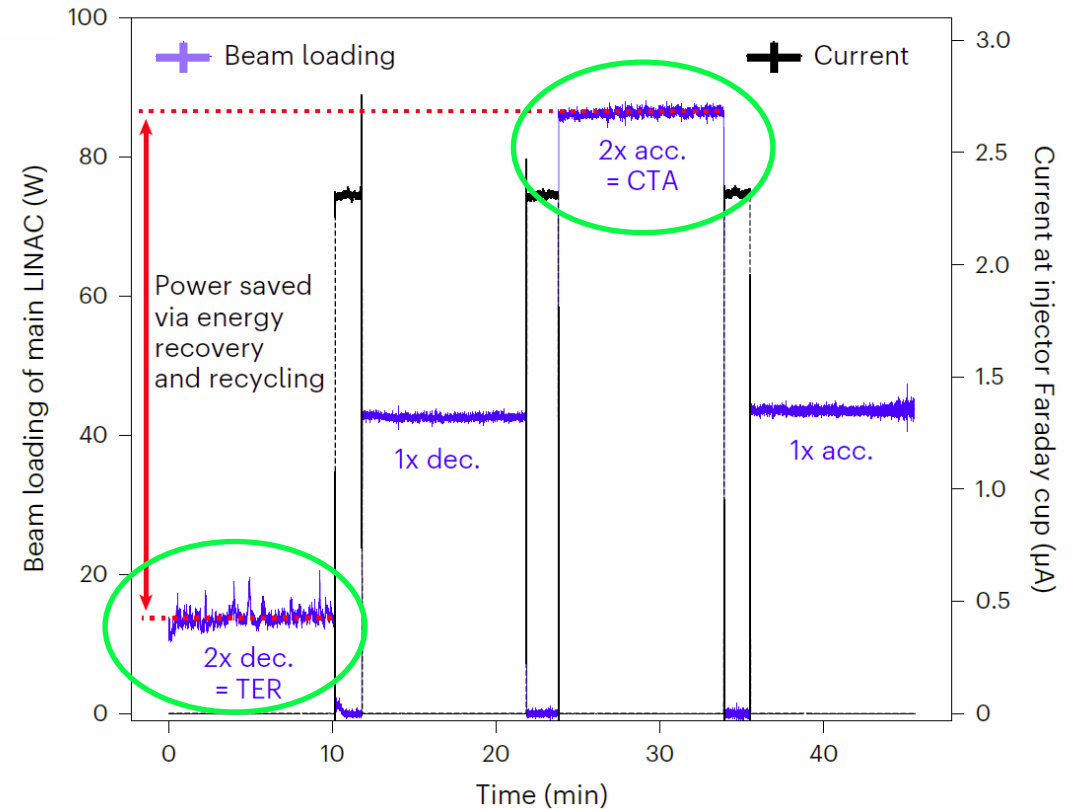
- Measurement of beam loadings of two-fold acceleration $P_{b,CTA}$ and two-fold ERL $P_{b,TER}$
- Energy recovery efficiency is then given by

$$\eta = \frac{P_{b,CTA} - P_{b,TER}}{P_{b,CTA}}$$

- Stable operation with a beam current of 2.3 μA :

Mode	Beam loading
CTA	$86.3 \pm 0.3 \text{ W}$
TER	$13.8 \pm 1.1 \text{ W}$

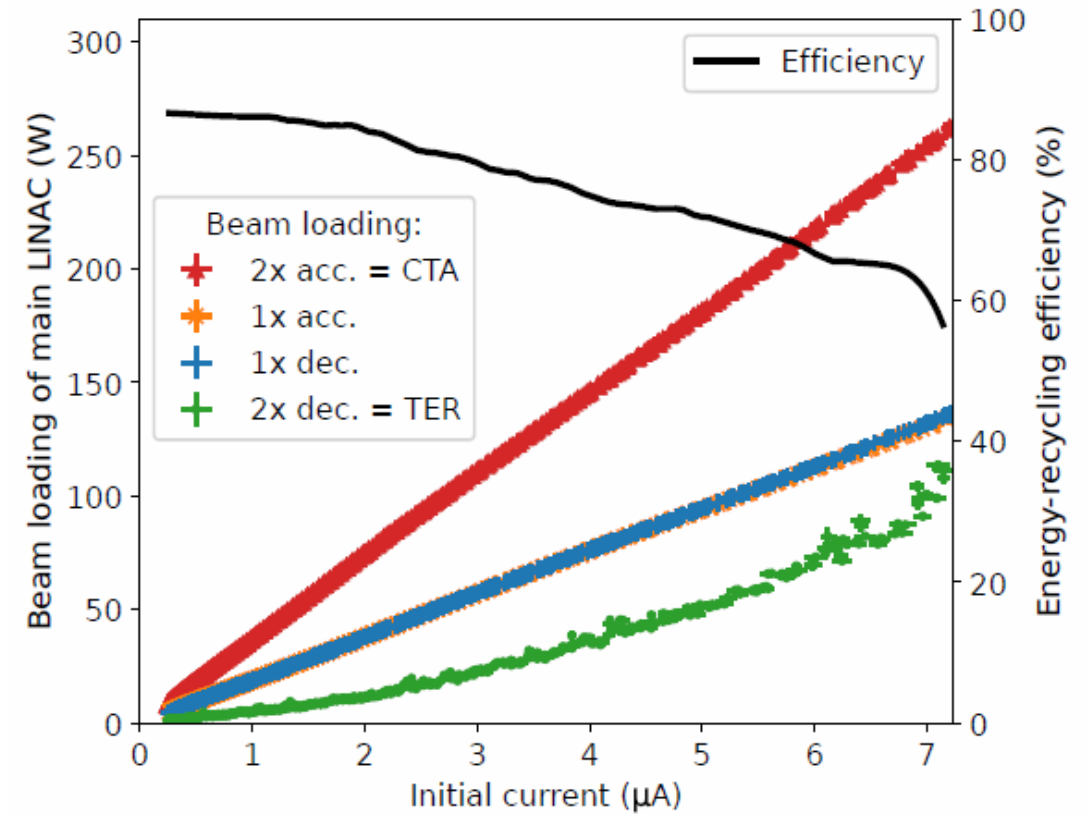
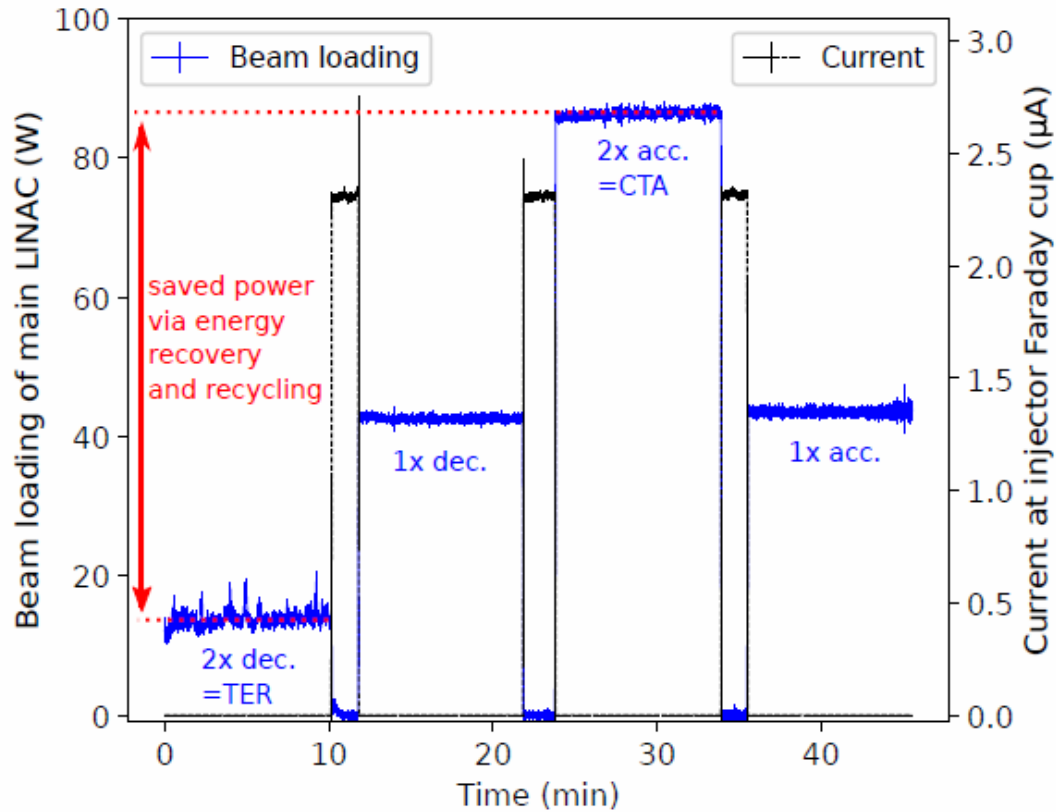
➤ $\eta = 84.0 \pm 1.2\%$



F. Schliessmann *et al.* Realization of a multi-turn energy recovery accelerator. *Nat. Phys.* **19**, 597 (2023).

<https://doi.org/10.1038/s41567-022-01856-w>

TWOFOLD ERL MODE (AUGUST 2021)

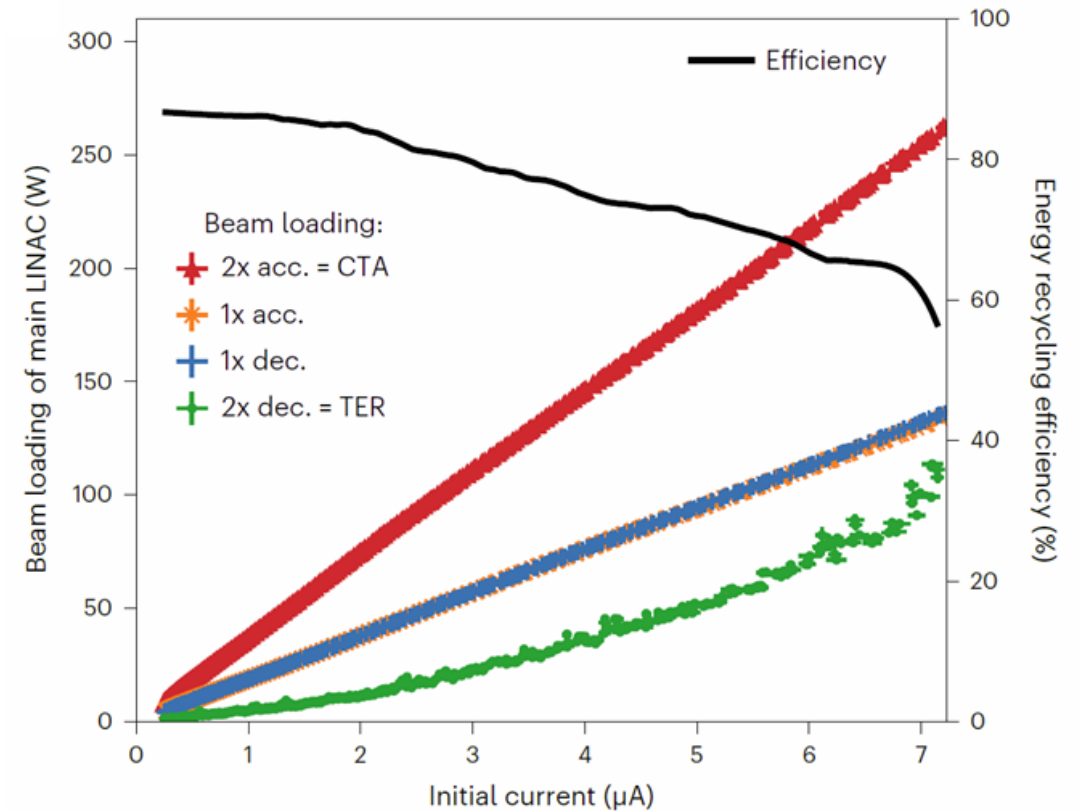


F. Schliessmann *et al.* Realization of a multi-turn energy recovery accelerator. *Nat. Phys.* **19**, 597 (2023).

<https://doi.org/10.1038/s41567-022-01856-w>

MULTI-TURN ERL MODE OF THE S-DALINAC | RECOVERY EFFICIENCY

- Beam loading measured for initial (injection) beam currents from 0.2 to above 7 μA
- Recovery efficiency **up to 87 %** for low currents
- 1x acc. and TER beam in *shared* beam pipe
 - Increase in transverse emittance
 - TER beam not fully kept in acceptance
- Efficiency decreasing with higher currents
- Extended measurements of beam properties as a function of beam intensity planned
- *individual* beam transport for future ERL accelerators under investigation

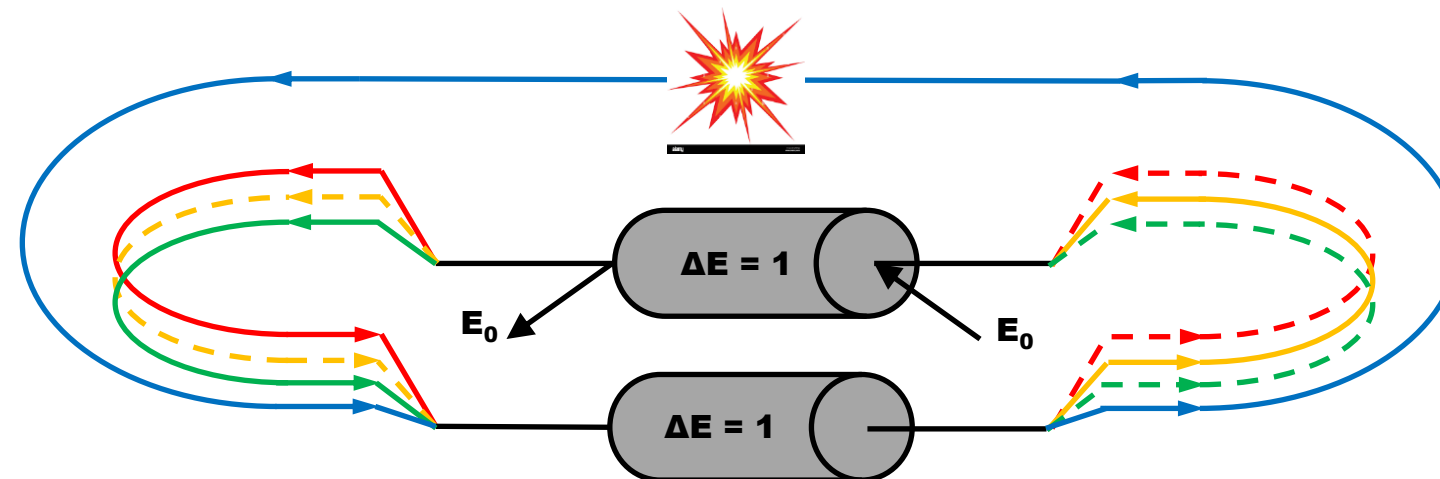


F. Schliessmann et al. *Nat. Phys.* (2023)

ERL – Applications

An ERL is the optimum collider

- best possible emittance
- high beam current with low beam load
- faint target => high beam current to be recovered

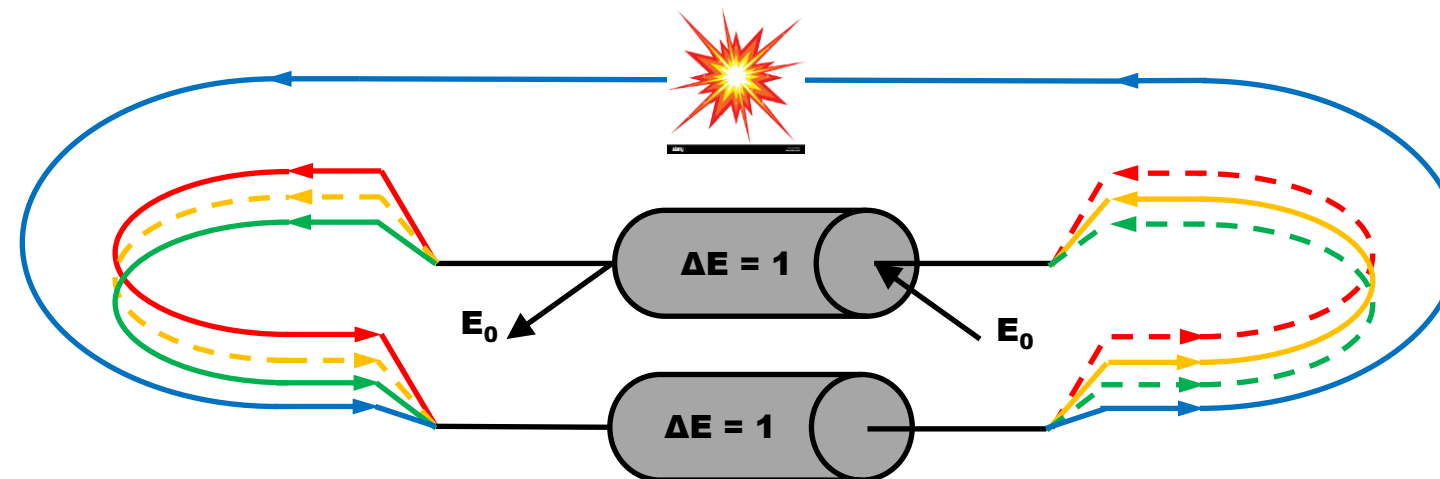


ERL – Applications

An ERL is the optimum collider

- best possible emittance
- high beam current with low beam load
- faint target => high beam current to be recovered

e.g. Laser-Compton backscattering

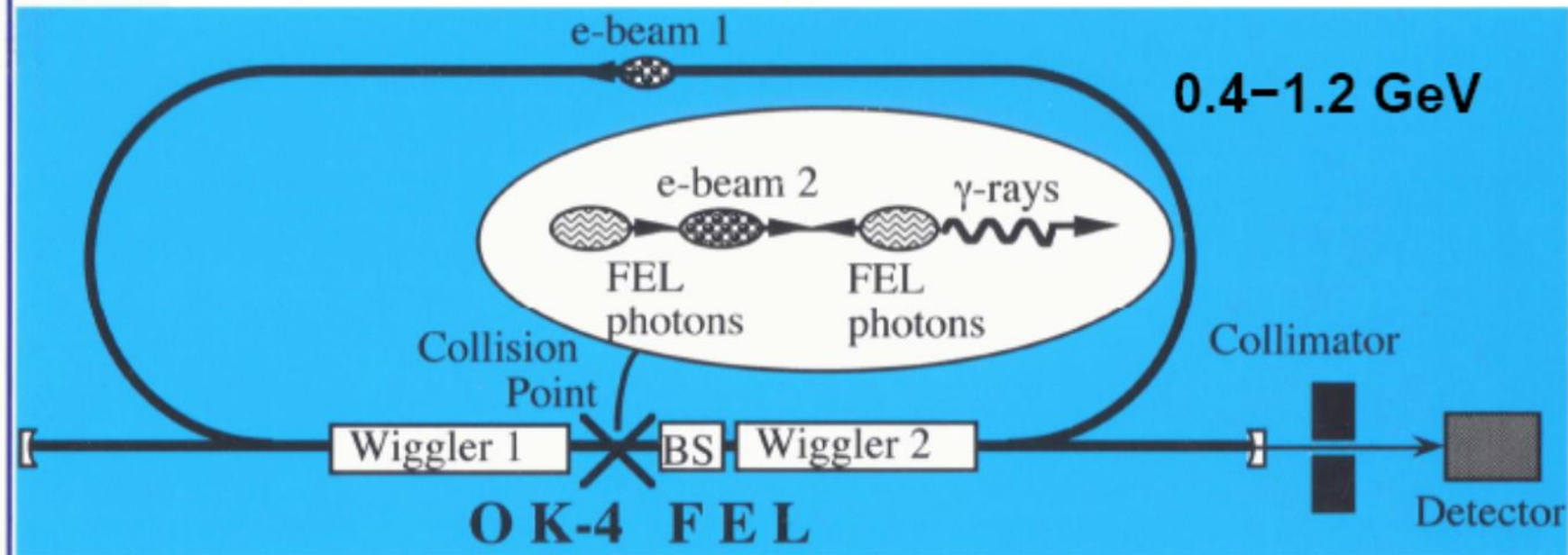


High Intensity γ -Ray Source (HlgS)



H.R.Weller, V.N.Litvinenko
Duke University, Durham, NC, U.S.A.

Compton Backscattering of Intra-cavity Laser Light



historic transparency
V.Litvinenko, ~ 2000

at the time with
OK-4
from Novosibirsk

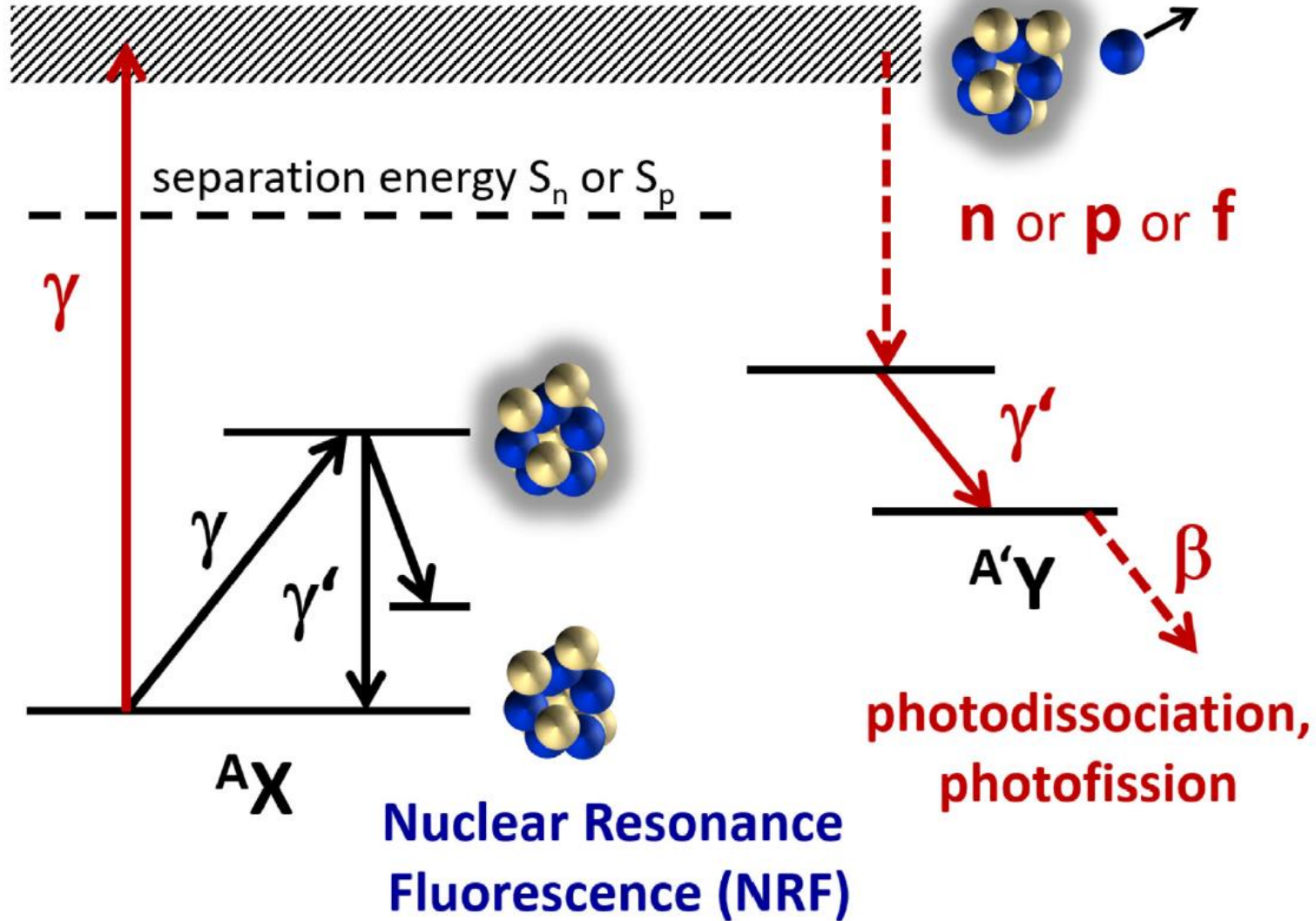
2 – 60 MeV

1.7 – 6.4 eV

~ 1000

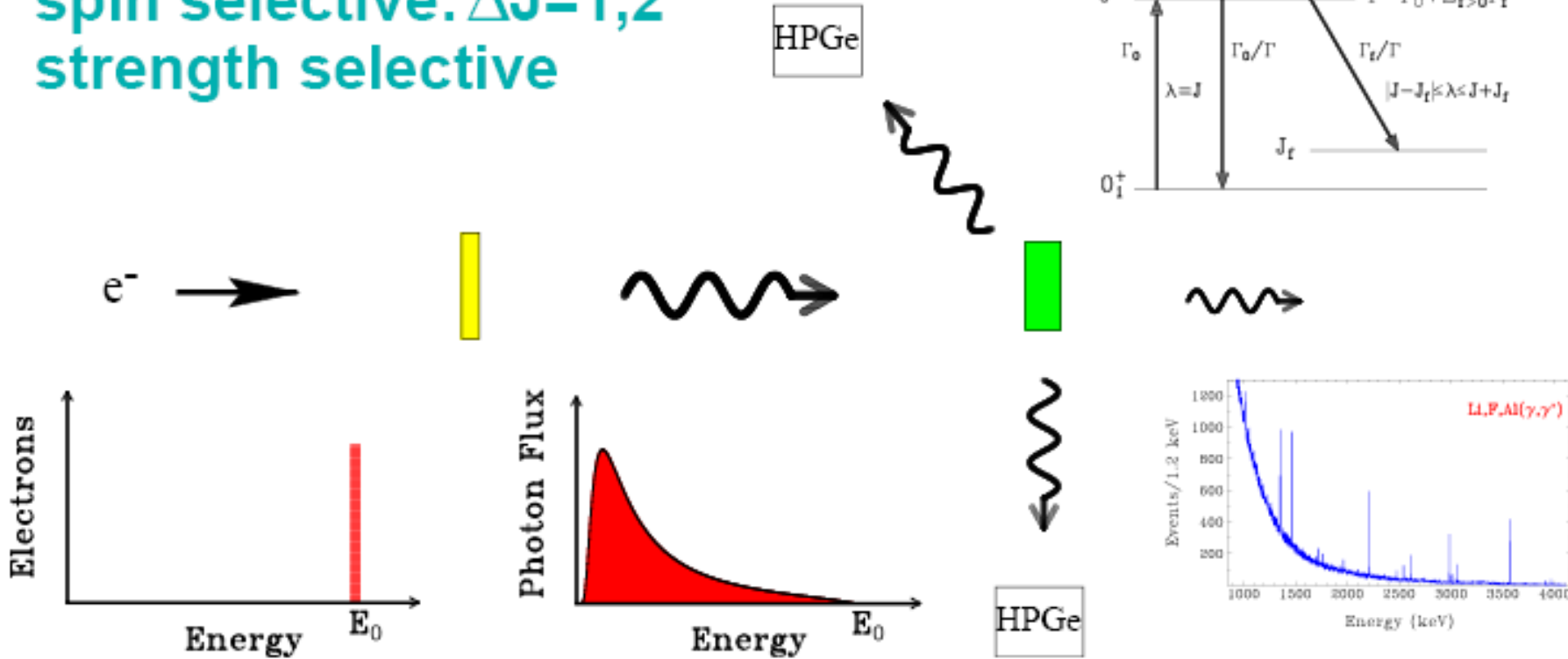
$$E_{\gamma} = \frac{4\gamma^2 E_{ph}}{(1+r+\gamma^2\theta^2)}; \quad r = \frac{4\gamma E_{ph}}{mc^2}; \quad E_{ph} = \frac{2\gamma^2 hc}{\lambda_w(1+K_w^2/2)}; \quad \gamma = \frac{E_e}{mc^2};$$

nearly monochromatic, tunable, completely polarized



Photon Scattering (Nuclear Resonance Fluorescence)

high energy resolution
spin selective: $\Delta J=1,2$
strength selective

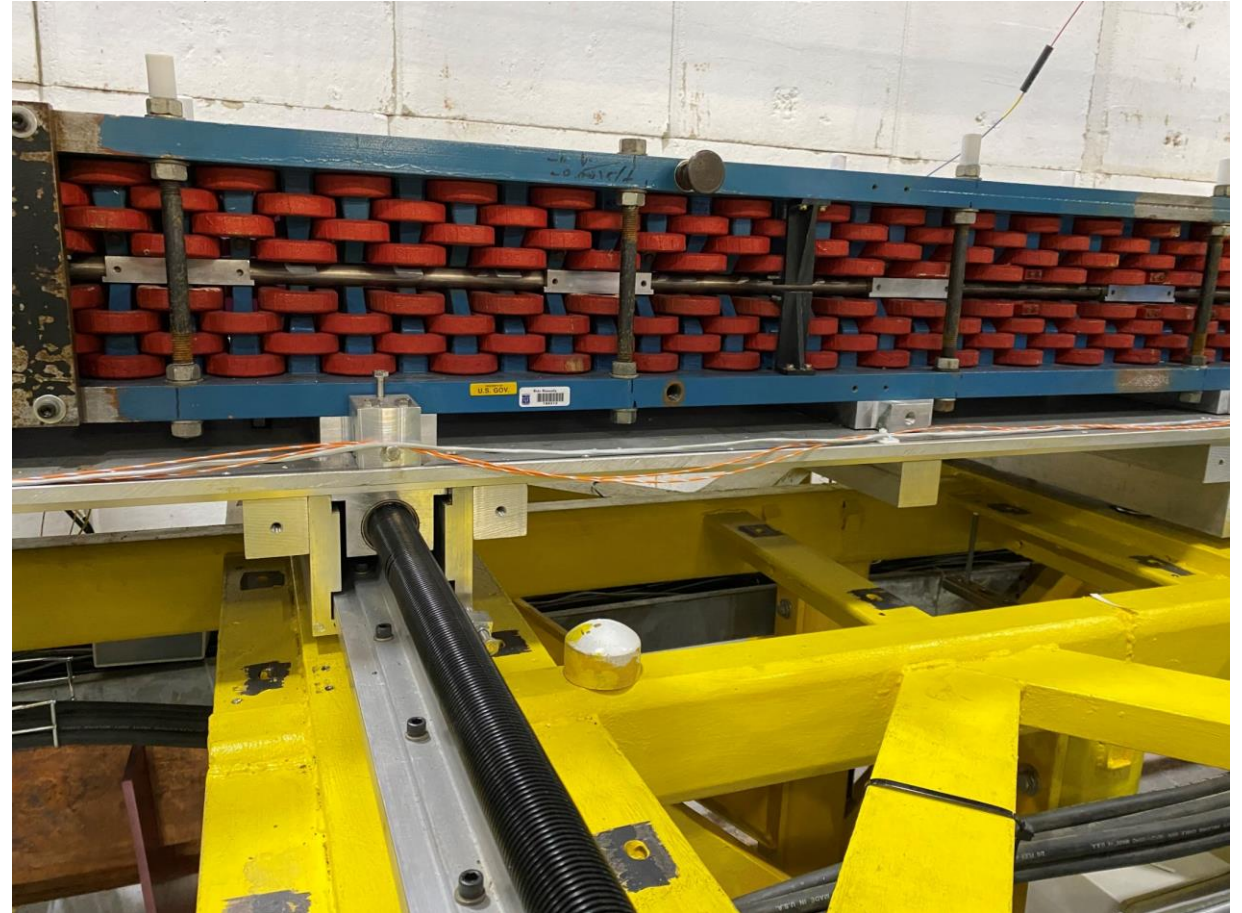
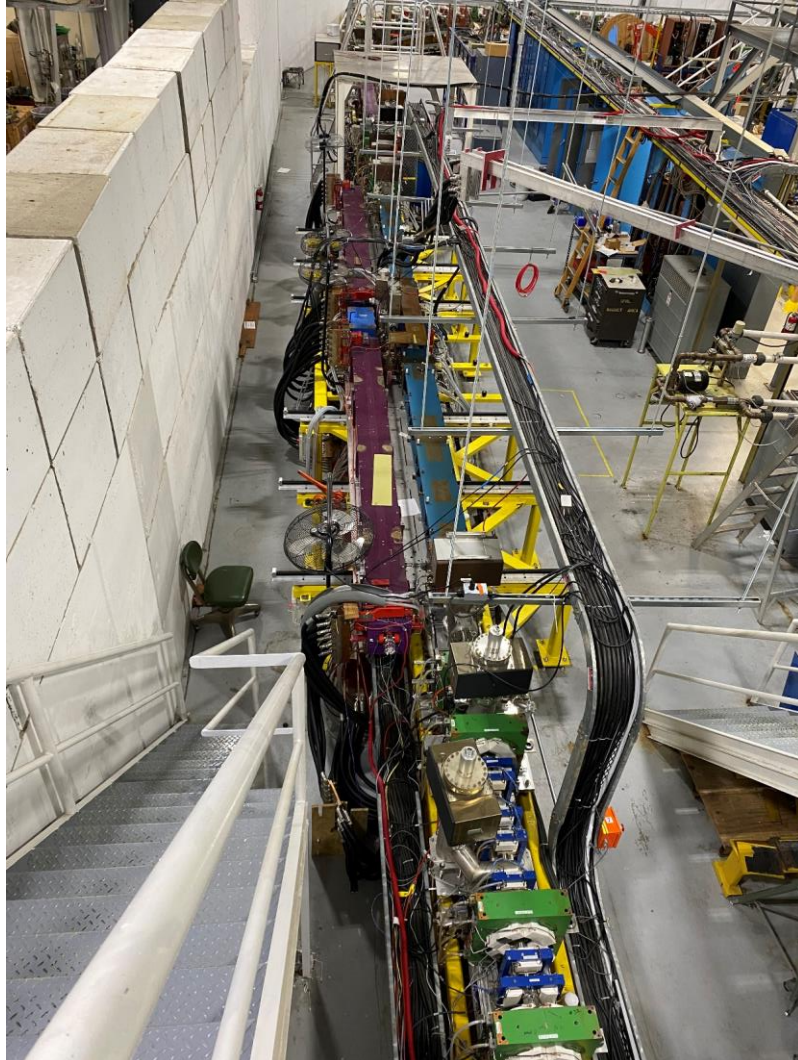


Observables

- Excitation Energy E_r
- Spin J
- Parity π
- Decay Energies E_γ
- Partial Widths Γ_i/Γ_0
- K-quantum numbers
- Multipole Mixing δ
- Decay Strengths $B(\pi\lambda)$
- Level Width Γ (eV)
- Lifetime τ (ps – as)

OVERVIEW ON MEV-RANGED GAMMA-RAY SOURCES – LASER-COMPTON BACKSCATTERING (LCB)

photos from Sept. 2023

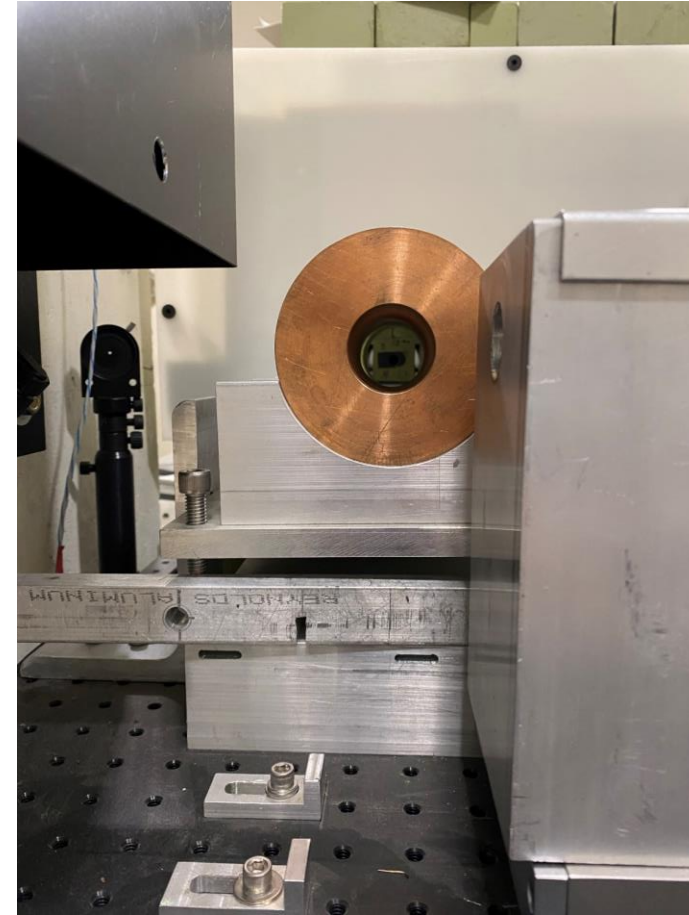


OK-5: this is a lamp!

OVERVIEW ON MEV-RANGED GAMMA-RAY SOURCES - LASER-COMPTON BACKSCATTERING (LCB)

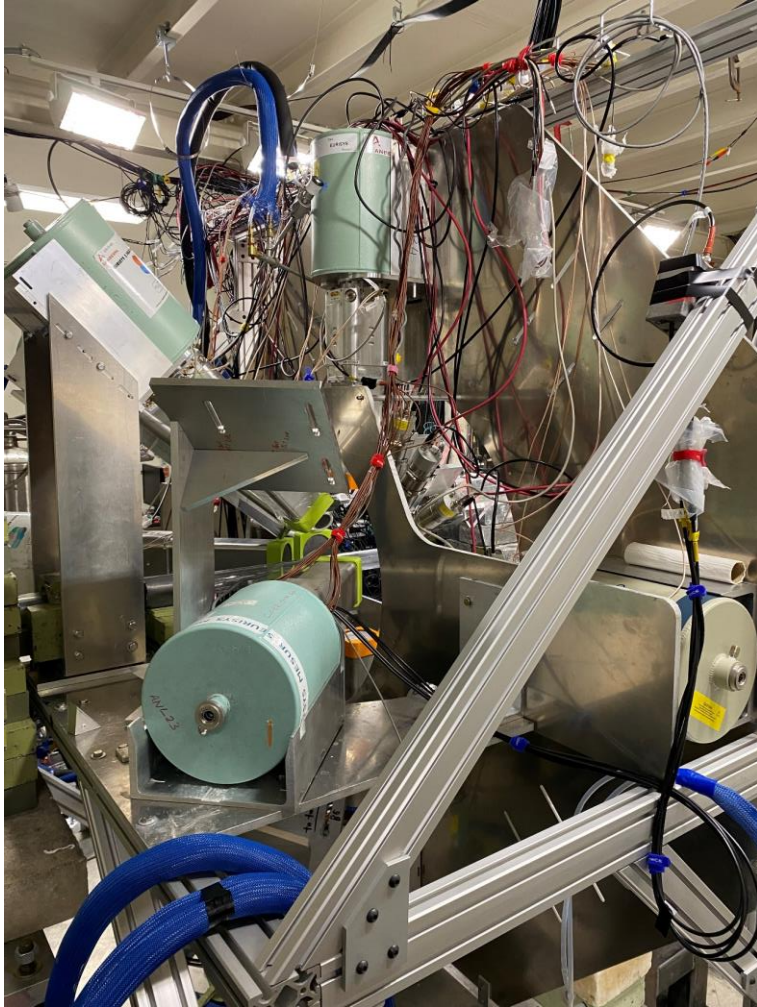


TECHNISCHE
UNIVERSITÄT
DARMSTADT



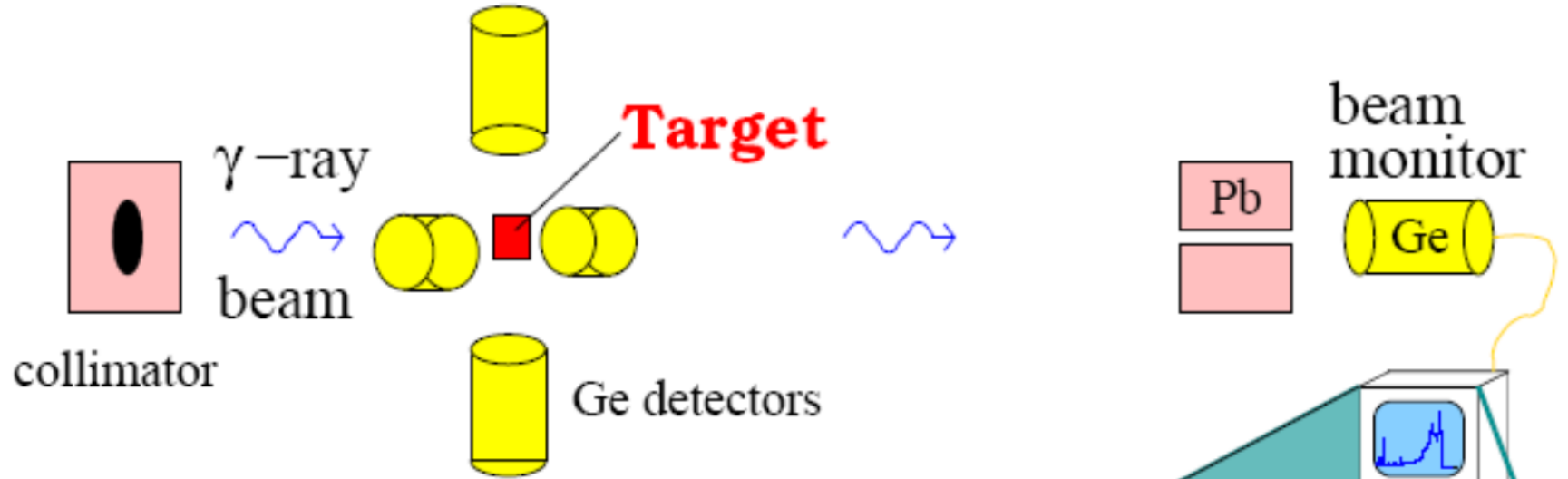
collimators

OVERVIEW ON MEV-RANGED GAMMA-RAY SOURCES - LASER-COMPTON BACKSCATTERING (LCB)

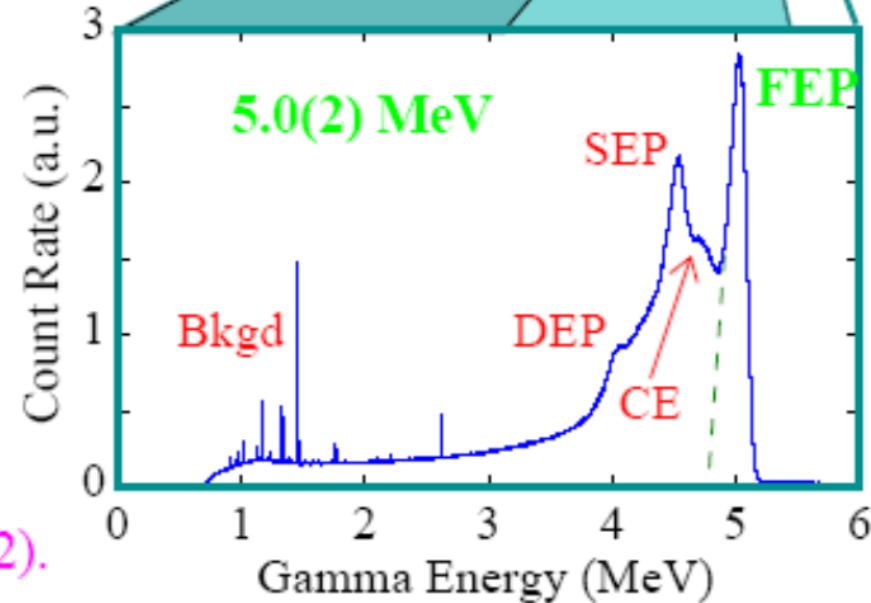


γ -ray
detectors
in the
target room

Looking at the HIGS Gamma-Ray Beam

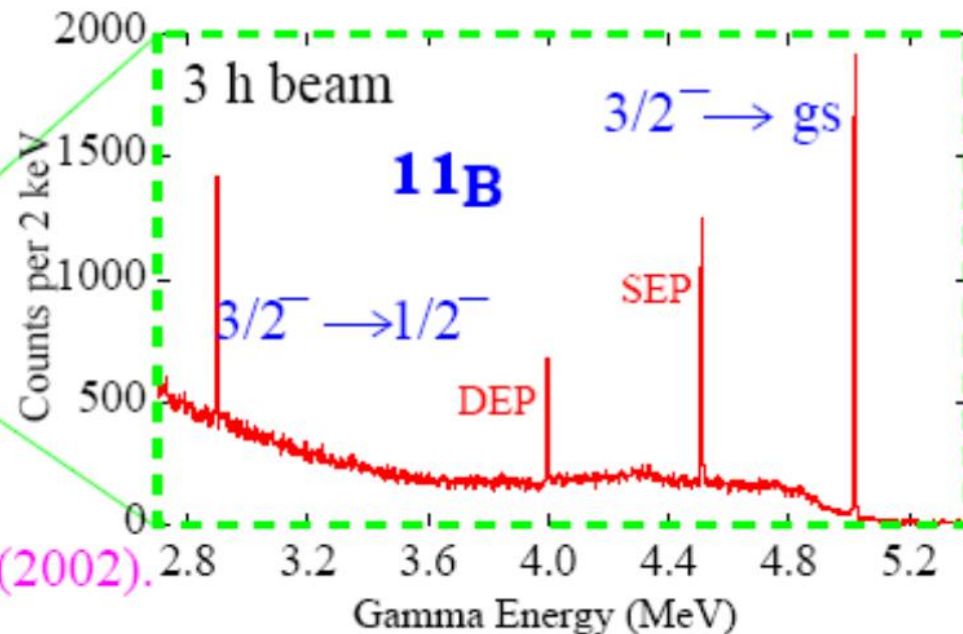
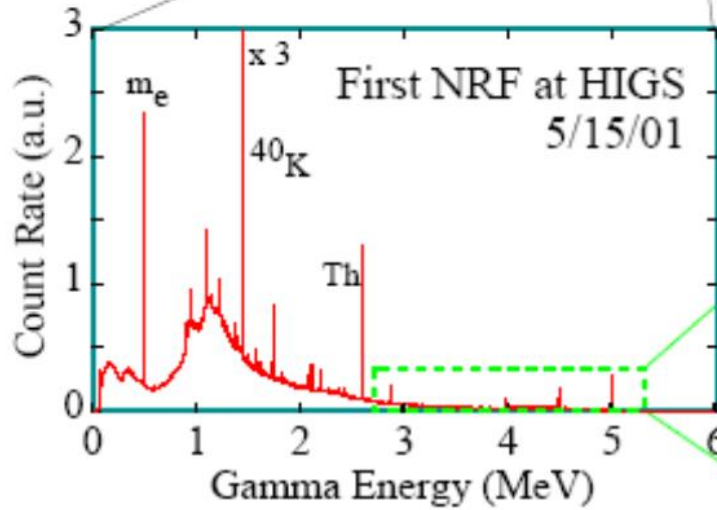
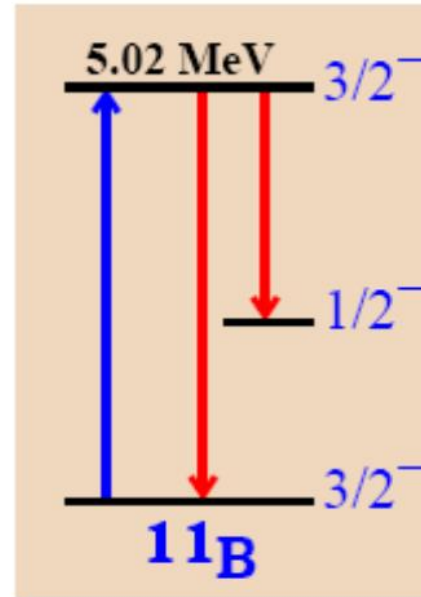
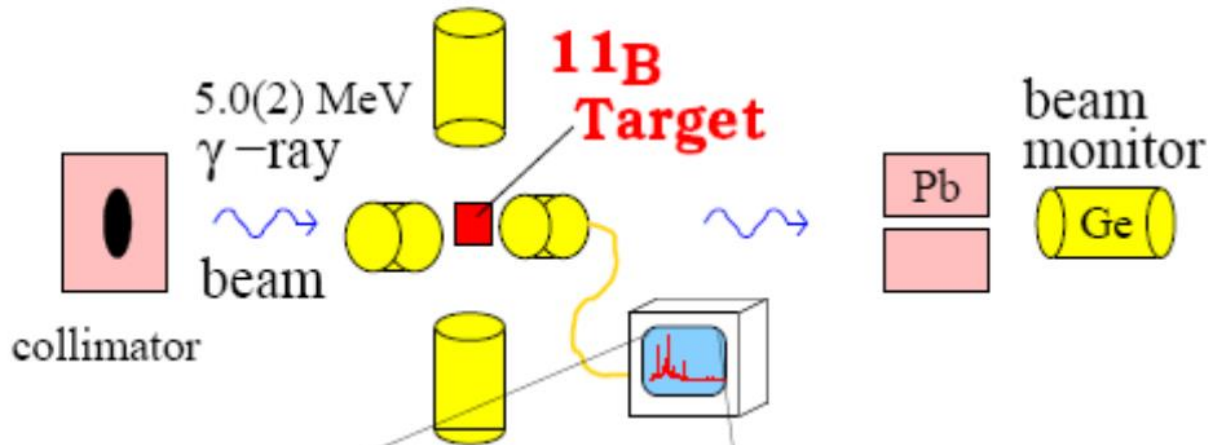


Flux at target: $10^7/s$
at maximum: $10^5/(s \text{ keV})$
Resolution: 3%
(with 1" collimator)

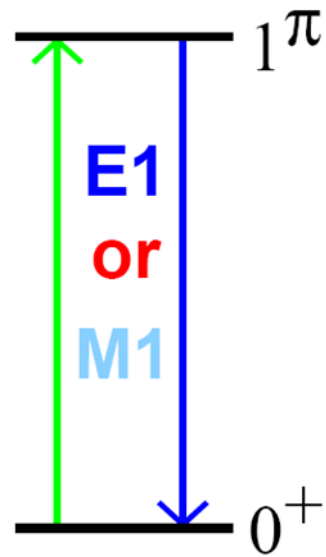


N.Pietralla et al.
Nucl.Instrum.Methods A 483, 556 (2002).

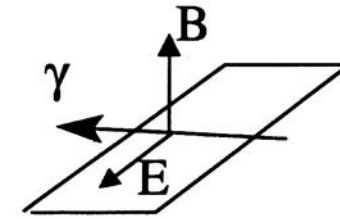
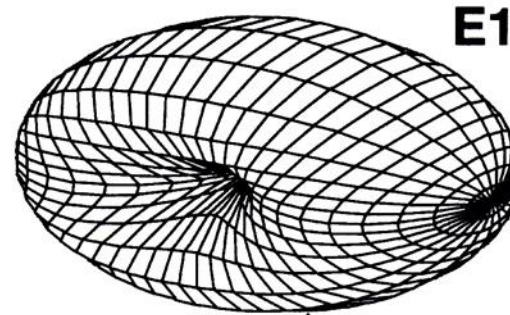
Looking at the Target



N. Pietralla et al.
Nucl. Instrum. Methods A483, 556 (2002).

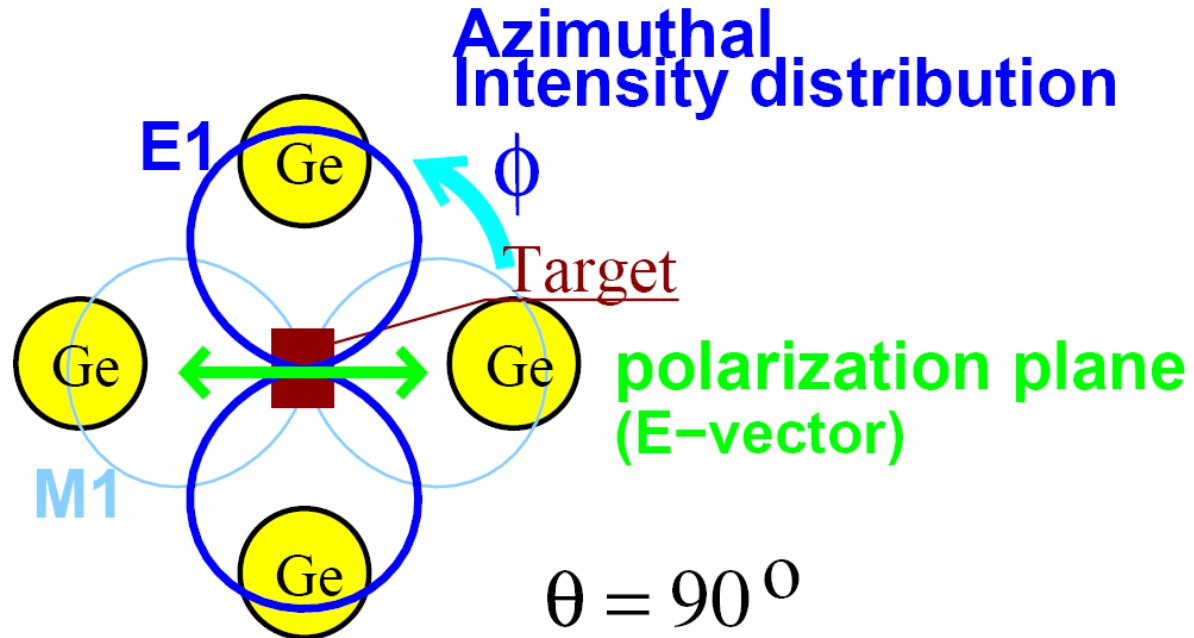
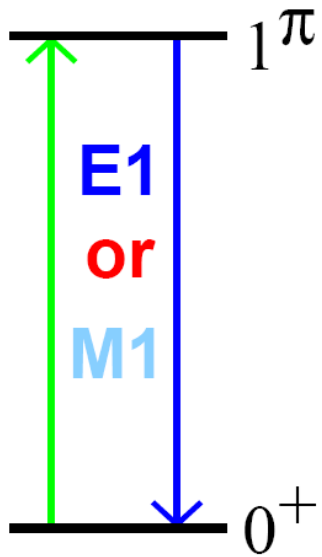


$$\Sigma = \frac{W(90^\circ, 0^\circ) - W(90^\circ, 90^\circ)}{W(90^\circ, 0^\circ) + W(90^\circ, 90^\circ)} = \pi_x = \begin{cases} +1 & \text{for } J^\pi = 1^+ \\ -1 & \text{for } J^\pi = 1^- \end{cases}$$



- Elastic scattering distribution not isotropic about incident polarization plane.
- No intensity along oscillating dipole vector
- Azimuthal rotation by 90° for $M1$ and $E1$ distributions
- Observable only for linearly polarized beam

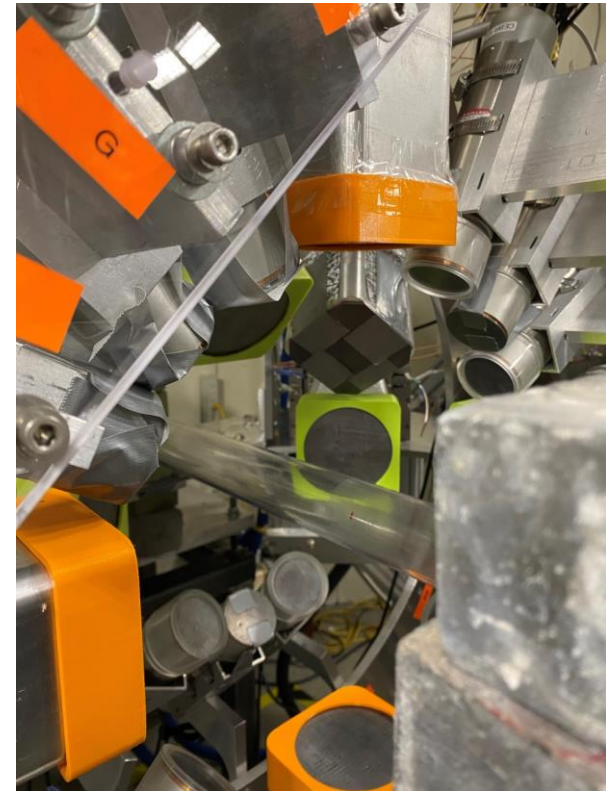
NUCLEAR RESONANCE FLUORESCENCE (NRF)



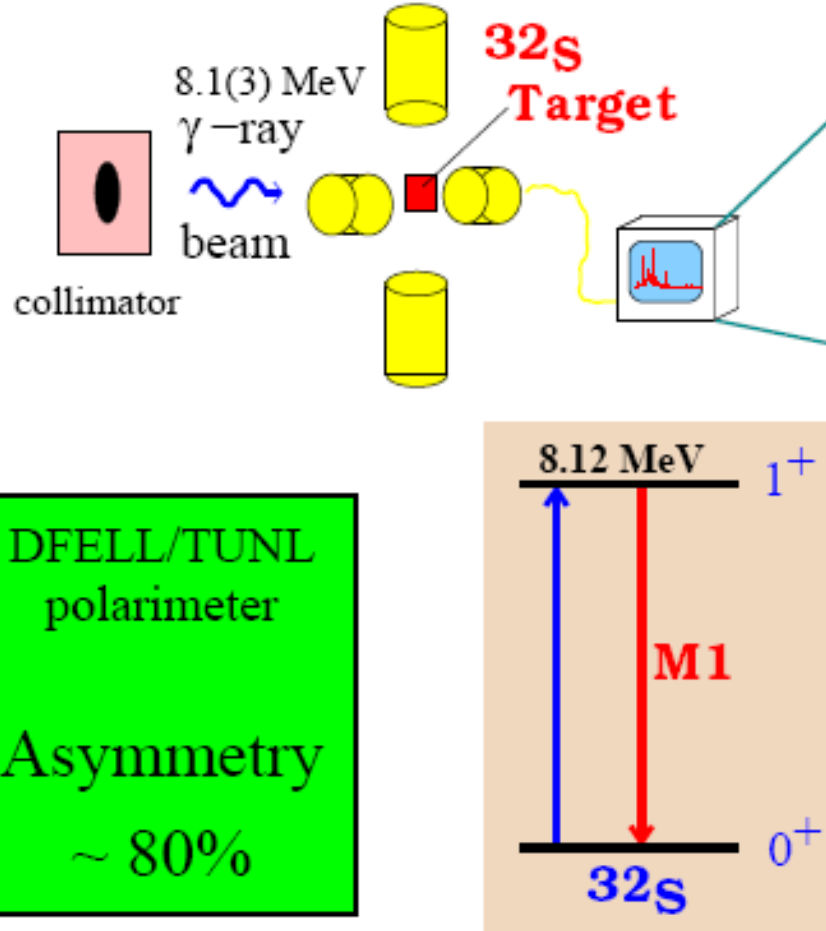
H γ S
2001



H γ S
2023

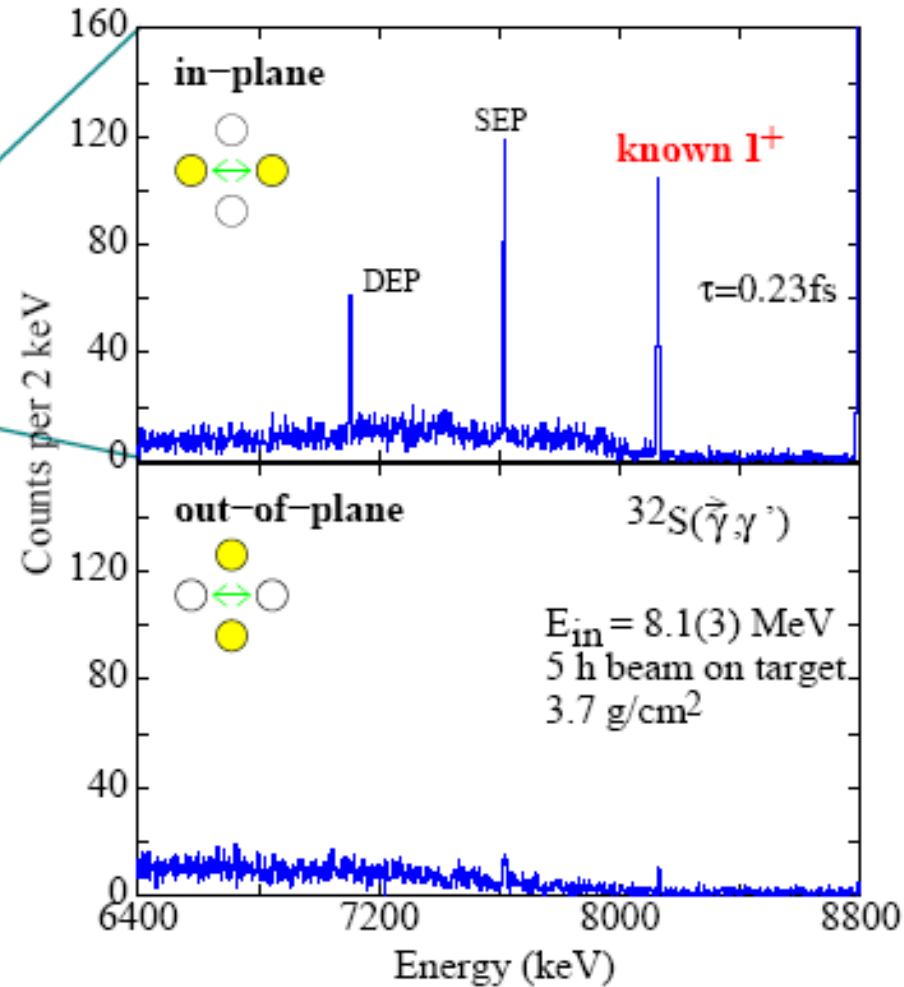


Proof of Principle



DFELL/TUNL
polarimeter

Asymmetry
~ 80%



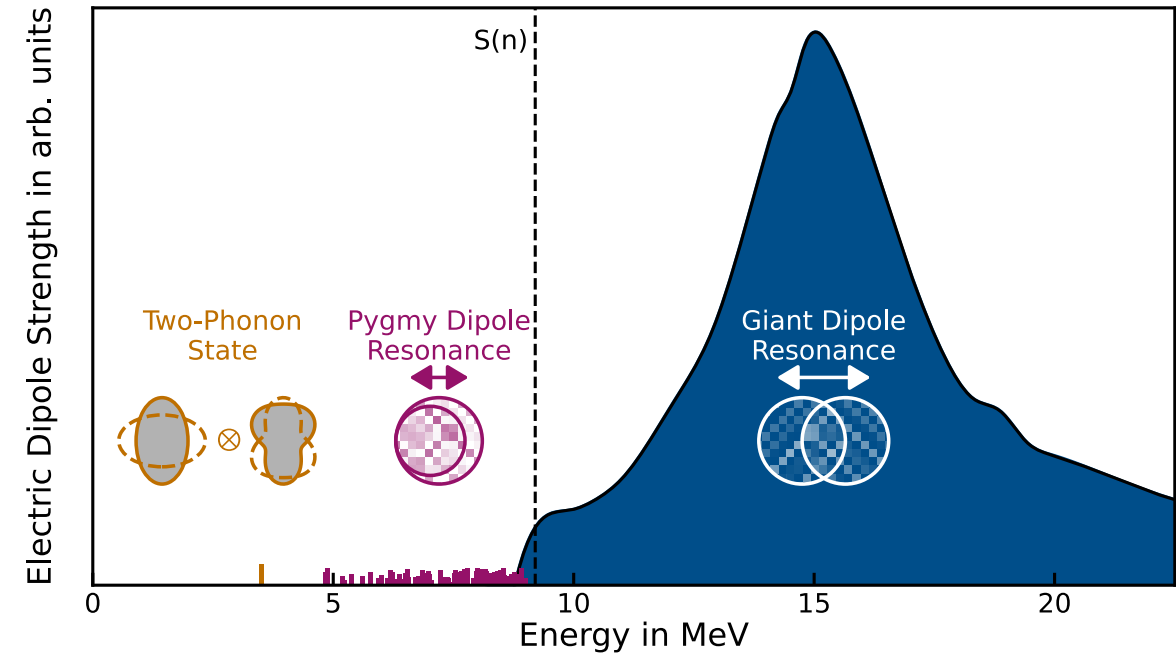
HI γ S 2001

N.Pietralla et al., Nucl.Instrum.Methods A483, 556 (2002).

Challenge to my PhD student
Jörn Kleemann:



„Study the γ -decay of the GDR in
a deformed nucleus as a function
of excitation energy!“

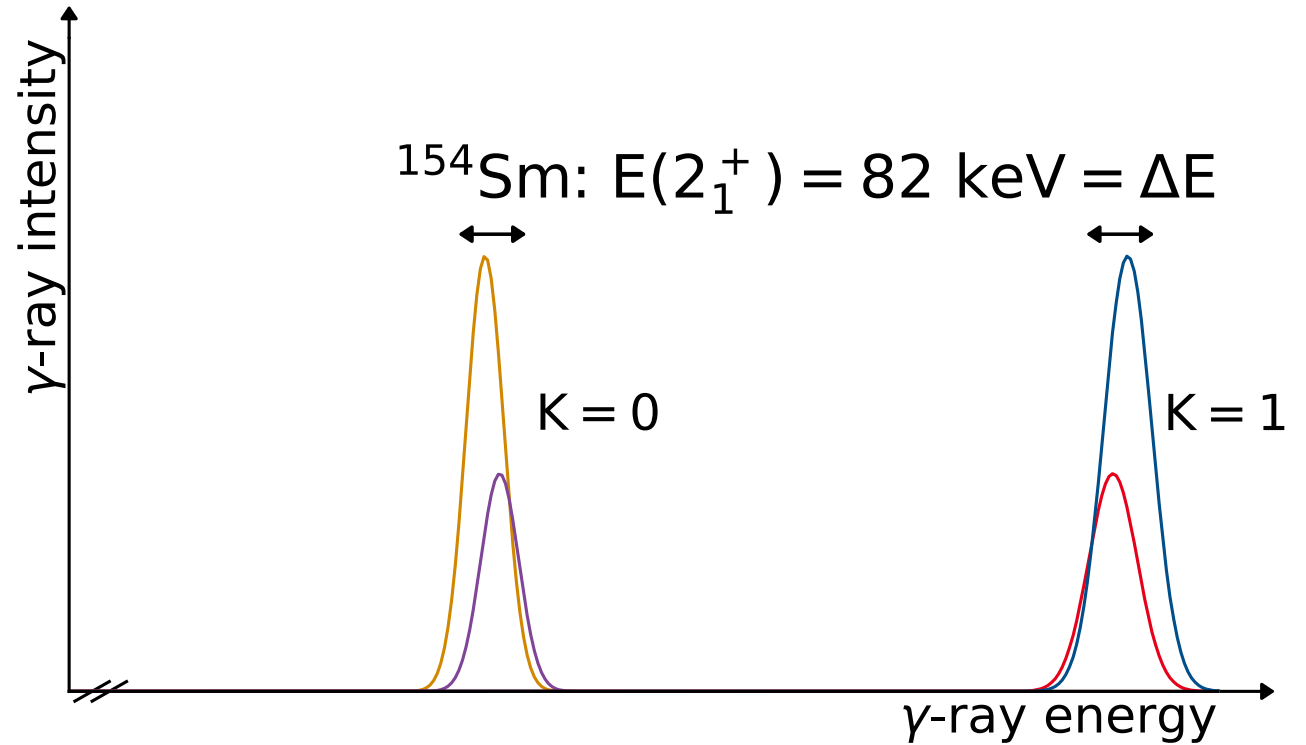
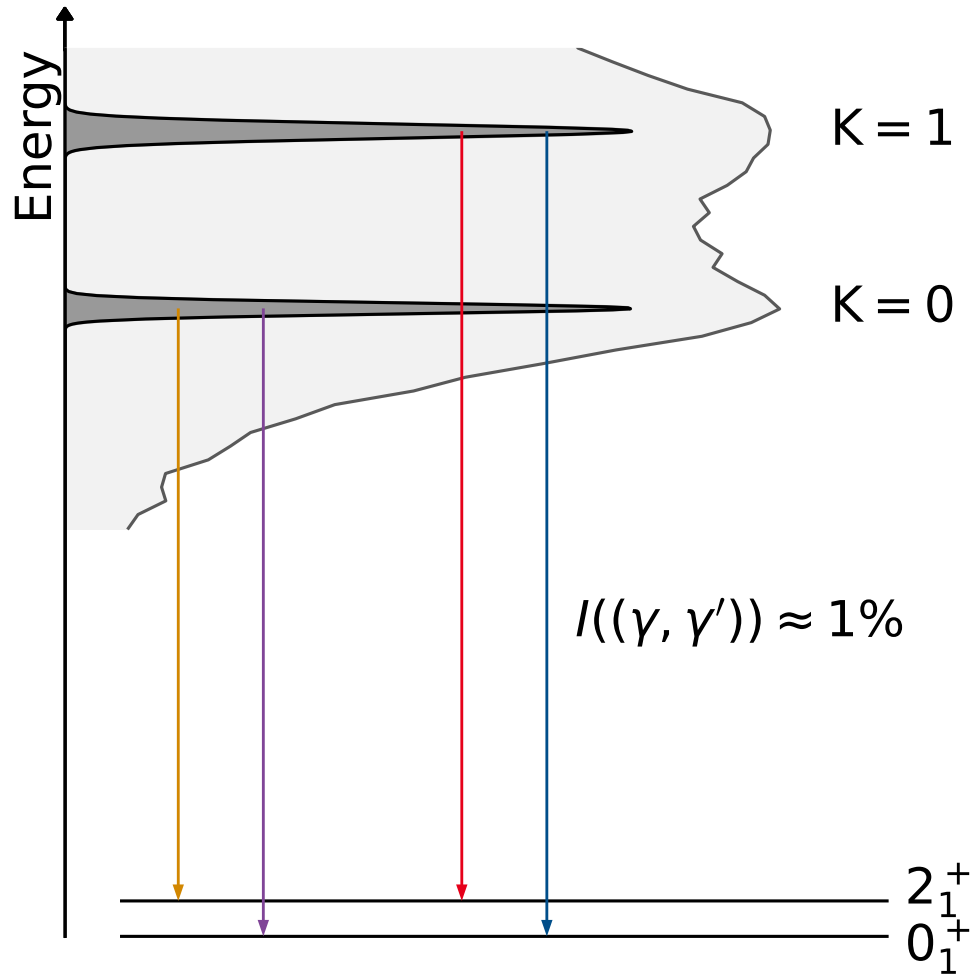


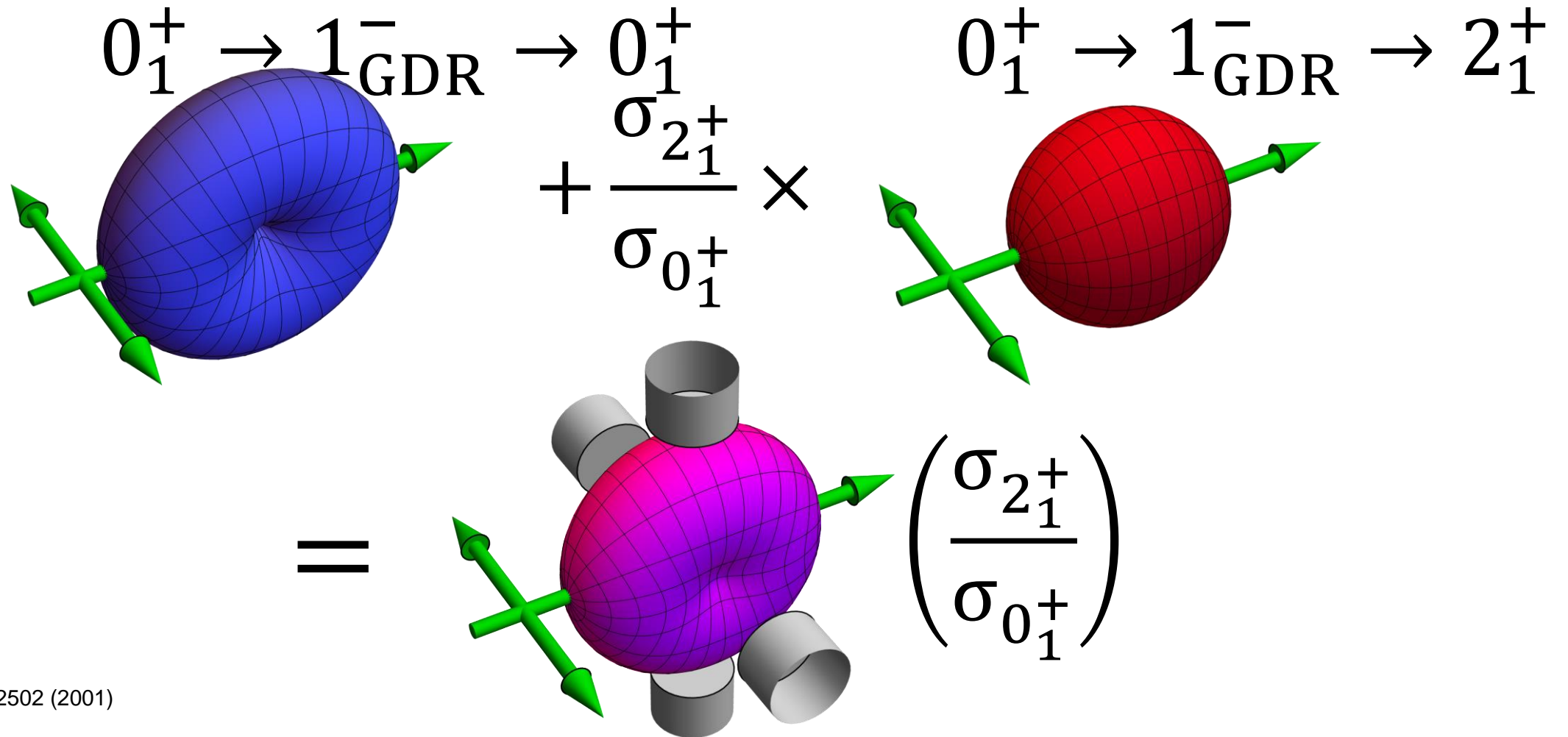
Particle unbound
 $\approx 99\%$ n-decay
 $\approx 1\%$ γ -decay

J. R. Beene *et al.*, Phys. Rev. C **41**, 920 (1990)

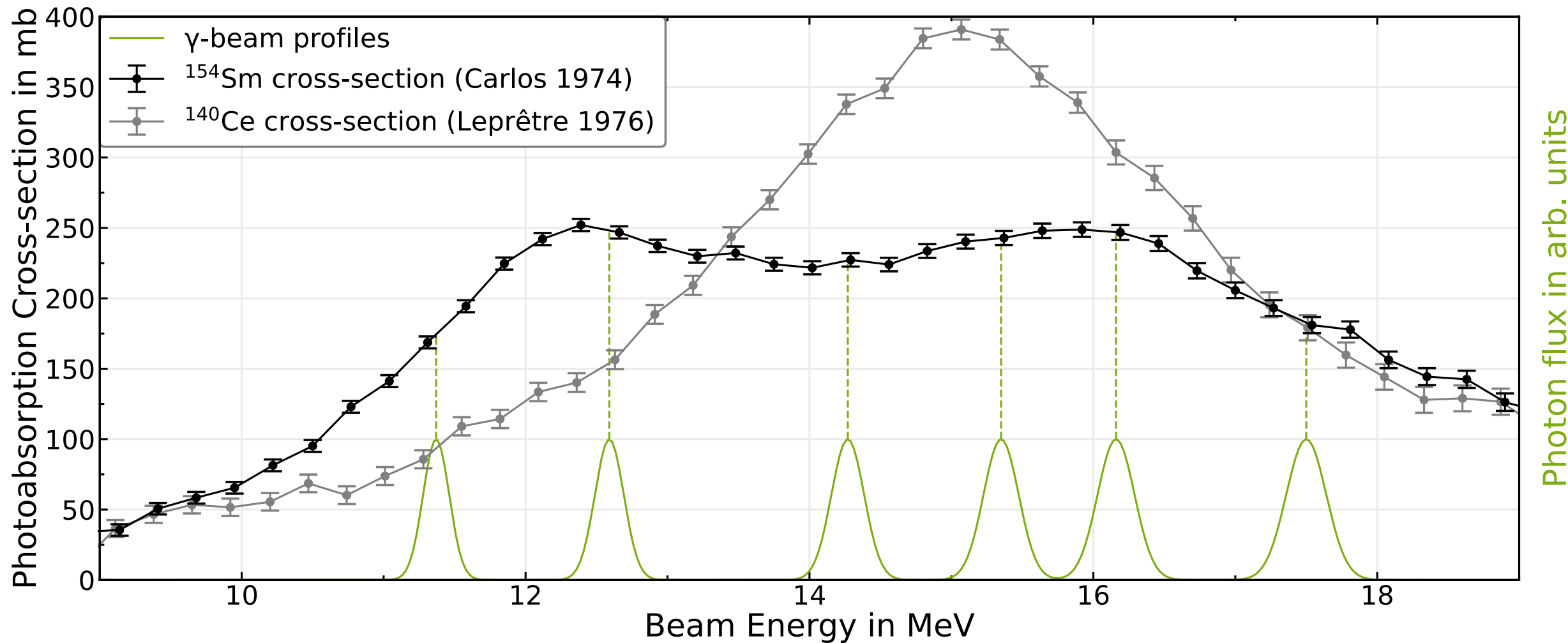
K. Boretzky *et al.*, Phys. Lett. B **384**, 30 (1996)

EXPERIMENTAL PRINCIPLE

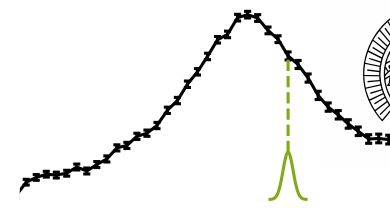




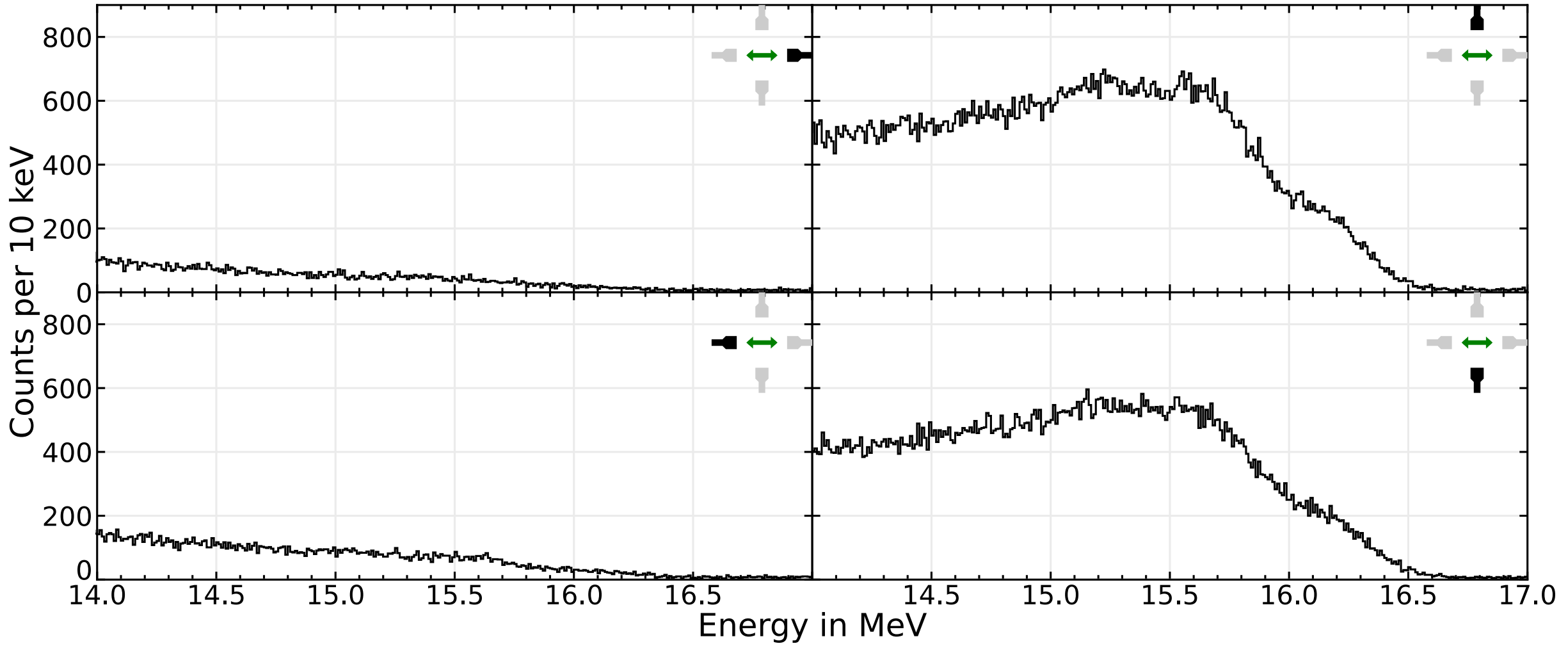
N. Pietralla *et al.*,
Phys. Rev. Lett. **88**, 012502 (2001)



^{140}Ce IN 16.2 MEV LINEARLY POLARIZED Γ -BEAM



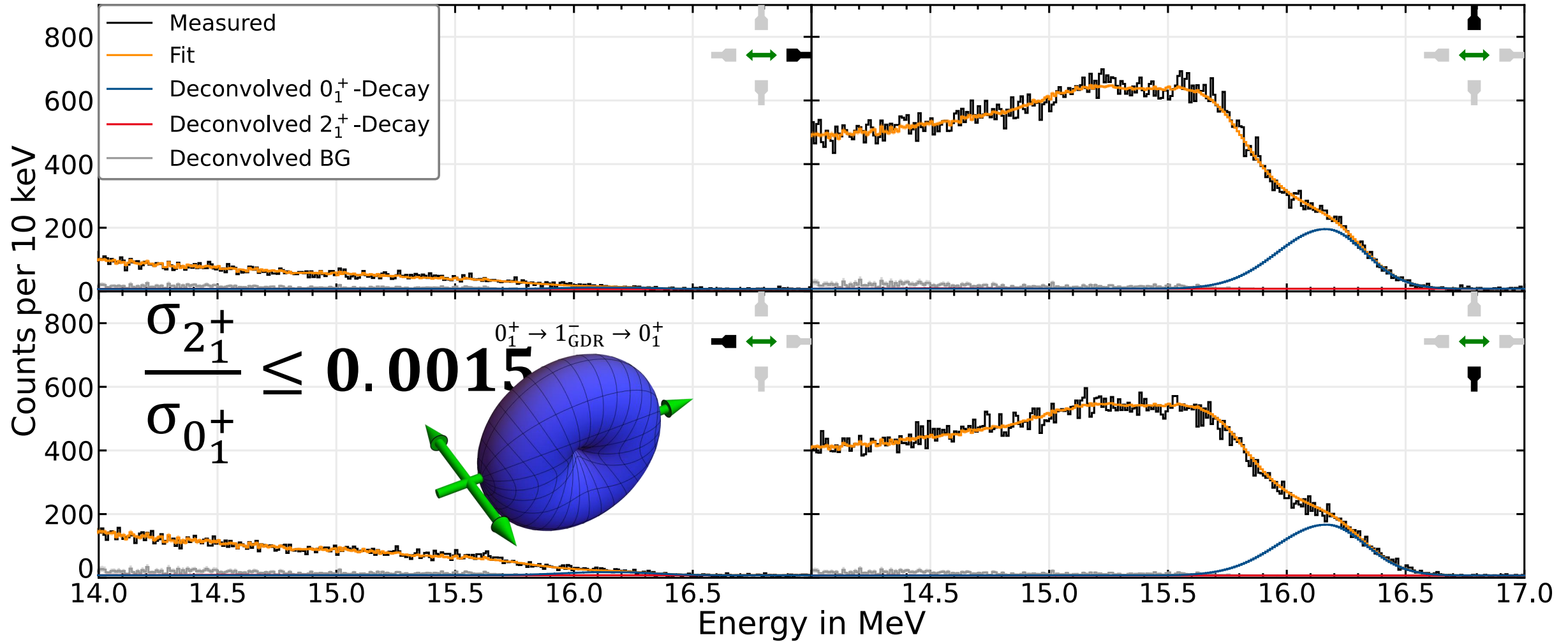
TECHNISCHE
UNIVERSITÄT
DARMSTADT



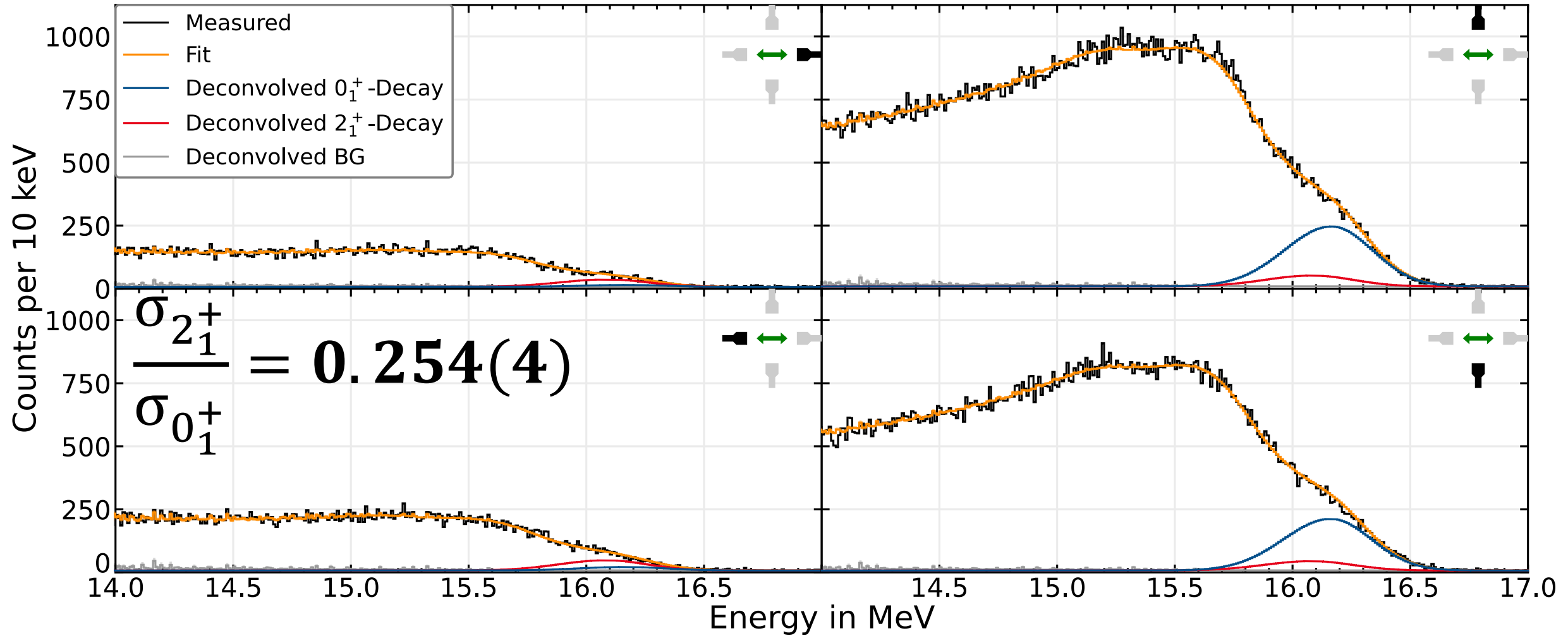
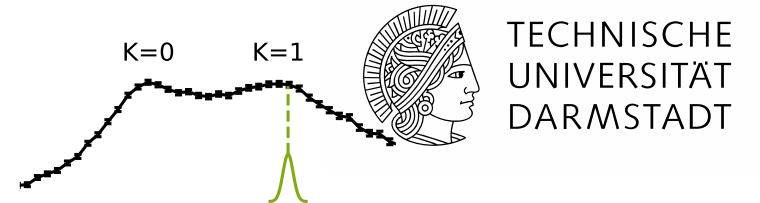
^{140}Ce IN 16.2 MEV LINEARLY POLARIZED Γ -BEAM



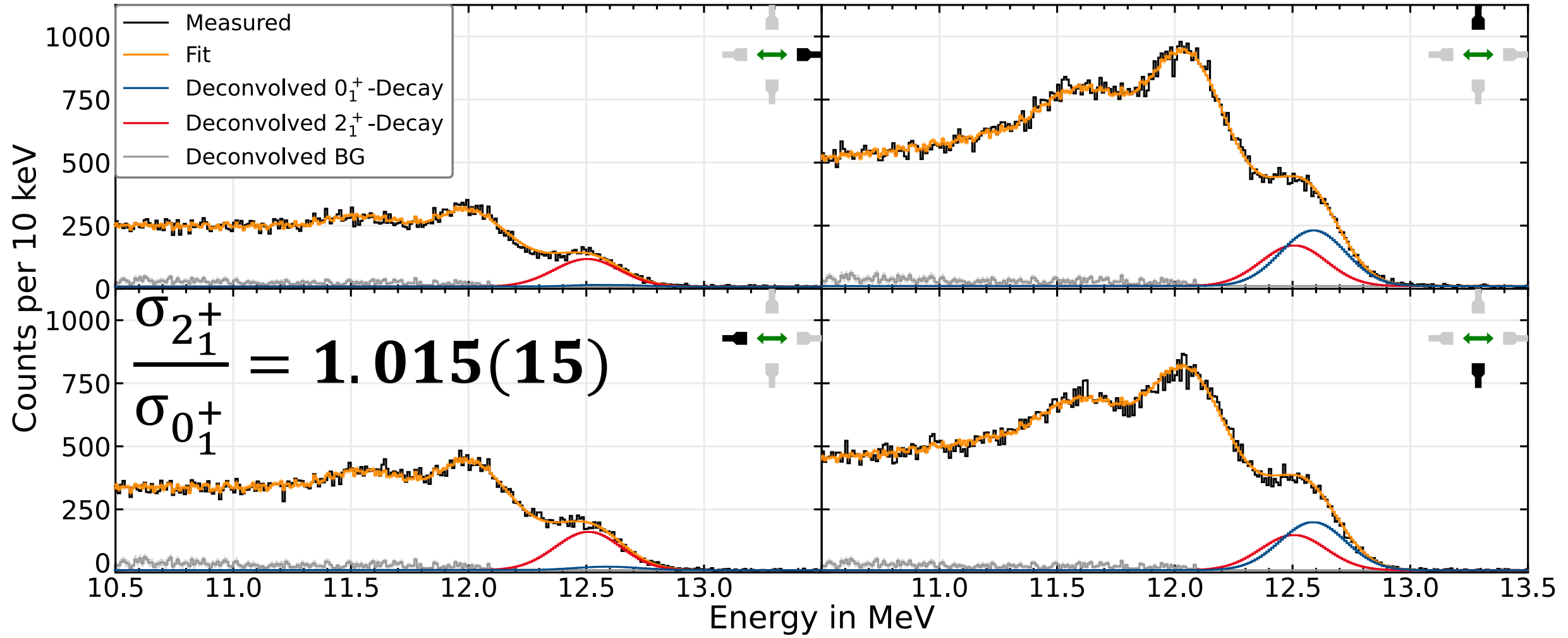
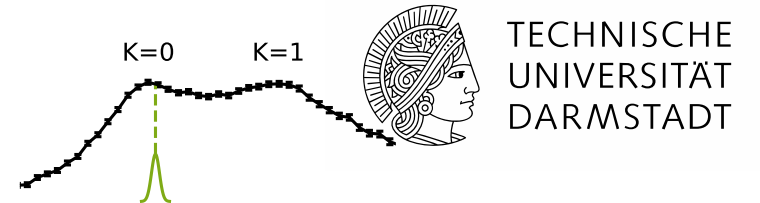
TECHNISCHE
UNIVERSITÄT
DARMSTADT

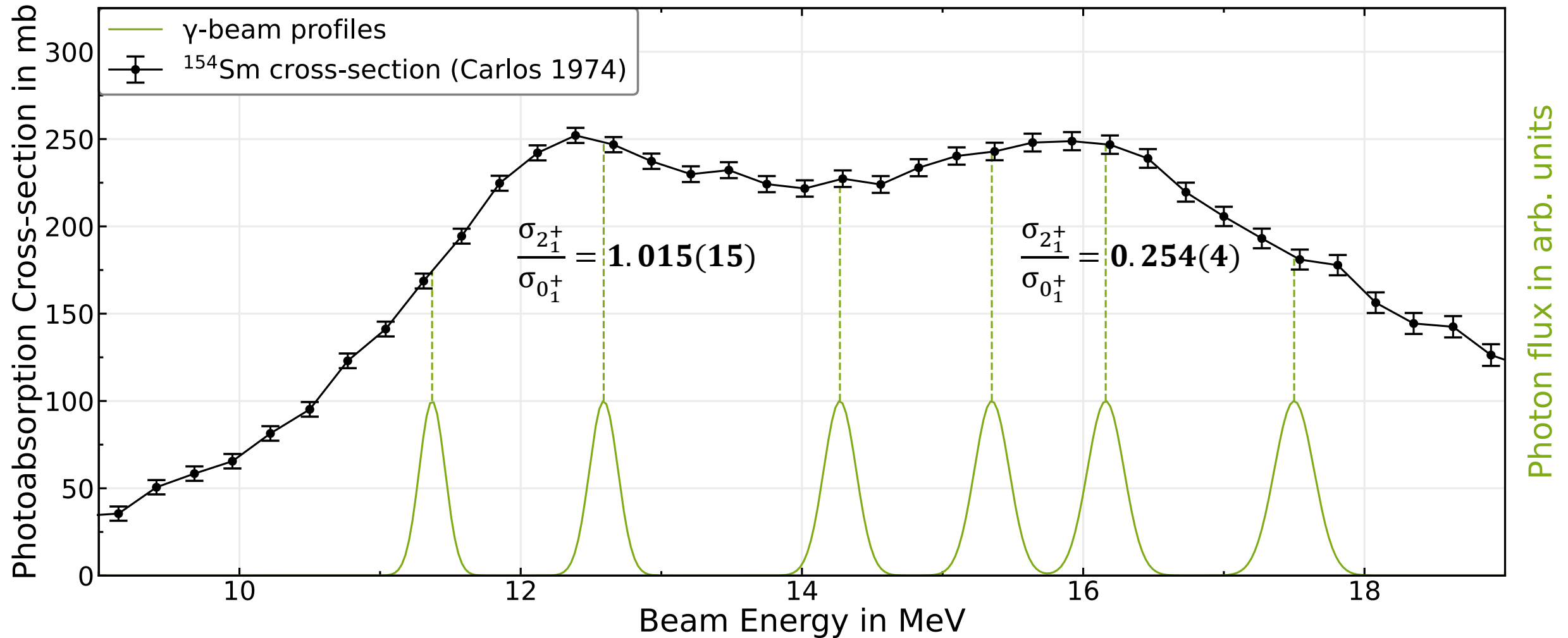


^{154}Sm IN 16.2 MEV LINEARLY POLARIZED Γ -BEAM

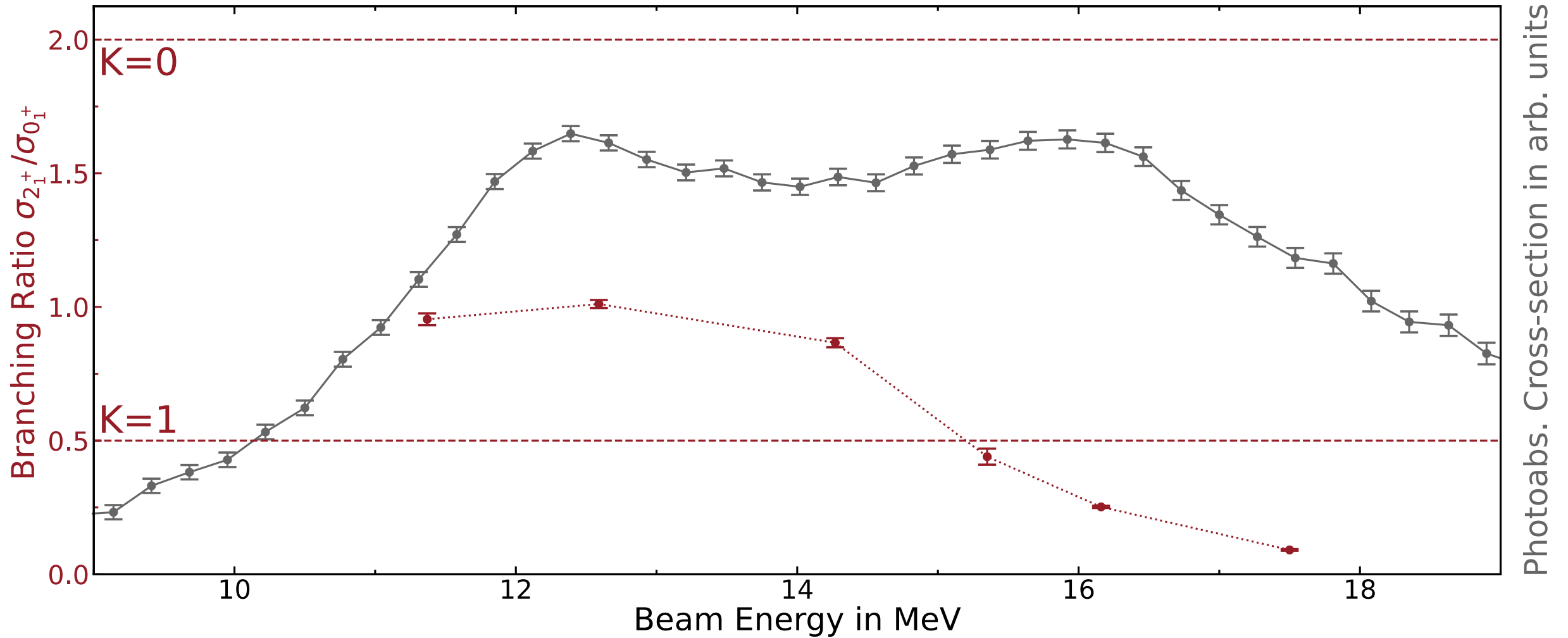


^{154}Sm IN 12.6 MEV LINEARLY POLARIZED Γ -BEAM





RESULTS ON Γ -DECAY BEHAVIOR OF GDR OF ^{154}Sm



Interference effects in the GDR

E. G. Fuller and E. Hayward, Nucl. Phys. **30**, 613 (1962)

- Thomson scattering interferes with GDR's γ -decay to 0_1^+

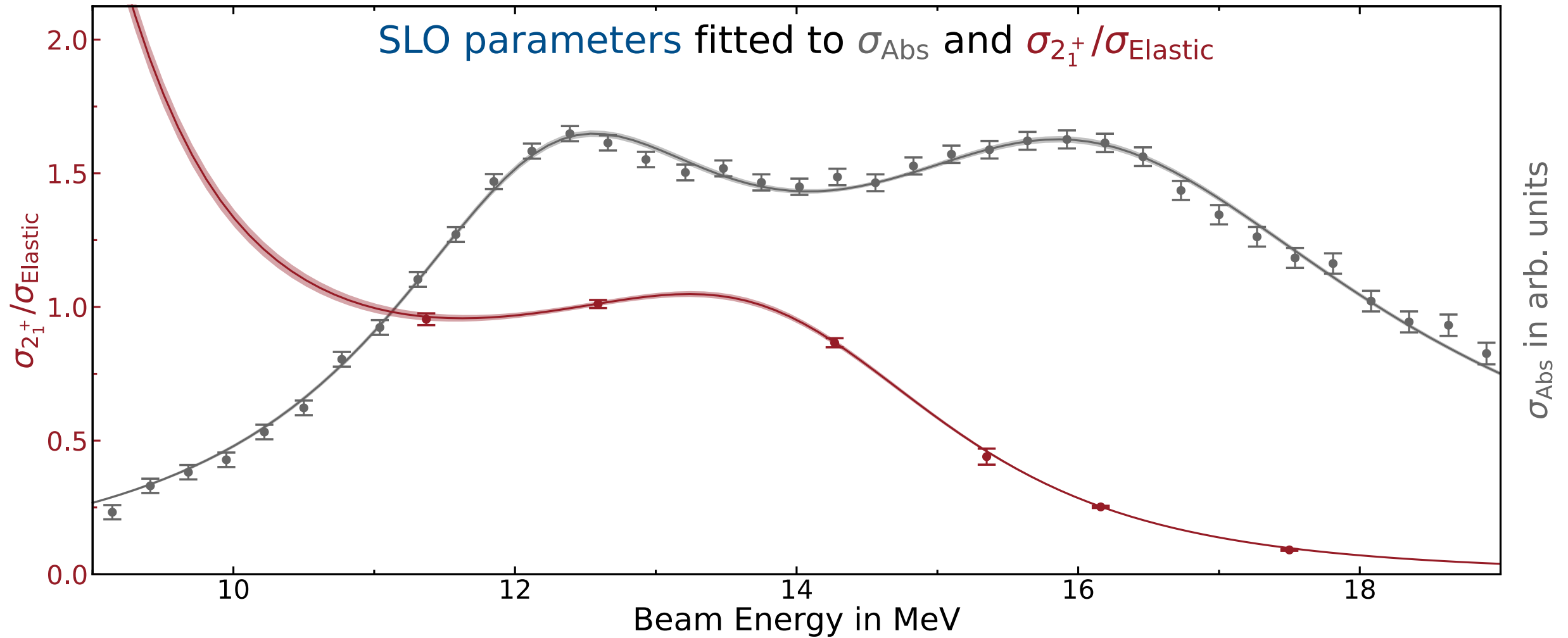
$$\sigma_{\text{Elastic}}(E) = \left| f_{\text{Th}} + f_{0_1^+ \text{ NRF}}(E) \right|^2$$

⇒ Need scattering amplitudes $\mathbf{f}(\mathbf{E}) \in \mathbb{C}$ for both processes for correction

⇒ Obtainable from σ_{Abs} through optical theorem and dispersion relations

$$\sigma_{\text{Abs}}(E) = \sum_{k \in \{0,1\}} \sigma_k \frac{E^2 \Gamma_k^2}{(E_k^2 - E^2)^2 + E^2 \Gamma_k^2}$$

⇒ Corrections up to 35%



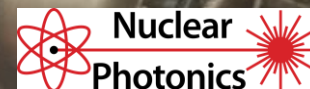
- Measured the γ -decay behavior of the GDRs of ^{154}Sm and ^{140}Ce
→ γ -decay of GDR very sensitive to SLO parameters of GDR
- $E_{K=0} = 12.367(21) \text{ MeV}$, $\Gamma = 3.27(6) \text{ MeV}$, $\sigma_{\text{tot}, K=0} = 0.644(15) \text{ MeV b}$ for ^{154}Sm
- $E_{K=1} = 16.119(20) \text{ MeV}$, $\Gamma = 5.05(5) \text{ MeV}$, $\sigma_{\text{tot}, K=1} = 1.052(17) \text{ MeV b}$ for ^{154}Sm
- Simultaneous activation of natural Ce, Sm and Au samples
→ γ/n branching (“ $\approx 1\%$ ”) and absolute cross-sections from activation
- Additional data on GDRs of ^{164}Dy , ^{232}Th & ^{208}Pb measured in April 2023



Jörn Kleemann



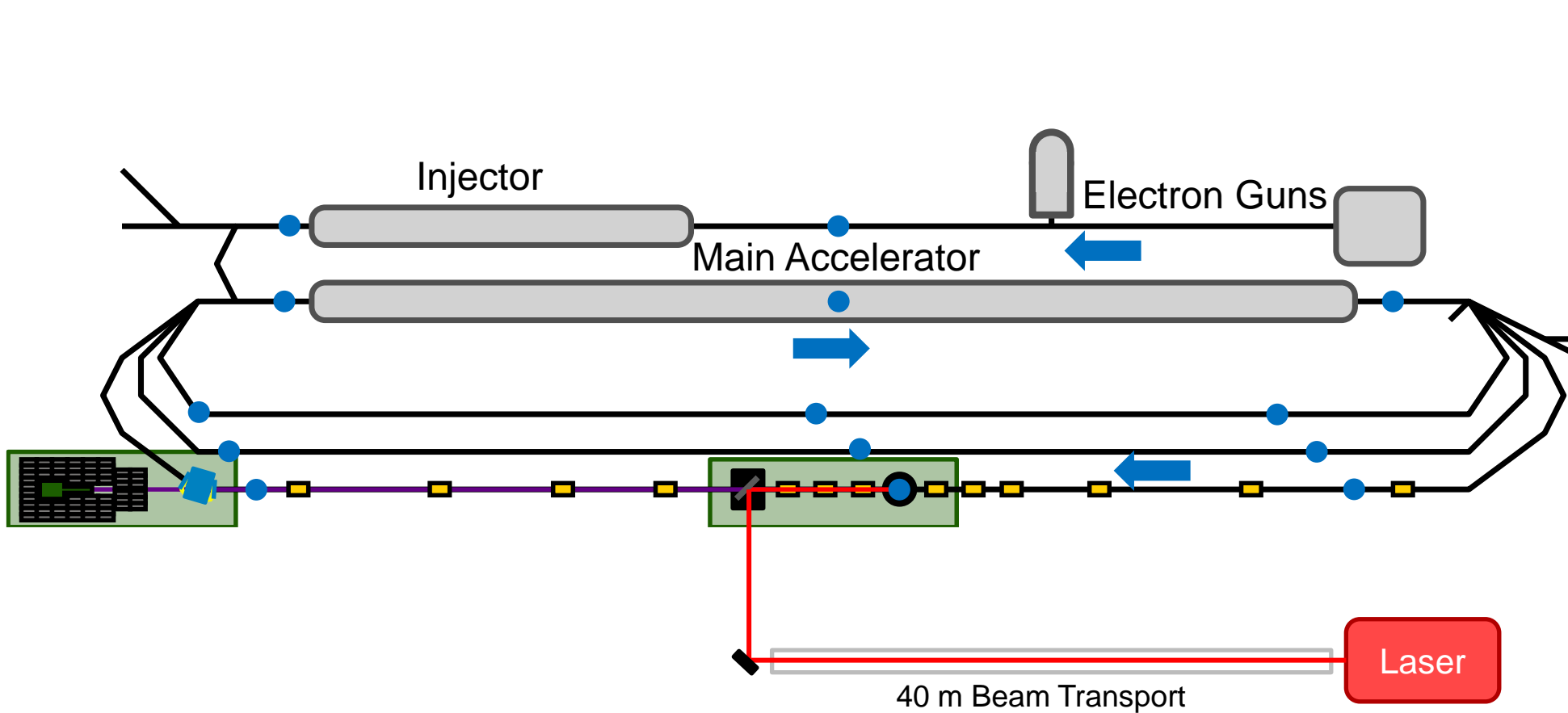
TECHNISCHE
UNIVERSITÄT
DARMSTADT



M. MEIER, M. ARNOLD, V. BAGNOUD, J. ENDERS & N. PIETRALLA

LASER-COMPTON BACKSCATTERING SOURCE AT THE S-DALINAC

LASER COMPTON BACKSCATTERING @ S-DALINAC



Higher photon energy preferred

Head-On Collision ✓

- ❖ For higher Energy
- ❖ Easier overlap

High Laser Pulse Energy (N_L)

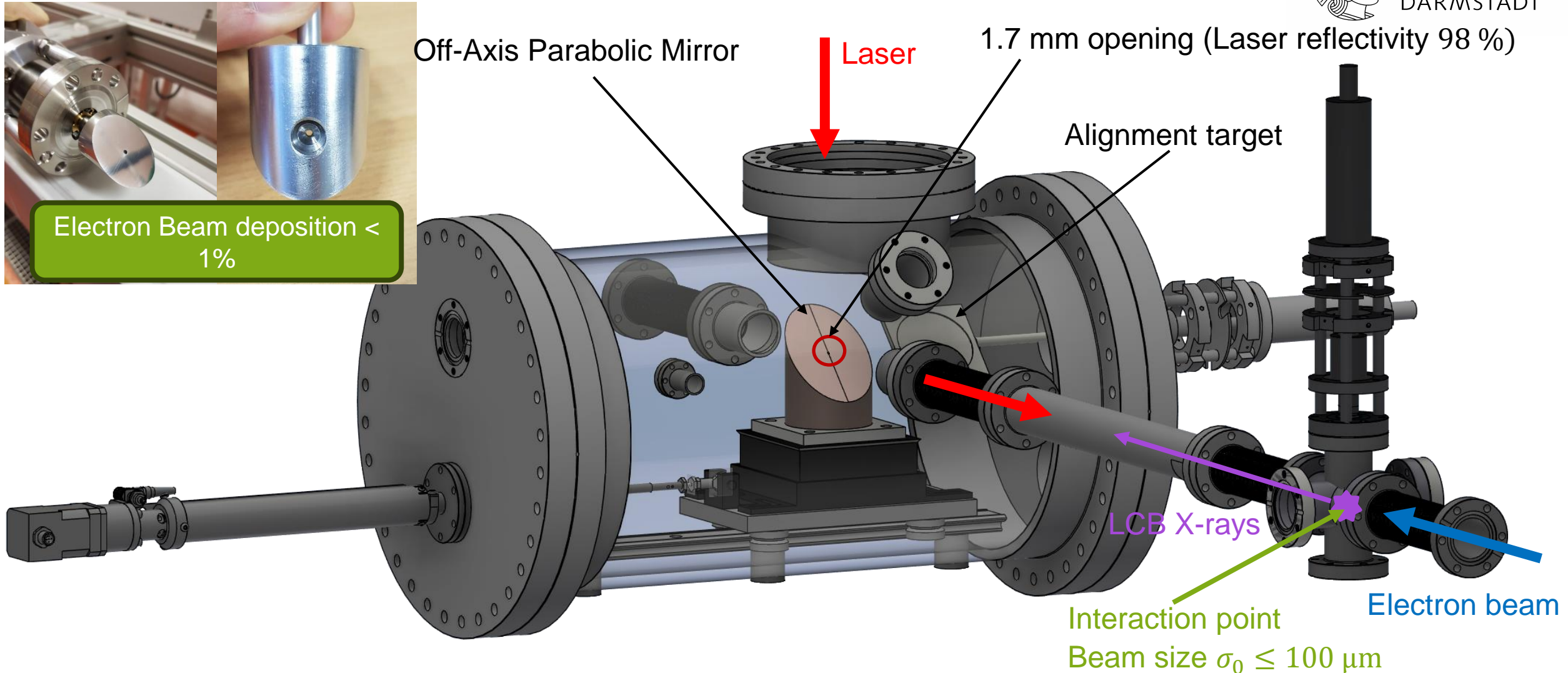
High scattering frequency (f)

Small beam size at IP

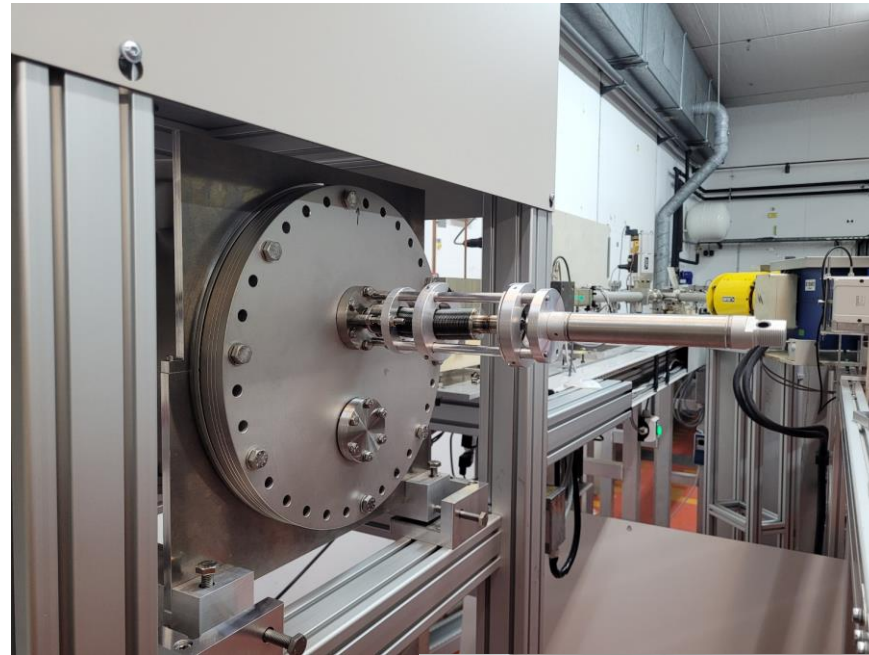
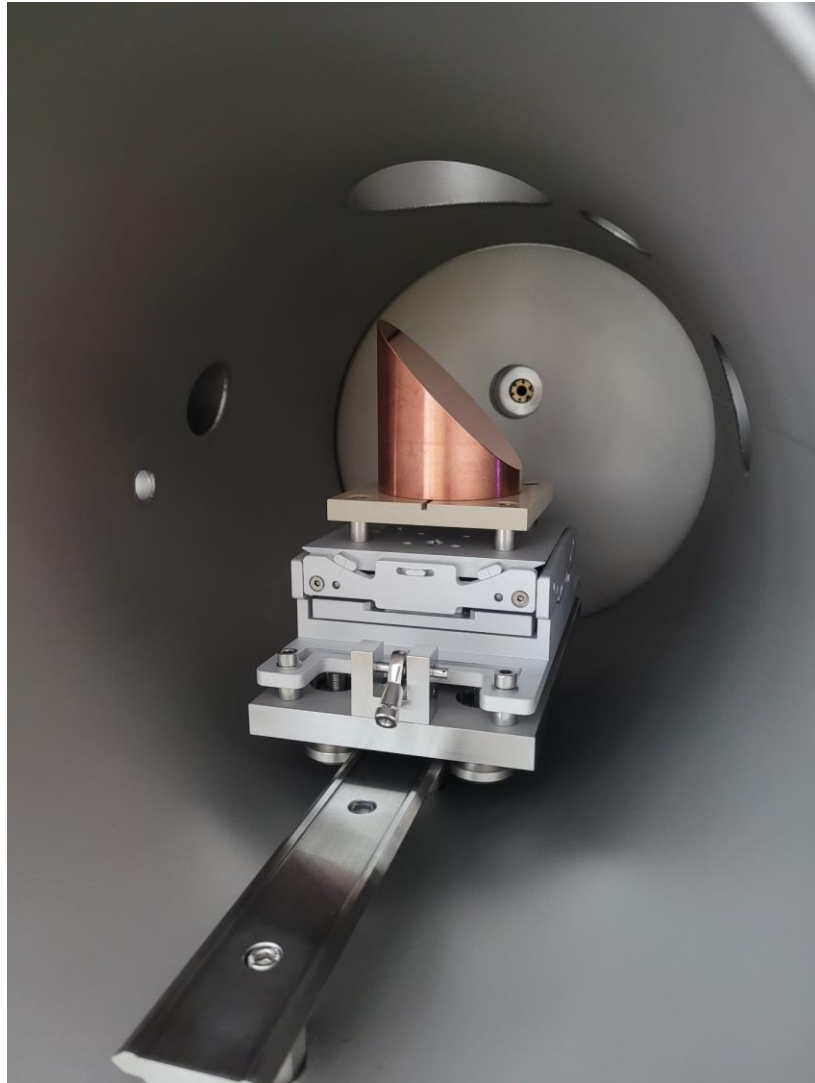
Low M^2

Low $\sigma_{\Delta E_p}$; $\frac{\sigma_{\Delta E_L}}{E_L} \leq \frac{\sigma_{\Delta E_e}}{E_e}$

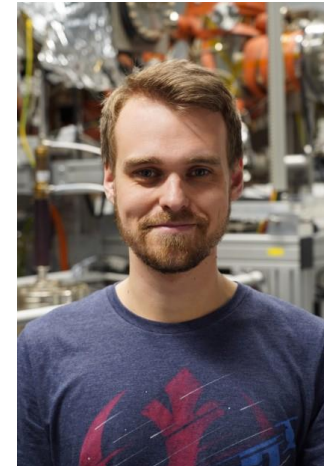
COUPLING CHAMBER OF LCB-SOURCE



COUPLING CHAMBER OF LCB-SOURCE



TECHNISCHE
UNIVERSITÄT
DARMSTADT



Maximilian Meier

LASER SYSTEM



Amplitude – Laser Tangor 100

- ❖ $\lambda = 1030 \text{ nm}$
(Ytterbium)
- ❖ $\frac{\Delta\lambda}{\lambda} \sim 2 \cdot 10^{-4}$
- ❖ $P_{avg} = 100 \text{ W}$
- ❖ $E_{pulse} \leq 0.5 \text{ mJ}$
- ❖ $f = 200 \text{ kHz} - 40 \text{ MHz}$
- ❖ $M^2 < 1.3$
- ❖ $\sigma_z = 3 \text{ ps}$

Higher Harmonic Generation

- ❖ SHG:
 $\lambda = 515 \text{ nm}$
 $\eta > 50 \%$
- ❖ THG:
 $\lambda = 343 \text{ nm}$
 $\eta > 25 \%$

Higher photon energy
preferred

Head-On Collision ✓

- ❖ For higher Energy
- ❖ Easier overlap

High Laser Pulse
Energy (N_L) ✓

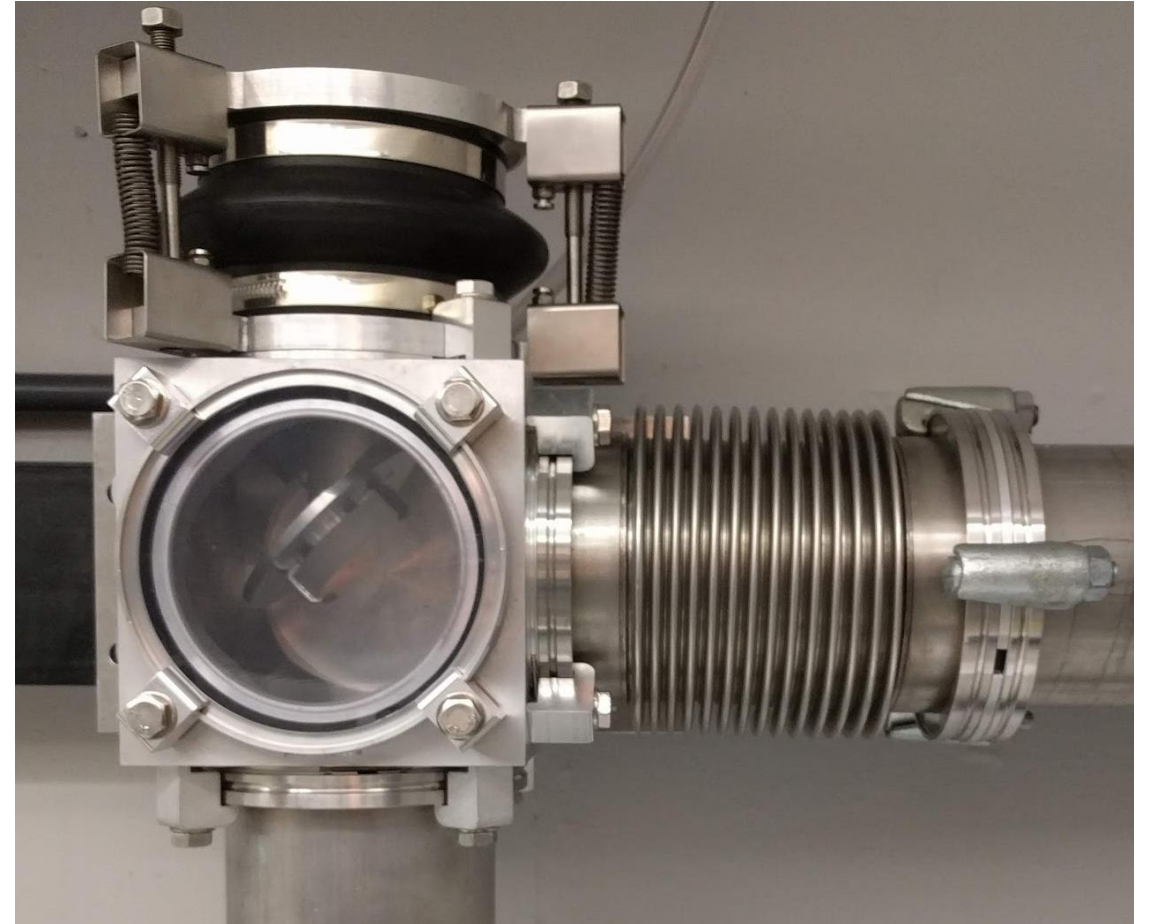
High scattering
frequency (f) ✓

Small beam size at IP ✓

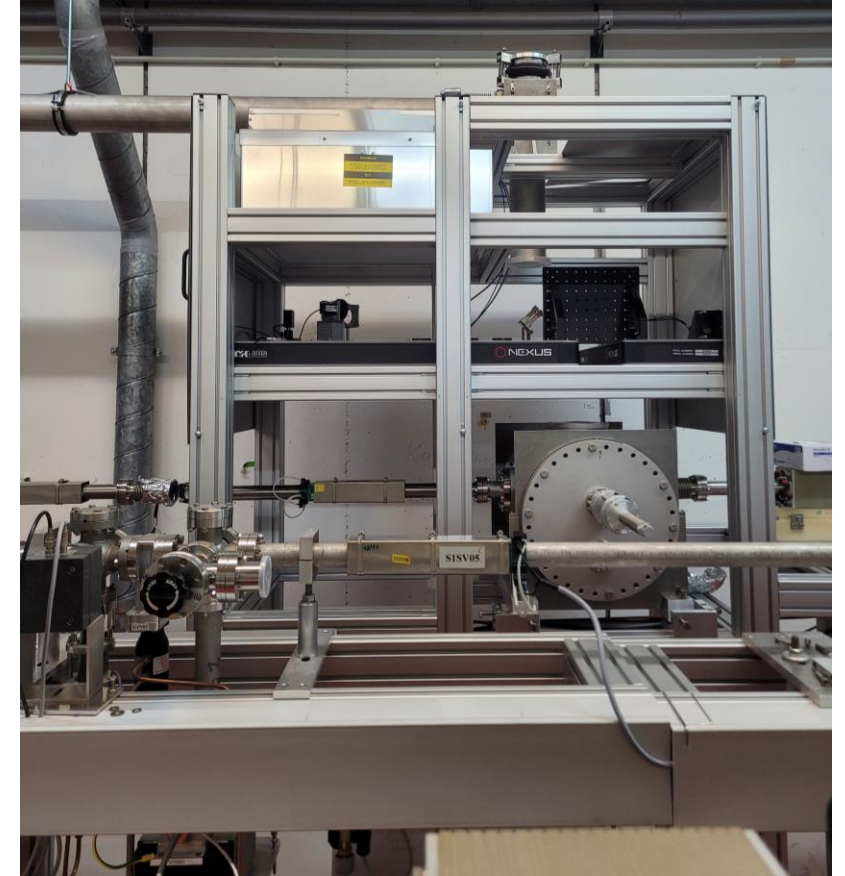
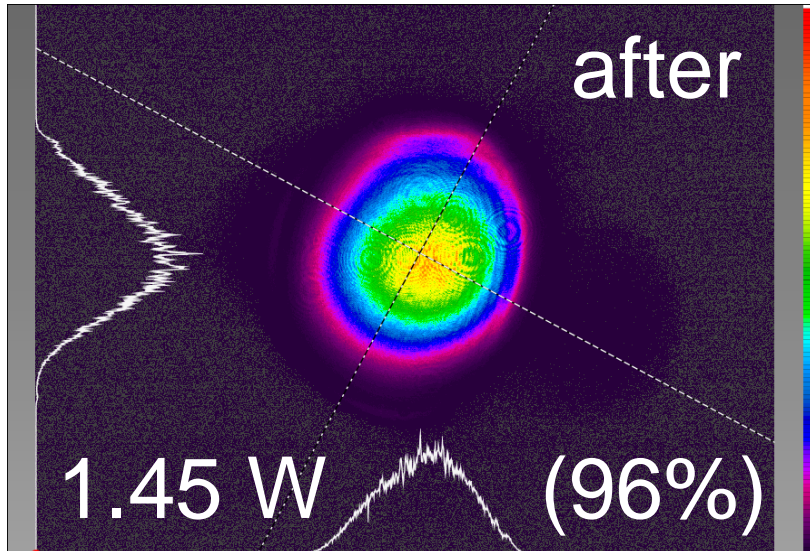
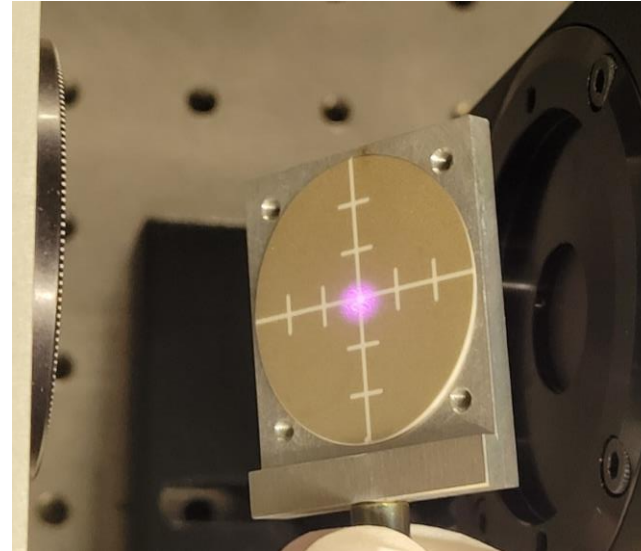
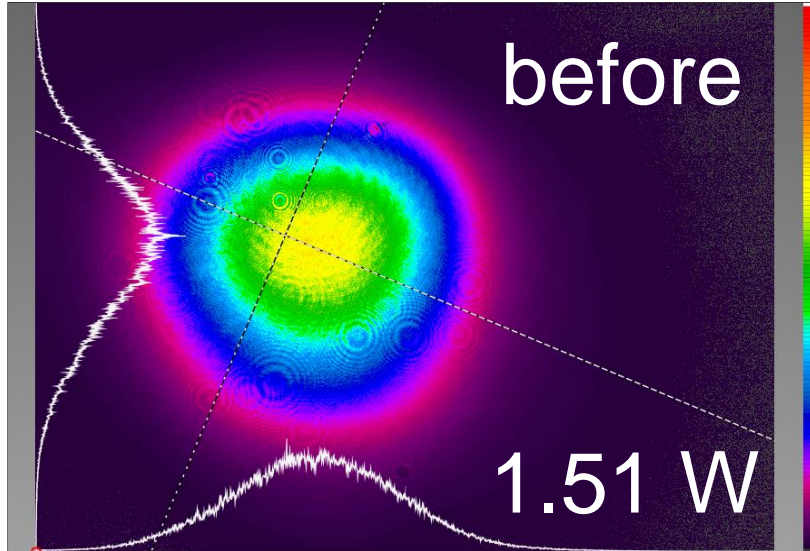
Low M^2 ✓

Low $\sigma_{\Delta E_p}$; $\frac{\sigma_{\Delta E_L}}{E_L} \leq \frac{\sigma_{\Delta E_e}}{E_e}$ ✓

LASER BEAM TRANSPORT



LASER BEAM TRANSPORT



STAY TUNED!

Thank you very much!



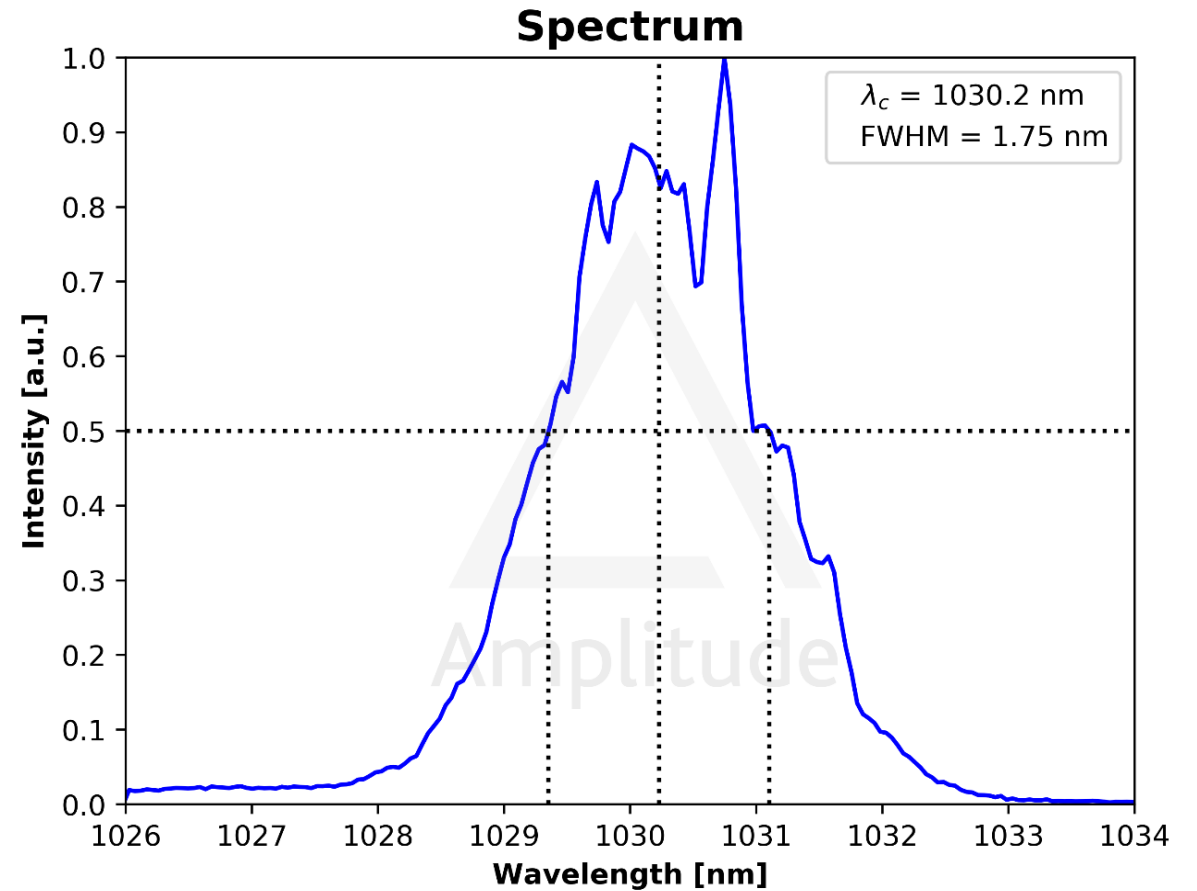
Jörn Kleemann



Maximilian Meier

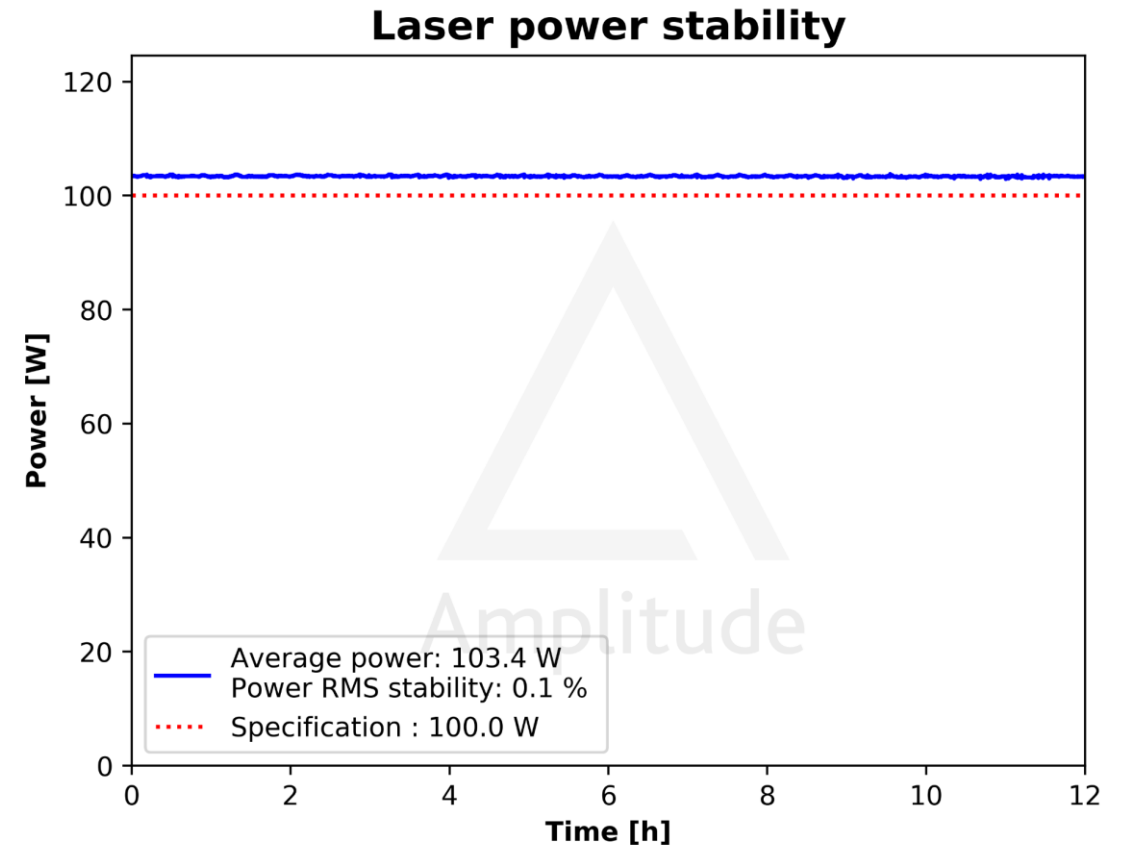
LASER SYSTEM

Laser Parameter		Unit	Measurement
Center wavelength		nm	1030.2
Bandwidth FWHM		nm	1.8
Average power		W	103.4
Energy per pulse		μJ	517.0
Short-term energy stability	RMS	%	0.89
Long-term energy stability	RMS	%	0.99
Pulse duration		fs	740
M ²	M ² _x		1.08
	M ² _y		1.11
Astigmatism		%	11.6
Waist asymmetry		%	0.5
Beam diameter	2W _{max}	mm	3.26
	2W _{min}	mm	3.11
Beam ellipticity		%	4.6
Short-term pointing stability	Radial	μrad	4.5
Short-term position stability	Radial	μm	1.58
Absolute timing jitter		fs	175.0
Long term jitter on 12h		fs	192.9
Repetition rate adjustability			Single shot – 40 MHz



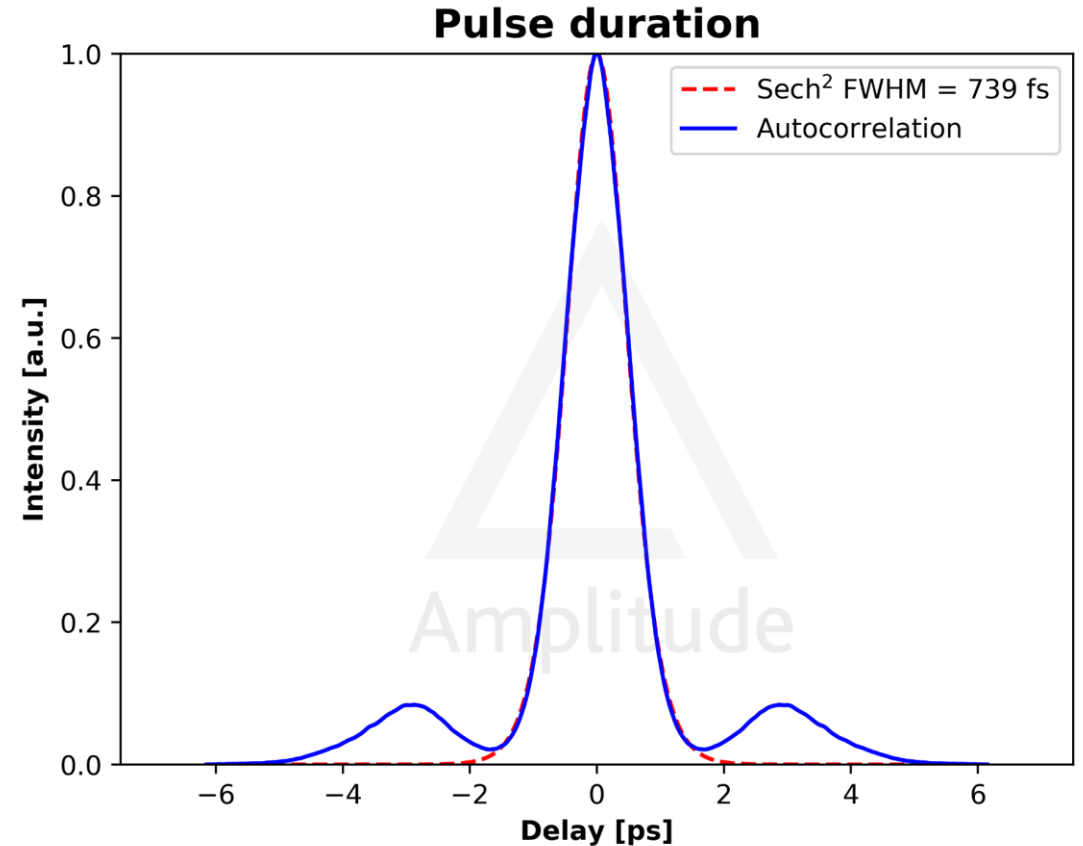
LASER SYSTEM

Laser Parameter		Unit	Measurement
Center wavelength		nm	1030.2
Bandwidth FWHM		nm	1.8
Average power		W	103.4
Energy per pulse		μJ	517.0
Short-term energy stability	RMS	%	0.89
Long-term energy stability	RMS	%	0.99
Pulse duration		fs	740
M ²	M ² _x		1.08
	M ² _y		1.11
Astigmatism		%	11.6
Waist asymmetry		%	0.5
Beam diameter	2W _{max}	mm	3.26
	2W _{min}	mm	3.11
Beam ellipticity		%	4.6
Short-term pointing stability	Radial	μrad	4.5
Short-term position stability	Radial	μm	1.58
Absolute timing jitter		fs	175.0
Long term jitter on 12h		fs	192.9
Repetition rate adjustability			Single shot – 40 MHz



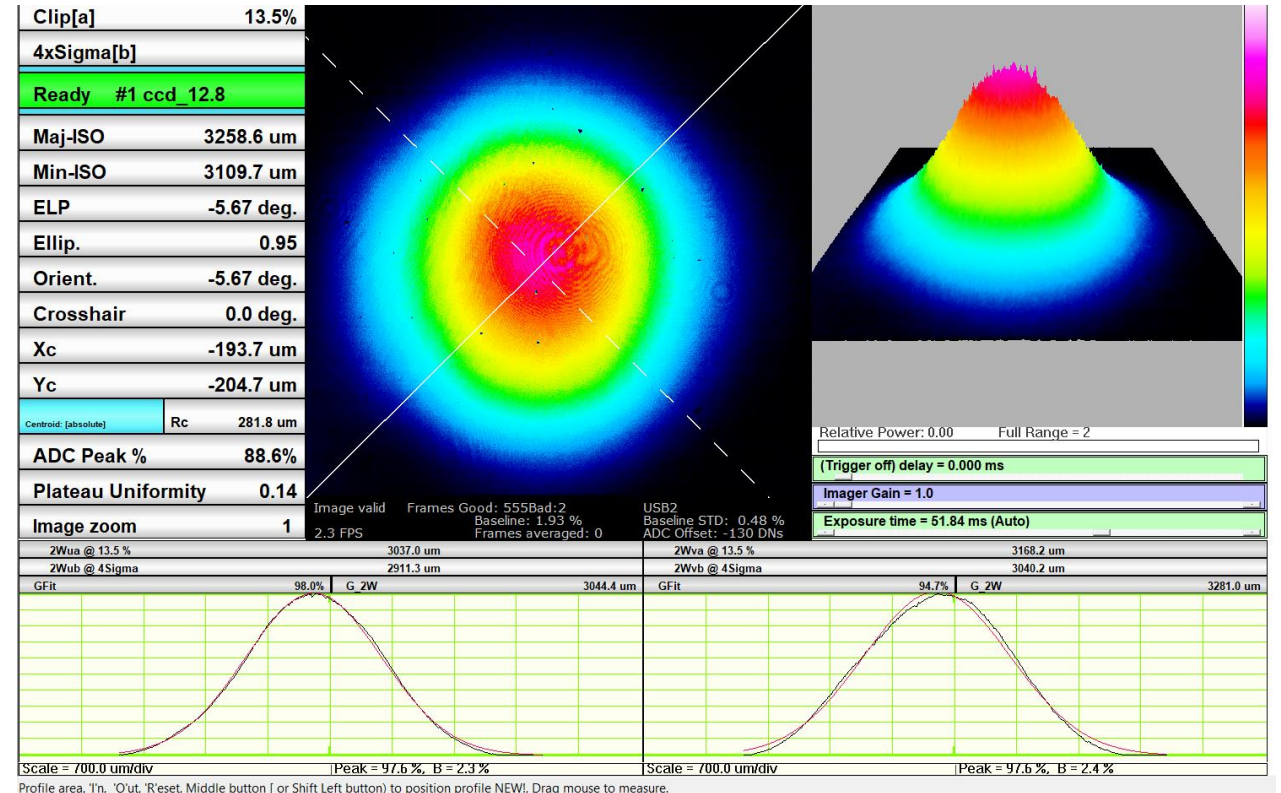
LASER SYSTEM

Laser Parameter		Unit	Measurement
Center wavelength		nm	1030.2
Bandwidth FWHM		nm	1.8
Average power		W	103.4
Energy per pulse		μJ	517.0
Short-term energy stability	RMS	%	0.89
Long-term energy stability	RMS	%	0.99
Pulse duration		fs	740
M ²	M ² _x		1.08
	M ² _y		1.11
Astigmatism		%	11.6
Waist asymmetry		%	0.5
Beam diameter	2W _{max}	mm	3.26
	2W _{min}	mm	3.11
Beam ellipticity		%	4.6
Short-term pointing stability	Radial	μrad	4.5
Short-term position stability	Radial	μm	1.58
Absolute timing jitter		fs	175.0
Long term jitter on 12h		fs	192.9
Repetition rate adjustability			Single shot – 40 MHz



LASER SYSTEM

Laser Parameter		Unit	Measurement
Center wavelength		nm	1030.2
Bandwidth FWHM		nm	1.8
Average power		W	103.4
Energy per pulse		μJ	517.0
Short-term energy stability	RMS	%	0.89
Long-term energy stability	RMS	%	0.99
Pulse duration		fs	740
M ²	M ² _x		1.08
	M ² _y		1.11
Astigmatism		%	11.6
Waist asymmetry		%	0.5
Beam diameter	2W _{max}	mm	3.26
	2W _{min}	mm	3.11
Beam ellipticity		%	4.6
Short-term pointing stability	Radial	μrad	4.5
Short-term position stability	Radial	μm	1.58
Absolute timing jitter		fs	175.0
Long term jitter on 12h		fs	192.9
Repetition rate adjustability			Single shot – 40 MHz

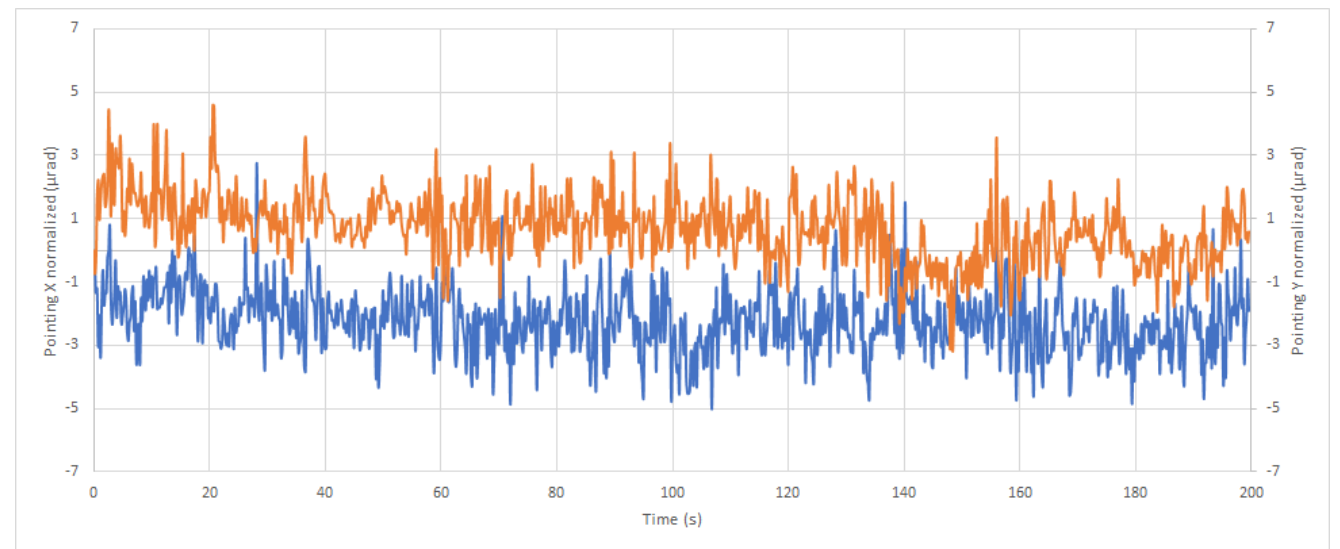
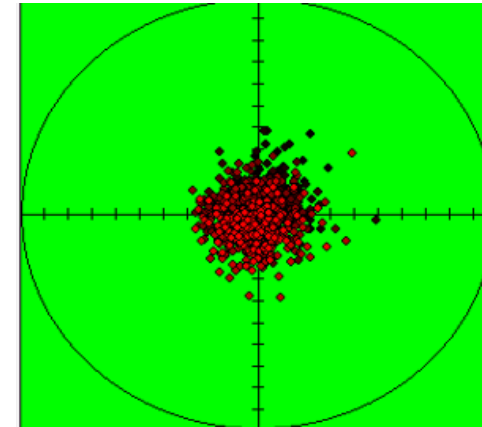


LASER SYSTEM

Laser Parameter		Unit	Measurement
Center wavelength		nm	1030.2
Bandwidth FWHM		nm	1.8
Average power		W	103.4
Energy per pulse		μJ	517.0
Short-term energy stability	RMS	%	0.89
Long-term energy stability	RMS	%	0.99
Pulse duration		fs	740
M^2	M^2_x		1.08
	M^2_y		1.11
Astigmatism		%	11.6
Waist asymmetry		%	0.5
Beam diameter	2Wmax	mm	3.26
	2Wmin	mm	3.11
Beam ellipticity		%	4.6
Short-term pointing stability	Radial	μrad	4.5
Short-term position stability	Radial	μm	1.58
Absolute timing jitter		fs	175.0
Long term jitter on 12h		fs	192.9
Repetition rate adjustability			Single shot – 40 MHz



TECHNISCHE
UNIVERSITÄT
DARMSTADT

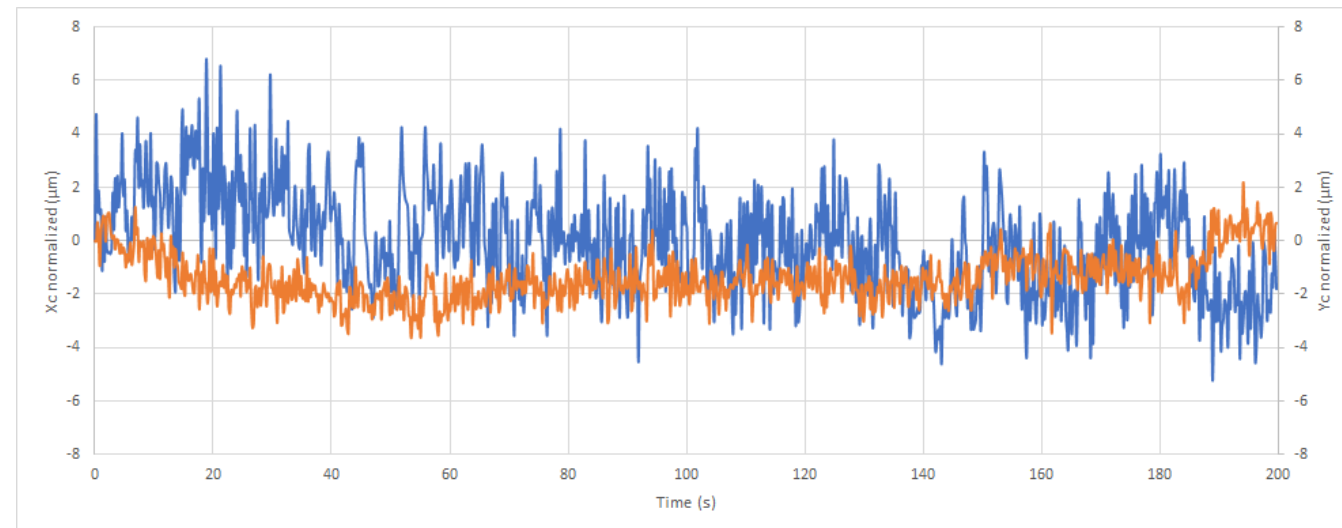
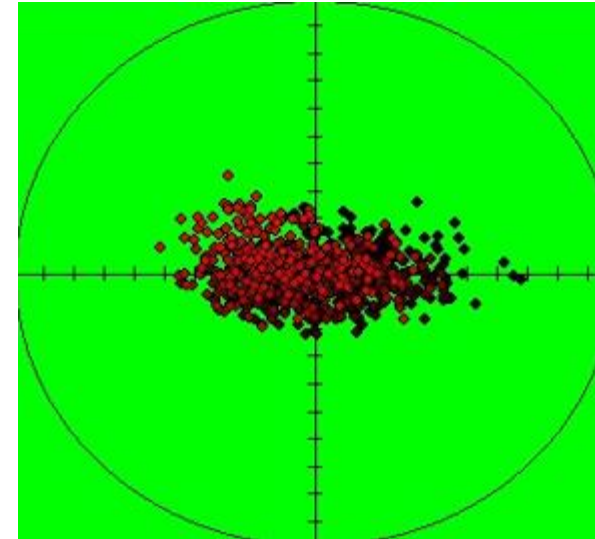


LASER SYSTEM

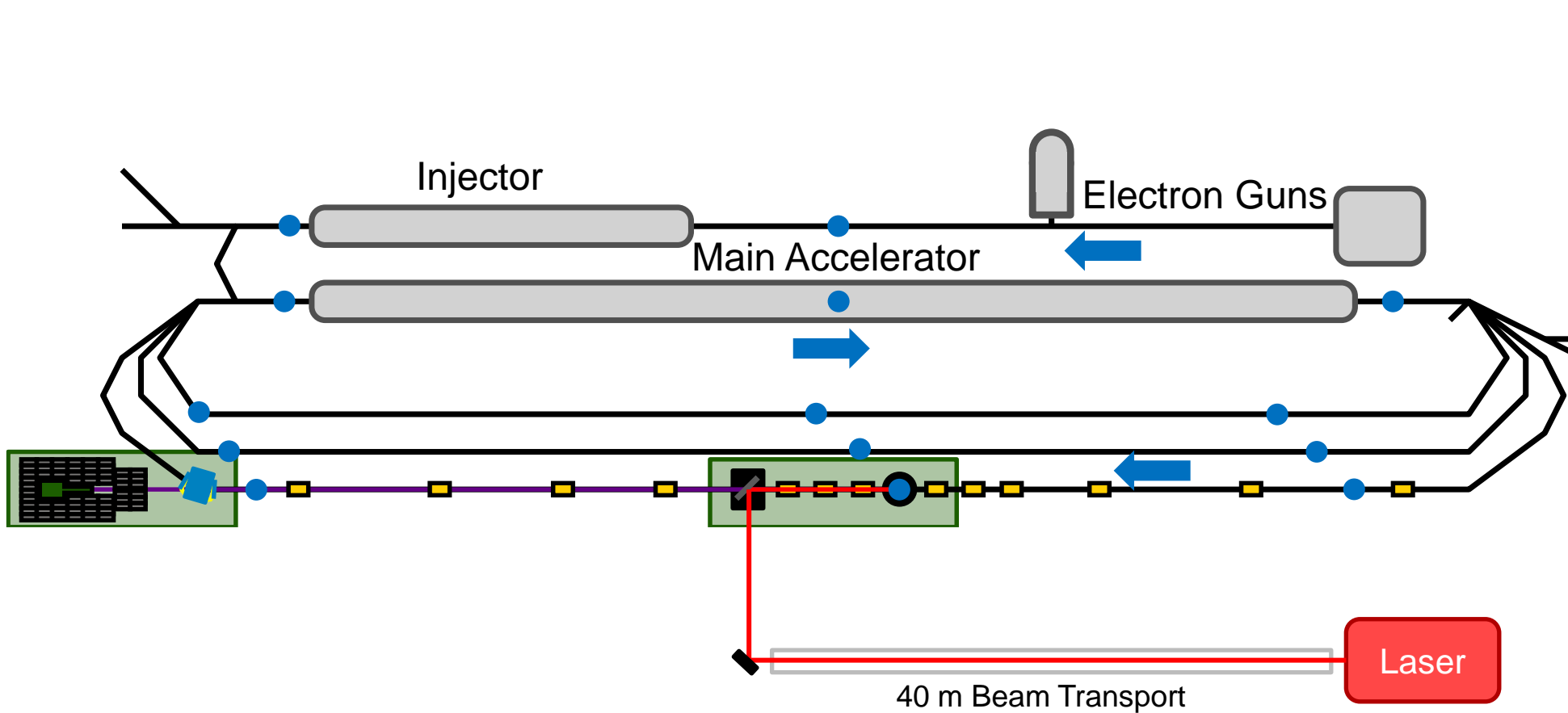
Laser Parameter		Unit	Measurement
Center wavelength		nm	1030.2
Bandwidth FWHM		nm	1.8
Average power		W	103.4
Energy per pulse		μJ	517.0
Short-term energy stability	RMS	%	0.89
Long-term energy stability	RMS	%	0.99
Pulse duration		fs	740
M ²	M ² _x		1.08
	M ² _y		1.11
Astigmatism		%	11.6
Waist asymmetry		%	0.5
Beam diameter	2W _{max}	mm	3.26
	2W _{min}	mm	3.11
Beam ellipticity		%	4.6
Short-term pointing stability	Radial	μrad	4.5
Short-term position stability	Radial	μm	1.58
Absolute timing jitter		fs	175.0
Long term jitter on 12h		fs	192.9
Repetition rate adjustability			Single shot – 40 MHz



TECHNISCHE
UNIVERSITÄT
DARMSTADT



LASER COMPTON BACKSCATTERING @ S-DALINAC



Higher photon energy preferred

Head-On Collision ✓

- ❖ For higher Energy
- ❖ Easier overlap

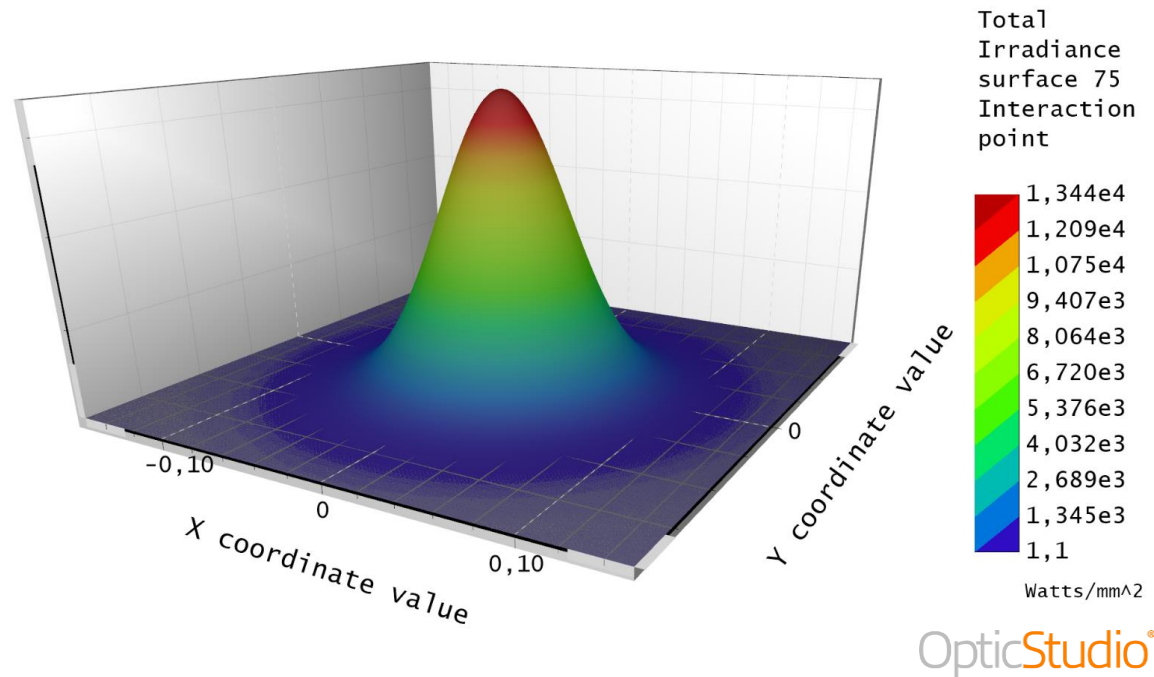
High Laser Pulse Energy (N_L)

High scattering frequency (f)

Small beam size at IP

Low M^2

Low $\sigma_{\Delta E_p}$; $\frac{\sigma_{\Delta E_L}}{E_L} \leq \frac{\sigma_{\Delta E_e}}{E_e}$



Simulation:

- Zemax OpticStudio
 - Physical optics propagation
- 40 m beam transport
- Telescopes and “relay imaging“
- Off-axis parabolic mirror with hole

Physical optics propagation @ IP:

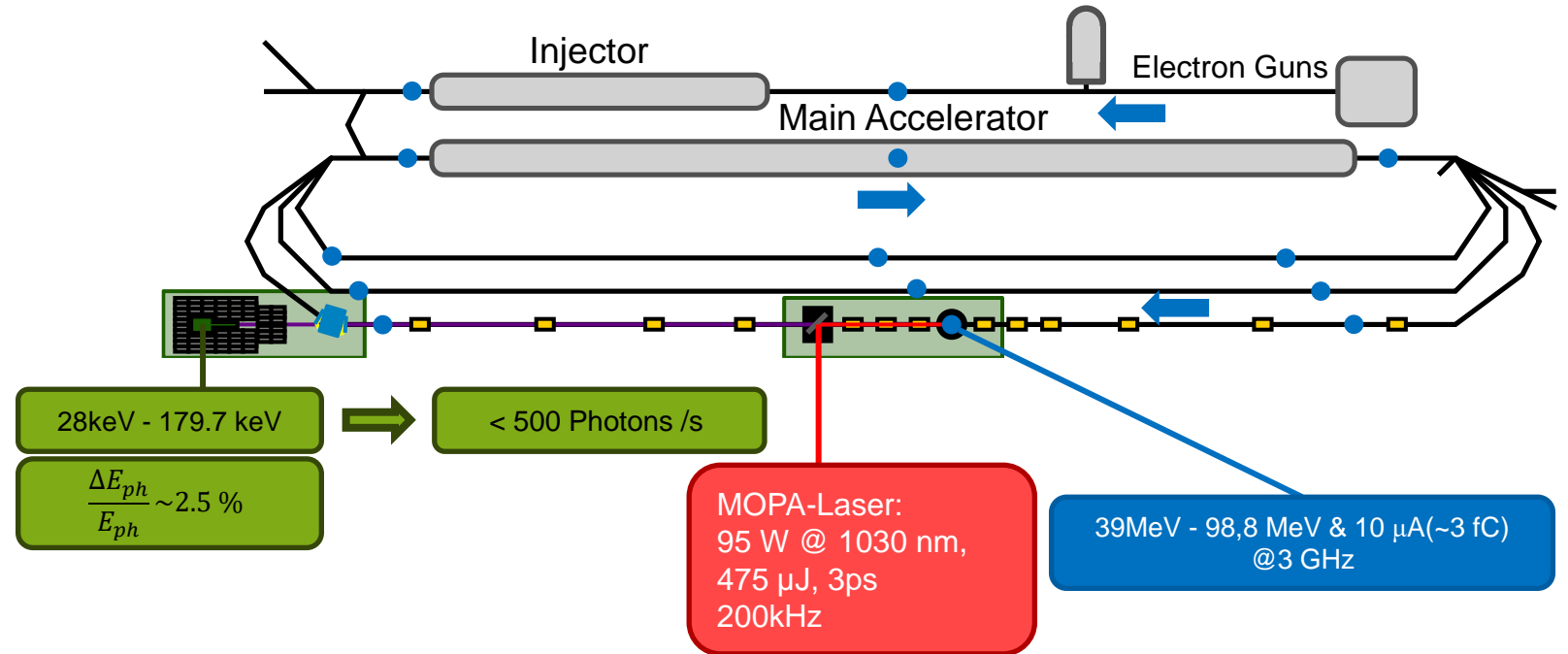
- Total power: 94.5 W (100 W)
- Waist size: 53.6 μm (12 mm)
- Rayleigh length: 8.8 mm

Total Irradiance surface 75 Interaction point

Beam wavelength is 1,03000 μm in the media with index 1,00000 at 0,0000 (deg)
 Display X Width = 3,0766E-01, Y Height = 3,0767E-01 Millimeters
 Peak Irradiance = 1,3439E+04 Watts/Millimeters², Total Power = 9,8445E+01 Watts
 Pilot: Size= 6,7106E-02, Waist= 5,3623E-02, Pos= 6,5988E+00, Rayleigh= 8,7703E+00

LASER COMPTON BACKSCATTERING @ S-DALINAC

Parameters	Values
Electron Beam	
Electron Energy (E_e)	39 MeV – 98.8 MeV
Rel. Error of Electron Energy (ΔE_e)	$< 10^{-3}$
Beam Current (I)	10 μ A
Beam normalized emittance	$5 \cdot 10^{-6}$ m rad
Electron Beam Size ($\sigma_{e,rms}$)	$\leq 100 \mu$ m
Laser Beam	
Wavelength (λ)	1030 nm
Photon Energy (E_L)	1.2 eV
Error Photon Energy (ΔE_L)	$1 \cdot 10^{-3}$ eV
Pulse Energy (E_{pulse})	0.25 mJ
Repetition Rate (f_{rep})	200 kHz
Beam Size ($\sigma_{pulse,rms}$)	$\leq 100 \mu$ m
Scattered Photon – Results for Head-On Collision	
Energy	28 keV – 179 keV
Min. rel. Energy Bandwidth, FWHM	0.7 %
Total Flux	$6 \cdot 10^3$ Ph/s
Spectral Flux at min. Bandwidth	38 Ph/s



MULTI-TURN ERL MODE OF THE S-DALINAC | RELATED PROJECTS

AKBP 16.4: Design and Status of the Laser-Compton Backscattering Source at the S-DALINAC

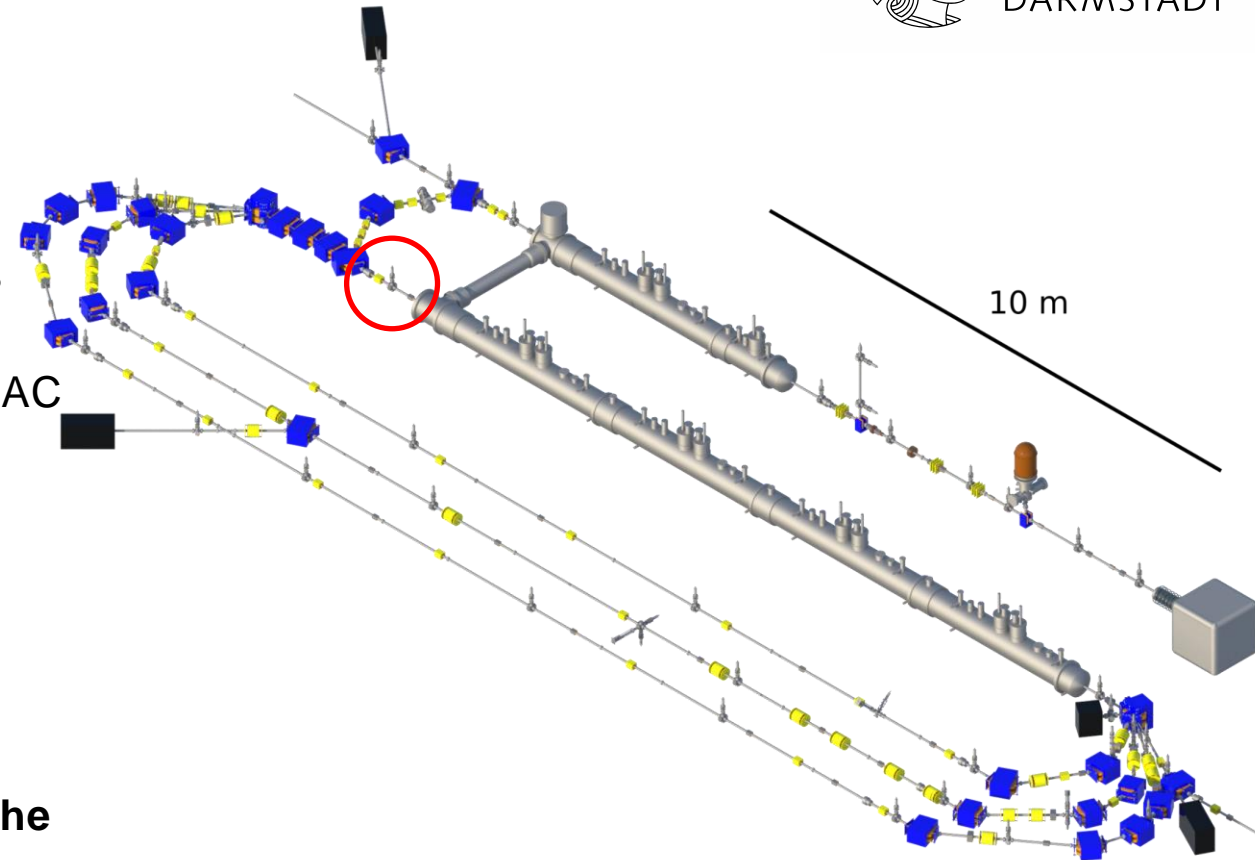


TECHNISCHE
UNIVERSITÄT
DARMSTADT



MULTI-TURN ERL MODE OF THE S-DALINAC | RELATED PROJECTS

1. AKBP 1.2: Automated Activation Procedure for GaAs Photocathodes
2. AKBP 8.4: Sensitivity Analysis and Online Surrogate Construction at the S-DALINAC Using Polynomial Chaos and Neural Networks
3. AKBP 9.6: Design of a Solenoid Magnet for the S-DALINAC
4. AKBP 14.1: System for Bunch Length Measurements behind the Injector of S-DALINAC
5. AKBP 14.2: Simulationen zur Optimierung von Vakuumsystemen für Beschleunigerstrahlführungen
6. AKBP 16.4: Design and Status of the Laser-Compton Backscattering Source at the S-DALINAC
7. **AKBP 16.5: Development of a 6 GHz Cavity BPM for the Multi-Turn ERL Operation at the S-DALINAC**



MULTI-TURN ERL MODE OF THE S-DALINAC | RELATED PROJECTS

AKBP 16.5: Development of a 6 GHz Cavity BPM for the Multi-Turn ERL Operation at the S-DALINAC

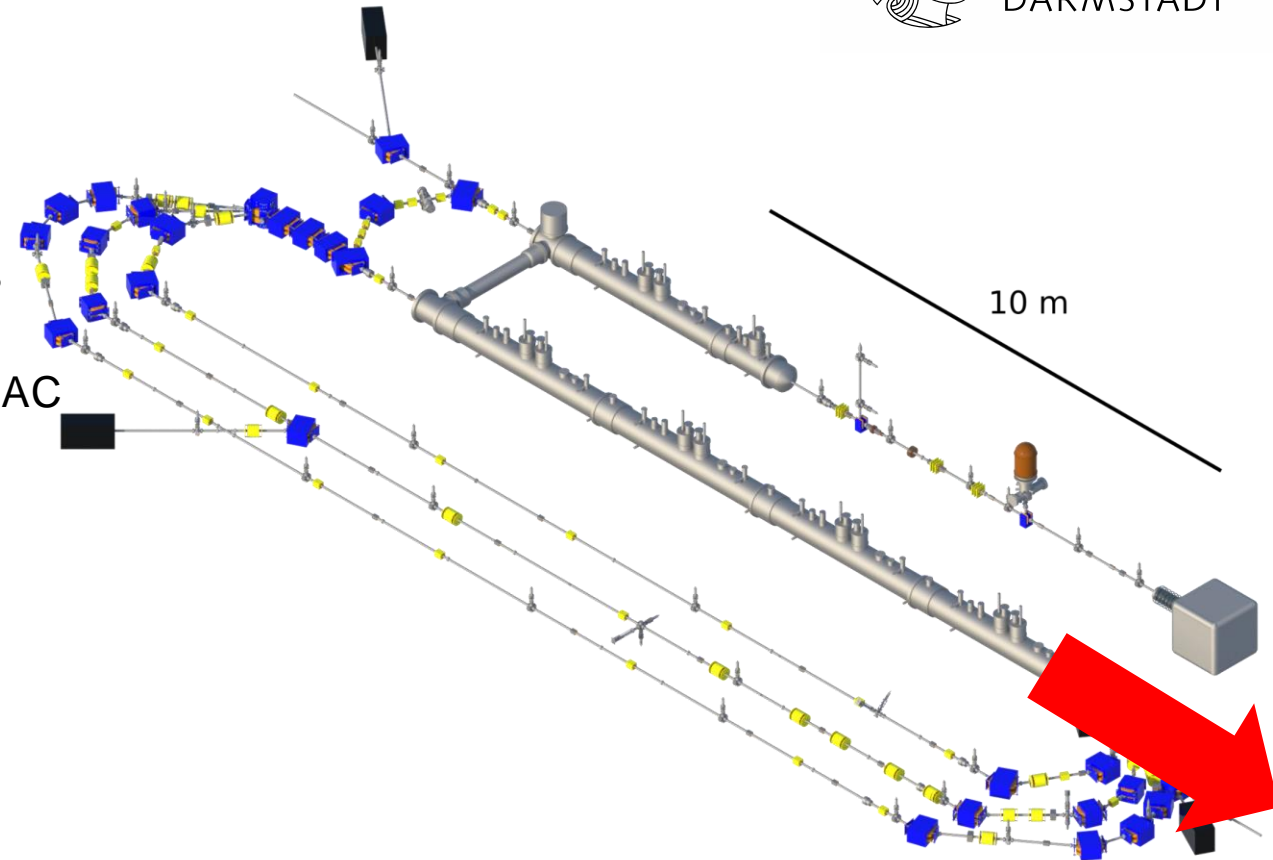


TECHNISCHE
UNIVERSITÄT
DARMSTADT



MULTI-TURN ERL MODE OF THE S-DALINAC | RELATED PROJECTS

1. AKBP 1.2: Automated Activation Procedure for GaAs Photocathodes
2. AKBP 8.4: Sensitivity Analysis and Online Surrogate Construction at the S-DALINAC Using Polynomial Chaos and Neural Networks
3. AKBP 9.6: Design of a Solenoid Magnet for the S-DALINAC
4. AKBP 14.1: System for Bunch Length Measurements behind the Injector of S-DALINAC
5. AKBP 14.2: Simulationen zur Optimierung von Vakuumsystemen für Beschleunigerstrahlführungen
6. AKBP 16.4: Design and Status of the Laser-Compton Backscattering Source at the S-DALINAC
7. AKBP 16.5: Development of a 6 GHz Cavity BPM for the Multi-Turn ERL Operation at the S-DALINAC
8. **AKBP 16.15: The Scraper System at S-DALINAC and ERL application**



MULTI-TURN ERL MODE OF THE S-DALINAC | RELATED PROJECTS
AKBP 16.15: The Scraper System at S-DALINAC and ERL application

- Machine protection
- Improving beam quality
- Background reduction
- Beam cleaning

- Simulation of an ERL interaction point with possible scraper placement

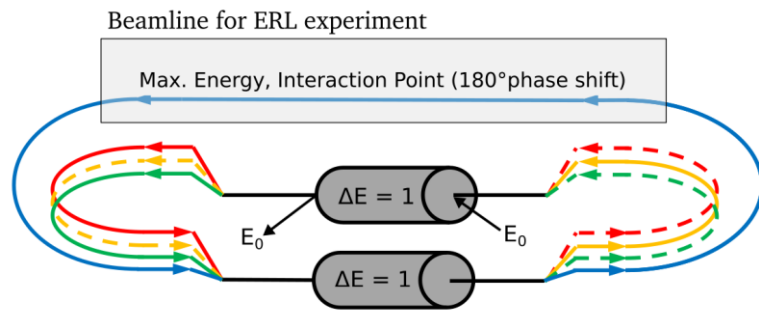


Table 1: Design parameters of S-DALINAC

Design Energy:	130 MeV
Beam current @ 130 MeV:	20 μ A
Frequency:	2.997 GHz

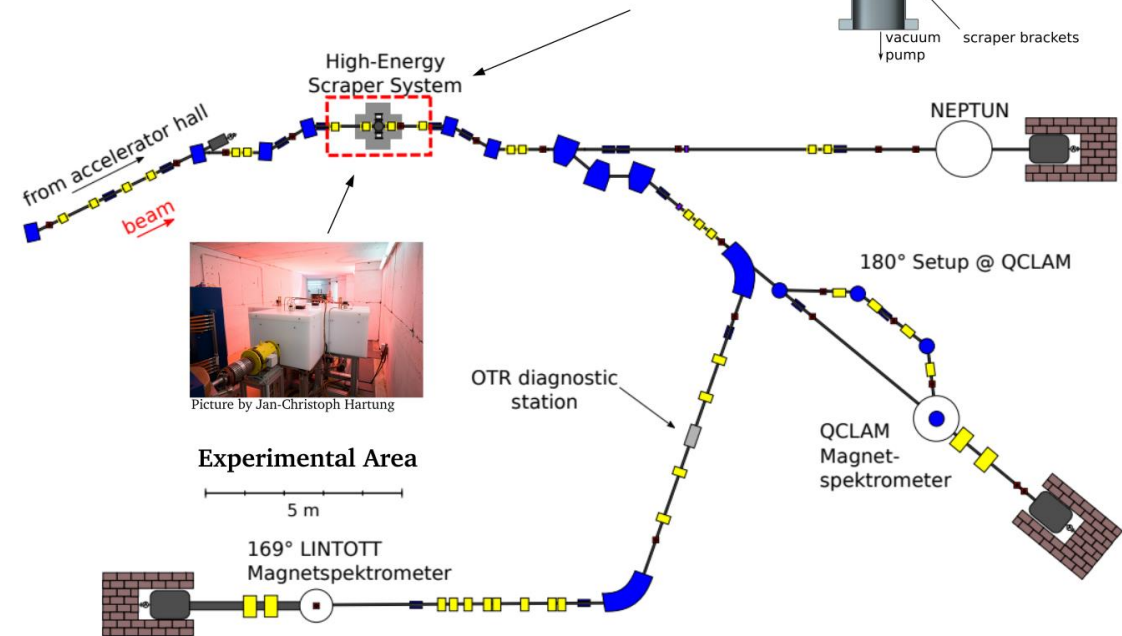
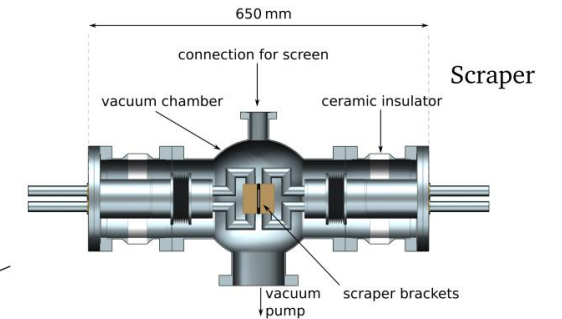


Figure 1: Experimental Area of S-DALINAC

- We successfully implemented a **two-fold energy recovery** (TER) mode at the S-DALINAC with an efficiency of **up to 87 %** (at low currents)
 - RF power required for a given beam current is substantially reduced
- Methods to increase the efficiency under investigation
- Implementation of a three-fold energy recovery mode in planning

- We have many **projects related to the ERL** operation of the S-DALINAC or future ERL accelerators, some of them **presented at this DPG Spring Meeting**



MULTI-TURN ERL MODE OF THE S-DALINAC

**THANK YOU FOR YOUR
ATTENTION**